

2020

Wearable Technology For Healthcare And Athletic Performance

Amanda Annette Watson

William & Mary - Arts & Sciences, volleyballmathlete@gmail.com

Follow this and additional works at: <https://scholarworks.wm.edu/etd>



Part of the [Computer Sciences Commons](#)

Recommended Citation

Watson, Amanda Annette, "Wearable Technology For Healthcare And Athletic Performance" (2020).
Dissertations, Theses, and Masters Projects. Paper 1593091706.
<http://dx.doi.org/10.21220/s2-4wzt-9387>

This Dissertation is brought to you for free and open access by the Theses, Dissertations, & Master Projects at W&M ScholarWorks. It has been accepted for inclusion in Dissertations, Theses, and Masters Projects by an authorized administrator of W&M ScholarWorks. For more information, please contact scholarworks@wm.edu.

Wearable Technology for Healthcare and Athletic Performance

Amanda Watson

College of William and Mary
Williamsburg, VA

Bachelor of Arts, Drury University, Springfield, MO 2014
Master of Science, College of William and Mary, Williamsburg, VA 2016

A Dissertation presented to the Graduate Faculty
of The College of William and Mary in Candidacy for the Degree of
Doctor of Philosophy

Department of Computer Science

College of William and Mary
May 2020

APPROVAL PAGE

This Dissertation is submitted in partial fulfillment of
the requirements for the degree of

Doctor of Philosophy

Amanda Watson

Amanda Watson

Approved by the Committee, April 17, 2020

Gang Zhou

Committee Chair

Gang Zhou, Professor, Computer Science
College of William and Mary

Robert Michael Lewis

Robert Michael Lewis, Associate Professor, Computer Science
College of William and Mary

Weizhen Mao

Weizhen Mao, Professor, Computer Science
College of William and Mary

Qun Li

Qun Li, Professor, Computer Science
College of William and Mary

Erik Korem

Erik Korem, William & Mary Athletics
College of William and Mary

COMPLIANCE PAGE

Research approved by

The College of William and Mary Protection of Human Subjects Committee

Protocol number(s):

PHSC-2015-03-25-11109-aawatson

PHSC-2017-11-11-12454-gzhou

PHSC-2018-01-15-12609-gzhou

PHSC-2018-03-23-12874-gzhou

PHSC-2019-01-17-13359-gzhou

PHSC-2019-04-17-13617-gzhou

PHSC-2019-04-26-13632-gzhou

PHSC-2019-06-12-13707-gzhou

PHSC-2019-08-12-13800-gzhou

Date(s) of approval:

04/11/2016

11/11/2017

02/22/2018

04/01/2018

01/30/2019

04/17/2019

04/26/2019

06/12/2019

08/12/2019

ABSTRACT

Wearable technology research has led to advancements in healthcare and athletic performance. Devices range from one size fits all fitness trackers to custom fitted devices with tailored algorithms. Because these devices are comfortable, discrete, and pervasive in everyday life, custom solutions are created to fit specific needs. In this dissertation, we investigate how wearable technology can advance research in healthcare and athletic performance by designing wearable sensors, features, algorithms, and intelligent feedback systems.

First, we present Magneto: a body mounted electromagnet-based sensing system for joint motion analysis. Magneto uses the combination of an electromagnet and magnetometer to remove environmental interference from a magnetic field reading. We localized the electromagnet with respect to the magnetic field reader, allowing us to apply Magneto in two pilot studies: measuring elbow angles and calculating shoulder positions. We calculated elbow angles to the nearest 15° with 93.8% accuracy, shoulder position in two-degrees of freedom with 96.9% accuracy.

Second, we present TracKnee: a sensing knee sleeve designed and fabricated to unobtrusively measure knee angles using conductive fabric sensors. We propose three models that can be used in succession to calculate knee angles from voltage. We evaluated our models and our device by conducting a user study where we collected 240 knee angles. Our results show that our model is 94.86% accurate to the nearest 15^{th} degree angle and that our average error per angle is 3.69° .

Third, we present ServesUp: a sensing shirt designed to monitor shoulder and elbow motion during the volleyball serve using conductive fabric sensors. ServesUp is comfortable, washable, and can be worn during and without impeding volleyball play. We conducted a user study with ten volleyball players for a total of 1000 volleyball serves which were classified using a KNN with an accuracy of 89.2%.

Fourth, we present BreathEZ, the first smartwatch application that provides both choking first aid instruction and real-time tactile and visual feedback on the quality of the abdominal thrusts. We evaluated our application through two user studies involving 20 subjects and 200 abdominal thrusts. The results of our study show that BreathEZ achieves a classification accuracy of 90.9% for abdominal thrusts and that BreathEZ was able to improve the quality of abdominal thrusts.

Finally, we present BBAid: the first smartwatch-based system that provides real time feedback back blows while instructing the user on choking first aid. We evaluated our application through two user studies involving 26 subjects and 260 back blow events. The results show that BBAid achieves a classification accuracy of 93.75% for back blows and was able to improve the quality of back blows.

TABLE OF CONTENTS

Acknowledgments	vii
Dedication	viii
List of Tables	ix
List of Figures	x
1 Introduction	2
1.1 Problem Statements	3
1.1.1 Improving Wearable Device Development Methods and Materials	3
1.1.2 Enhancing Skill Classification and Quantification Through Modeling and Machine Learning Techniques	4
1.1.3 Improving Skill Performance Using Intelligent Feedback System	4
1.2 Contributions	5
1.3 Dissertation Organization	8
2 Related Work	9
2.1 Wearable Technology Research	9
2.2 Sensing Using Magnets	10
2.3 Joint Angle Estimation	12
2.4 Athletics Performance Analysis	13
2.5 First Aid Skill Monitoring	14

3	Magneto: Joint Motion Analysis Using an Electromagnet-Based	
	Sensing Method	17
	3.1 Introduction	17
	3.2 Magneto Hardware Design	20
	3.3 Elimination of Environmental Interference	22
	3.3.1 Evaluation	24
	3.4 Localization of the Electromagnet	30
	3.4.1 Magnetic Field	30
	3.4.2 Evaluation	33
	3.5 Application Scenarios	35
	3.5.1 Elbow Angle Pilot Study	36
	3.5.2 Shoulder Position Pilot Study	39
	3.6 Discussion and Future Work	45
	3.6.1 Increasing the Strength of the Electromagnet	45
	3.6.2 Increasing the Cycling Rate	46
	3.6.3 Multiple Electromagnets	46
	3.7 Conclusion	47
4	TracKnee: Knee Angle Measurement Using Stretchable Conductive Fabric	
	Sensors	48
	4.1 Introduction	48
	4.2 Modeling	52
	4.2.1 Change in Length to Angle Model	52
	4.2.2 Resistance to Change in Length Model	55
	4.2.3 Voltage to Resistance Model	56
	4.3 TracKnee Prototype Design	57
	4.3.1 Control Patch	58

4.3.1.1	Components	59
4.3.1.2	Fabrication	60
4.3.2	Sensor Sleeve	62
4.3.2.1	Components	62
4.3.2.2	Fabrication	63
4.3.3	TracKnee Prototype	63
4.3.4	Lessons Learned	64
4.4	Data Collection	65
4.4.1	Equipment	65
4.4.2	Parameters	68
4.4.3	Demographics	69
4.5	Experiment Results	70
4.6	Conclusion	72
5	ServesUp: Using Wearables to Improve the Volleyball Serve	73
5.1	Introduction	73
5.2	Prototype Design: Sensing Shirt	75
5.2.1	Control Swatch	76
5.2.1.1	Components	76
5.2.1.2	Connection	77
5.2.1.3	Conductive Thread Wiring	77
5.2.2	Sensor Shirt	77
5.2.2.1	Conductive Fabric Bend Sensors	78
5.2.2.2	Conductive Thread Wiring	83
5.2.3	Lessons Learned	83
5.2.3.1	Conductive Thread Choices	84
5.2.3.2	Conductive Thread Stitch Patterns	84

5.2.3.3	Bridges and Barrier Layers	85
5.3	User Study	85
5.3.1	Equipment	85
5.3.2	Parameters	86
5.3.3	Demographics	87
5.4	Results	88
5.4.1	Serve Classification	88
5.4.1.1	Naive Serve Classifier	89
5.4.1.2	Weka Serve Classifiers	90
5.4.2	Results from Questionnaires	90
5.5	Discussion and Future Work	91
5.5.1	Evaluating the System on Other Volleyball Players	91
5.5.2	Sensing Shirt Upgrade	91
5.5.3	Other Applications for the Sensing Shirt	92
5.6	Conclusion	93
6	BreathEZ: Using Smartwatches to Improve Choking First Aid	94
6.1	Introduction	94
6.2	Pre-User Study	97
6.2.1	Choking First Aid Background	98
6.2.2	Study Design	99
6.2.3	Results	101
6.3	System Design	103
6.3.1	System Architecture	103
6.3.2	Feature Extraction	104
6.3.3	Event Detection	104
6.3.4	Metric Calculation	105

6.3.4.1	Quality of Thrusts	106
6.3.4.2	Quantity of Thrusts	106
6.4	BreathEZ Application	107
6.5	Post-User Study	108
6.5.1	Study Design	108
6.5.2	Results	111
6.5.2.1	Classification of Abdominal Thrusts	111
6.5.2.2	Abdominal Thrust Performance Feedback	112
6.5.2.3	Willingness and Fear	113
6.6	Discussion and Future Work	114
6.6.1	Angle of Abdominal Thrusts	114
6.6.2	Feedback After Each Abdominal Thrust	115
6.6.3	Back Blows	115
6.6.4	Choking First Aid for Infants	116
6.7	Conclusion	116
7	BBAid: Using Smartwatches to Improve Back Blows	118
7.1	Introduction	118
7.2	Preliminary Study	121
7.2.1	Study Setup	121
7.2.2	Study Results	123
7.3	System Design	125
7.3.1	System Architecture	125
7.3.2	Feature Extraction	127
7.3.3	Event Detection	127
7.3.4	Metric Calculation	128
7.4	BBAid Application	130

7.4.1	Instructions	130
7.4.2	Feedback	132
7.5	User Study	132
7.5.1	Study Setup	133
7.5.2	Study Results	135
7.5.2.1	Back Blow Classification	135
7.5.2.2	User Performance	135
7.5.2.3	User Knowledge	137
7.5.2.4	User Feedback	139
7.6	Discussion and Future Work	140
7.6.1	Abdominal Thrusts	140
7.6.2	First Aid Training	140
7.7	Conclusion	141
8	Conclusion and Future Work	142

ACKNOWLEDGMENTS

The completion of this dissertation would not have been possible without the help of many talented and hardworking people who have challenged, supported, and encouraged me through this process. Although not everyone's names may be enumerated, their contributions are sincerely appreciated and gratefully acknowledged.

First, I would like to thank my advisor, Professor Gang Zhou, for his feedback and guidance throughout all of my research. Many thanks to Professor Robert Michael Lewis, Professor Weizhen Mao, Professor Qun Li, and Dr. Erik Korem for serving on my dissertation committee.

Next, I would also like to thank all of the past and current members of the LENS lab research group and all of my collaborators, including but not limited to: Ken Koltermann, Andrew Lyubovsky, Shuangquan Wang, Ingrid Pretzer-Aboff, Kyle Wallace, Minglong Sun, Woosub Jung, George Simmons, Samhita Pendyal, and Hongyang Zhao.

Finally, I would like to extend my gratitude to the Computer Science Department. I especially would like to thank the administration team; Vanessa Godwin, Jacquelyn Johnson, and Dale Hayes.

This work was supported in part by the U.S. National Science Foundation under grants CNS-1841129 (CSR:EAGER) and CNS-1253506 (CAREER).

I would like to dedicate this dissertation to my parents, Robert and Helen Watson,
and to Shirley Guckenberger for their endless support of my pursuit of a Ph.D.

LIST OF TABLES

3.1 Cycling Rate Analysis	29
3.2 Equation 3.1 Variable Definitions	31
4.1 Participant Knee Motion Statistics	54
4.2 Participant Knee Range of Motion Statistics	69
4.3 Model Accuracy by Participant	71
5.1 Fabric Warping	79
5.2 Sensor Stretch Progression During a Serve	88
5.3 Evaluation of Classifiers	90
6.1 Classifier Evaluation	105
6.2 Group 1 Feedback	112
7.1 Evaluation of Multiple Classifiers	128
7.2 Participant Performance	136

LIST OF FIGURES

3.1 Circuit Diagram for Magneto	21
3.2 Calculation of Time Cycle Features	23
3.3 Averages and Environmental Noise Removal	23
3.4 Orientation Experiment	25
3.5 Movement Experiment	25
3.6 Magnetic Interference Experiment	27
3.7 Environments Tested	28
3.8 The Relationship Between the Magnet and the Reader	30
3.9 Ellipsoid of Location and Orientation Pairs	32
3.10 Experimental Setup	33
3.11 Distance and Orientation Results	34
3.12 Elbow User Study Setup	36
3.13 Elbow Angles	38
3.14 Elbow Angles Results	38
3.15 Shoulder Movements	40
3.16 Shoulder Motion	41
3.17 Direction of θ_N at Different Shoulder Locations	42
3.18 Intersection of Localization and Shoulder Motion Distance	43
4.1 Measured Knee Angles	52
4.2 Change in Length for Knee Angles Adjusted for Height	53
4.3 Change in Length to Angle model Adjusted for Height	55

4.4 Fabric Resistance to Stretch Distance	56
4.5 Voltage Divider	56
4.6 TracKnee Prototype	57
4.7 TracKnee Control Patch	58
4.8 Baby Lock Verve Sewing and Embroidery Machine	60
4.9 Circuit diagram of TracKnee	64
4.10 TracKnee Application	66
4.11 TracKnee Application States	67
4.12 User Study Setup	68
4.13 Comparison of Ground Truth Angle and Calculated Angle	70
4.14 Voltage of Battery Over Time	71
5.1 Sensing Shirt	75
5.2 Control Swatch and its Attachment Location	76
5.3 Sensor Placement Inside of Sensing Shirt	78
5.4 Elbow Sensor Design	79
5.5 Resistance Change of Conductive Fabric for Elbow	80
5.6 Resistance Change of Conductive Fabric for Shoulder	81
5.7 Stitch Patterns and Connections Points	83
5.8 Lessons Learned	84
5.9 Progression of the Volleyball Serve	87
5.10 Sensing Shirt Readings for a Single Serve	89
6.1 CPR Training Manikin	98
6.2 Participant Willingness	101
6.3 System Architecture for BreathEZ	102
6.4 Abdominal Thrust Features	103
6.5 Instructional Screens	107

6.6 Feedback Screens	108
6.7 Post-User Study Willingness	114
7.1 Willingness to Perform Choking First Aid	124
7.2 System Architecture of BBAid	126
7.3 Back Blow Features	126
7.4 Comparison of Expert and Participant Back Blow Accelerations	129
7.5 BBAid Instructional Screens	130
7.6 BBAid Feedback Screens	131
7.7 User Study Questionnaires	134
7.8 Correct Manikin Position	136
7.9 Choking First Aid Willingness	138

Wearable Technology for Healthcare and Athletic Performance

Chapter 1

Introduction

Wearable technology is a categorization of electronic devices that are worn on the body. These devices include but are not limited to devices embedded into clothing, implanted in the body, and even smart tattoos and bandages applied to the skin. Key qualities of these devices are that they are hands-free, can wirelessly communicate, and incorporate microprocessors that allow for computing functionality. These qualities promote the rapid growth in the number of devices worldwide from 526 million in 2016 to an expectation of more than 1.1 billion in 2022 [\[40\]](#). With the number of devices growing, their applications are ever-expanding and wearable technology is being leveraged to solve more specific problems ranging from health and fitness tracking to augmented reality to communication.

In the past, a trip to the physicians' office was required for individuals to have their overall health and well-being examined. Today, with the help of wearable technology, individuals can monitor their health from the comfort of their own home. The ability to collect remote health data supports early diagnosis of disease, monitoring of the progression of an illness, and more efficient post-operative recovery. Athletes take this data a step further. They optimize their training and resting periods to see the maximum improvements while preventing overtraining and injuries. These devices can even apply directly to their sports, giving feedback on the specific skills required. Overall, wearable technology is enabling new avenues for advancement in healthcare and athletics.

1.1 Problem Statements

In this dissertation, we investigate how wearable technology can advance research in healthcare and athletic performance by designing wearable sensors, features, algorithms, and intelligent feedback systems. Specifically, we answer three research questions:

RQ1: How can we design comfortable wearable sensors and devices that accurately sense biometric data?

RQ2: How can we develop features and algorithms that accurately classify and quantify the performance of a skill?

RQ3: How do we create intelligent feedback systems that promote an increase in the quality of the performance of a skill?

1.1.1 Improving Wearable Device Development Methods and Materials

To answer our first research question, we created customized wearable devices called SoftWear. These are soft wearable devices with sensors made from conductive fabric that integrate seamlessly into clothing. To the wearer, these sensors are undetectable. Since wires are rigid and uncomfortable, we replaced them with conductive thread. Further, our garments are washable as the electronics are confined to a removable patch. They even hold up to 200 washes in a washing machine. We leveraged our custom development method and materials in two projects: TracKnee and ServesUp. TracKnee is a sensing knee sleeve designed and fabricated to unobtrusively measure knee angles using a single conductive fabric sensor. ServesUp is a sensing shirt designed to monitor shoulder and elbow motion through the volleyball serve with four conductive fabric sensors that an athlete can wear without impeding volleyball play.

1.1.2 Enhancing Skill Classification and Quantification Through Modeling and Machine Learning Techniques

To answer our second research question, we developed features and algorithms to classify and quantify skills. In this dissertation, we focus on skills performed in athletic and choking first aid situations. In our joint angle sensing projects, Magneto and TracKnee, we developed mathematical models to derive joint angles from wearable sensor data. In Magneto, we calculated elbow angles to the nearest 15° with 93.8% accuracy, shoulder position in two-degrees of freedom with 96.9% accuracy, and shoulder positions in three-degrees of freedom with 75.8% accuracy. In TracKnee, we evaluated our models by conducting a user study with six participants where we collected 240 ground truth angles and sensor data from our TracKnee device. Our results show that our model is 94.86% accurate to the nearest 15^{th} degree angle and that our average error per angle is 3.69° . In ServesUp, we classified serving motion given data from our sensing shirt using a KNN with a classification accuracy of 89.2%. We evaluated our classifier by conducting a user study with ten volleyball players. In our choking first aid projects, BreathEZ and BBAid, we created features that represent abdominal thrusts and back blows and used machine learning algorithms to classify the choking first aid skills. Then, we created metrics that allowed us to quantify the quality of the performance of those skills.

1.1.3 Improving Skill Performance Using Intelligent Feedback System

To answer our third research question, we designed intelligent feedback systems that provided essential data to the user in real-time and during post data collection analysis. In our choking first aid projects, we developed a smartwatch application that demonstrated real-time feedback on choking first aid performance to the user. We designed this application to give choking first aid instructions, classify and analyze the performance of the skill, and then provide feedback to the user in a way that is easy to understand. We leveraged multiple methods of feedback including colors, text, and vibration. This allowed the user

to make immediate changes that led to improved performance of choking first aid skills.

1.2 Contributions

The overall results of this dissertation advance the applications of wearable technology in healthcare and athletic performance by designing wearable sensors, features, algorithms and intelligent feedback systems.

Electromagnet-based Sensing System for Joint Motion Analysis. First, we developed an electromagnet based wearable sensing system that localizes a magnet without magnetic interference from the surrounding environment. Based on our results, we leveraged this sensor data to monitor joint angles. Our main contributions are:

- We developed a method that removes environmental interference from a magnetic field reading. We evaluated this method to show its performance when removing the interference in three movement dimensions, in six environments, and with six different cycling rates.
- We designed an algorithm that allows us to localize a magnet with respect to a magnetic field reader. Our algorithm calculated orientation of the magnet with an average error of 3.43° and distance from the reader to the magnet with an average error of 2.34%.
- We conducted two pilot studies to evaluate Magneto: elbow angles and shoulder position. We conducted a user study where we recorded 650 elbow angles from 13 participants in which we examined 12 different elbow angles for a total data set of 650 angles. Overall, our method saw an accuracy of 93.82% when classifying elbow angles to the nearest 15° angle and an average error of 2.52° . We modelled the motion of the shoulder in two and three dimensional space. We calculated the correct shoulder position (within 2.5 millimeters) in 96.87% of test cases in two dimensional space and in 75.79% of test cases in three dimensional space.

Conductive Fabric Sensor Based Knee Angle Monitor. Second, we explore the use of conductive fabric as an accurate on body joint angle sensor. We target the knee as it is a hinge joint and only displays one degree of motion. The results from this study are promising and provide us with the ability to study more complicated joints. Our contributions are summarized as follows:

- We propose three models that can be used in series to calculate knee angles from voltage. First, we model change in length across the front of the knee to the knee angle with respect to the height of an individual. Second, we model resistance of the fabric to change in length of the conductive fabric. Third, we model voltage to the resistance of the fabric.
- We designed and fabricated a wireless sensing knee sleeve to unobtrusively measure knee angles called TracKnee. TracKnee utilizes a soft and stretchable conductive fabric sensor to monitor knee angles. We designed it to be washable by making any non-washable electronic components removable. We also designed to be easy to put on and take off so that it would be as easy for the user to wear as a non-sensing knee sleeve.
- We conducted a user study with six participants where we collected ground truth angles and sensor data from our TracKnee device. To do this, we developed a data collection application on an Android smartphone to collect and store the data.
- We evaluated our models on the user study data. Our results show that our model is 94.86% accurate to the nearest 15th degree angle and that our average error per angle is 3.69°.

Conductive Fabric Sensor Based Shoulder and Arm Motion Monitor. Third, we examine how conductive fabric sensors can apply to a more complicated joint: the shoulder. The results from this research work show that the three dimensional dynamic

motion of the shoulder can be monitored by an array of conductive fabric sensors. Our contributions are summarized as follows:

- We designed and implemented a wearable device, called the sensing shirt, with sensors embedded into the fabric of a shirt to recognize volleyball serve in real time.
- We collected data using our shirt on 1000 serves collected from 10 volleyball players. We developed a classifier that achieves 89% serve classification accuracy.

Choking First Aid Abdominal Thrust Monitoring Smartwatch. Fourth, we examine the ability of smartwatches to be used as not only a monitoring device but also a tool that can provide real-time feedback to the user during the abdominal thrust portion of choking first aid. Our results show that our application not only improves the quality of choking first aid skill performance but also the willingness of the user to perform the skill. Our contributions may be summarized as follows:

- We introduce BreathEZ, a smartwatch application that improves choking first aid by providing auditory and tactile feedback to the user and improves bystander performance of abdominal thrusts as part of choking first aid.
- We conduct two user studies with the first comprised of 135 abdominal thrusts from 13 individuals and the second comprised of 100 abdominal thrusts from 10 individuals. Short surveys were administered to gain insight on the viability of using BreathEZ in real world scenarios.
- We present a model describing abdominal thrust performance using number and quality of the abdominal thrusts which are used to coach the user while they are performing choking first aid.

Choking First Aid Back Blow Monitoring Smartwatch. Fifth, we extended our last research work to encompass an additional choking first aid skill: back blows. Our results mirrored those of our last study and once again showed that our smartwatch

application improved skill quality performance and willingness. Our contributions are summarized as follows:

- We are the first to extract features from smartwatch accelerometer data and use it to accurately classify back blows. We selected five features to describe a single back blow. We feed these five features into a random forest classifier and see a 93.5% accuracy.
- We are the first to provide insightful feedback to enhance back blow performance. We calculate two metrics: quality and quantity of back blows that are used to provide feedback. In our final user study, all of our participants experienced an increase in performance while using BBAid.
- We propose and develop the first smartwatch application that incorporates our features, classifier, and feedback to combat the bystander effect. All of our participants saw an increase in their willingness to perform choking first aid when using the given choking first aid instructions.

1.3 Dissertation Organization

The remainder of this dissertation is organized as follows: Chapter 2 details the related work on wearable technology and its application to healthcare and athletics. In Chapter 3, we present Magneto, a body mounted electromagnet-based sensing system for joint motion analysis. In Chapter 4, we present TracKnee, a knee sleeve that measures knee angles using a conductive fabric sensor. In Chapter 5, we present ServesUp, a smart shirt that improves the volleyball serve. In Chapter 6, we present BreathEZ, a smartwatch application that improves the abdominal thrust portion of choking first aid. In Chapter 7, we present BBAid, a smartwatch application that improves the back blow portion of choking first aid. Finally, in Chapter 8, we summarize with plans for future work and our conclusion.

Chapter 2

Related Work

In this chapter, we discuss the related work for our research. Our related work is broken into five categories. First, we discuss wearable technology research. Second, we explore sensing using magnets. Third, we describe joint angle estimation using a variety of wearable devices. Fourth, we consider athletics performance analysis using smart devices. Fifth, we finish by examining first aid skill monitoring.

2.1 Wearable Technology Research

Enabling ubiquitous body motion tracking and modeling has received an increasing amount of attention from the medical science and computing disciplines [174, 144, 47, 141, 200]. Medical science research is mainly conducted in a lab setting [193] but there is a push to move data collection outside of the lab [155]. This will enable researchers to collect more data in the real world which is important when treating diseases. For example, in certain diseases, such as Parkinson's Disease specific symptoms such as freezing of gate and are difficult to reproduce in lab conditions [15]. Ubiquitous monitoring will enable the collection of more data on freezing of gate which can help to advance research on Parkinson's disease. In other diseases, such as Osteoarthritis, medical professionals see benefits in monitoring patients outside of the clinic [151] but currently, this is not widespread.

Smart fabrics and e-textiles have enabled the production of wearable devices that are flexible and thus comfortable when worn on the human body. Research into e-textiles has made progress in fields such as sports, healthcare, and gaming [74]. Using e-textiles, researchers have acquired signals such as the electrocardiogram (ECG) [189] and electromyogram (EMG) [173, 65, 152, 147]. Wearable e-textiles are also being used for touch-sensitive buttons [194] and pressure sensors [94]. Accelerometers have been imported in e-textiles to detect fall risks and monitor human activity recognition [122]. Large companies are expanding their research to include e-textiles. For example, Project Jacquard from Google is developing capacitive touch sensing textiles [158].

Conductive materials are being used to develop stretch, pressure, and bend sensors. Gioberto et al. [75] developed a stitched stretch sensor made with conductive thread. These sensors have been integrated into overalls to detect lower body posture [138] and to measure the flexion of the knee and the hip [76, 73]. Huang et al. [98] invented a glove using stretch sensors made from piezo-resistive yarn to take input from the user's hand gestures. Ashruf et al. [13] and Rothmaier et al. [167] have developed capacitive pressure sensors with a matrix of conductive thread. Dunne et al. uses foam sensors to monitor breathing, shoulder lift, and directional arm movement [59, 58]. Shyr et al. [175] used a conductive webbing made of conductive and elastic yarn to determine the flexion angle of the elbow. Bergmann et al. [19] used a flexible conductive polymer material that could be attached to clothing to measure knee joint angles. Papi et al. [150] designed a pair of smart leggings that used a conductive polymer strip to estimate the range of motion of the knee. Gholami et al. [72] used a thermoplastic-based stretchable strain sensor to gauge its ability to estimate knee flexion and simple tasks such as walking.

2.2 Sensing Using Magnets

Qu et al. [162] developed a wearable device to measure joint flexion and physical activity using neodymium magnets. They tested their device on human subjects for knee

motion and porcine subjects to monitor their physical activity. They tested several different sizes, shapes, and strengths of magnets ranging from 1.6 cm in diameter circle magnets to 10 cm by 1.3 cm by 0.6 cm bar magnets. Hullfish et al. [99] used a neodymium magnet and magnetometer combination to measure peak knee extension angles. They used a 1.5" by 0.5" by 0.25" neodymium bar magnet. They were able to accurately measure knee extension angles within 5° of the actual value. A challenge they encountered was sensor saturation below 65° . They further measured peak knee flexion during walking and averaged an RMSE of 10.1° . While both of these works were able to successfully use a static magnetic field as the input for a sensor, they do not address the effects of outside magnetic fields. Since they use the magnetic field reading to calculate distance, they assume that any change in magnetic field reading is a change in the distances between the magnetometer and the magnet. To remove the influences of outside magnetic fields, the magnetometer can be calibrated for a specific environment, but such calibration must be done every time the environment changes. Our sensing device, Magneto, accounts for the influence outside magnetic fields and is able to remove them without affecting the signal of our electromagnet.

Further, work has been done to attach magnets to the hand to monitor hand postures and gestures. Ma et al. [125] [126] attached small magnets to each fingernail on a hand and put magnetic sensors in a wristband. They used this sensor to calculate hand postures. Keyes et al. [127] patented the use of magnetometer in a head-mounted display such as smart glasses and a magnet mounted on a hand to classify gestures made with the hand. Osman et al. [148] patented a method where they placed magnetic readers on the hand and fingertips and three magnets on the wrist to compute the position of the fingertip. Chen et al. [38] placed magnetometers on fingers and a magnet on the thumb to track hand motion. These systems do not account for the influence of outside environmental field while Magneto does.

Bonnet et al. [25] used on-body magnetic field sensors to accurately monitor and analyze human movements including sit-to-stand, trunk inclination, and absolute acceleration.

Their sensor is limited by any rotation that occurs around the Earth’s magnetic field and any outside magnetic interference degrades their performance. O’Donovan et al. [146] uses magnetic sensors as well as inertial sensors to measure angles of the ankle. Since the Earth’s magnetic field was used as a reference, their angle measurements would be limited by orientation and location. Meina et al. [134] uses a permanent magnet to correct the drift of readings from an IMU. Magnetometers and magnetometer arrays have been used to locate and identify ferrous objects [130] [131]. These research works used the magnetic field of the Earth as a reference point. While they use this as an asset their sensors are still susceptible to magnetic interference from nearby ferrous objects.

2.3 Joint Angle Estimation

Joint angle estimation has been a focus of research in human motion tracking and modeling and is commonly used in athletics. Commonly, wearable sensors are used for monitoring of joint angles as they are small, durable, and can be worn outside of a lab. The most prevalent sensing technology is the inertial movement unit (IMU) as it is small, inexpensive, and widely tested [113] [41] [117] [118] [26] [61] [102] [66] [102] [69]. Wireless wearable ultrasonic sensors [161] [159] [160], optical sensors [183] [176] [109], liquid metal sensors [135] [136], potentiometers [54], acoustic sensors [188], force sensitive resistors [177], retractable string sensors [119], and galvanic coupling systems [39] are also used but they are intrusive and not comfortable for long term wear. Flexible sensors have also been used [197] [17] but even though they are small and flexible, they have hard edges that cannot seamlessly integrate into clothing. Conductive textile sensors [198] [175] and flexible conductive polymers [19] [150], solve this issue as there are not hard edges when integrated into clothing. Additionally, wireless signals have been used in joint angle analysis. Anderson et al. [6] and Qi et al. [161] used Ultra-Wideband (UWB) radios for mobile gait analysis and to measure joint flexion and extension angles. In TracKnee and ServesUp, we leverage these soft conductive textile sensors to provide insights in the forms of knee

angle monitoring and serve classification.

2.4 Athletics Performance Analysis

Most researchers have attempted to detect human activities from accelerometer data [18, 114, 164, 88, 112, 137, 89, 186], physiological sensor [116, 153, 187], microphone [184], location sensor [202] or other biometric data (e.g., electrocardiogram [156]). These wearable sensors are used for human activity recognition systems [18, 164, 112, 89], in which the sensors are located on a fixed body part. Sport-specific sensing research has also been done mainly using IMMUs. IMMUs have been used for activity recognition in skateboarding [82, 83], snowboarding [81, 97], skiing [84], soccer [169], rugby [105], table tennis [22, 21], basketball [143], and cricket [80]. One such work even targeted multiple sports: soccer and field hockey [139]. Research into volleyball has been focused on injury prevention and distinguishing the professional players from the amateurs. But to date, sensing research in this sport has not been well explored. This can be explained by the speed of the game or the difficulty of becoming familiar with volleyball at a high level. Human activity recognition has been well explored in sports and daily life. In this section, we will explore the research that has been done in sensing in volleyball and other sports and human activity detection with wearable and E-textile sensors.

In volleyball, players can jump upwards of 300 times in a single volleyball match [16]. Since volleyball players execute a high number of jumps, it is common for them to experience overuse injuries [68]. To combat these injuries, Jarning et al. [103] attempted to calculate jump frequency in volleyball players using an accelerometer. To do this, they calculated two metrics: peak vertical acceleration and peak resultant acceleration. They concluded that these measurements were not an applicable method for classifying jumps in volleyball. Vert [195] is a device being used by amateur and professional volleyball players alike to track the number of jumps, average height of jumps, and highest vertical jump. A number of studies have been done to using the Vert device [27, 128, 178, 36] in

which it was determined that the Vert device accurately calculated the number, height, and jump load of volleyball players in controlled, practice, and game situations.

Kautz et al. [106] designed a system that classified ten skills that occur in beach volleyball via wrist-worn acceleration sensors. They began by classifying when the ball made contact with the player's arm that wore the acceleration sensors. From this, they were able to classify their set of skills using a DCNN (Deep Concurrent Neural Network) with an accuracy of 83.2%. In their evaluation, they saw that the lowest classification accuracy was on the block skill. This skill is frequently performed without the contact of a ball and thus was not always classified correctly. While this work, makes a large step forward in classifying many different volleyball skills, they are limited by the necessity of a player contacting a volleyball with the arm in which the acceleration sensors are worn. Many times in this sport, skills are performed without making contact with the volleyball. In our work, ServesUp, is not limited by the player making contact with the volleyball. Cuspinera et al. [48] detected beach volleyball serves and potentially classified four common serve types using two accelerometers mounted on the wrist and hand. Their results show that they were able to classify one type of serve given a single semi-professional player's data. They do not include a comprehensive evaluation of the other three types of serves or data from players below the level of semi-professional. ServesUp also focuses on the volleyball serve but our sensor are soft and flexible and do not impede the athlete while playing volleyball.

2.5 First Aid Skill Monitoring

Smart devices make great tools for providing instructions and feedback for first aid because they are readily available and easy to use. Gruernerbl et al. [86], Elliot et al. [182], and Ahn et al. [1] developed applications for a smartwatch that provided real-time feedback for CPR chest compressions. Their applications were meant to enhance the performance of CPR chest compressions by measuring the frequency and depth of the compressions.

They tested their applications on chest compressions performed on a CPR manikin. They demonstrated that their application not only improves the user’s performance of CPR, but it also increases the user’s potential for performing it. Gruernerbl et al showed that a smartwatch feedback system provided a significant performance improvement on CPR techniques. Ahn et al. showed that CPR related feedback via a smartwatch could provide assistance with respect to the ideal range of chest compression depth, and this can easily be applied to patients with out-of-hospital arrest by rescuers who wear smartwatches. In *BreathEZ* and *BBAid*, we address choking first aid and show that our smartwatch feedback applications improve not only the technique but also the likelihood that the user will perform choking first aid.

Researchers have developed devices to aid in the performance of choking first aid. The first of these devices is outlined in a patent filed by Totman at Zoll Medical Corporation [190] that describes a method to measure abdominal thrusts. In this patent, a handheld device that uses accelerometers to determine the appropriate depth and speed of the abdominal thrusts is described. This device targets first aid training, but they do not have an extensive evaluation of how this device could improve user learning and performance. In contrast, our system provides in-situ instruction and real-time feedback on the quality of each set of abdominal thrusts. The second of these devices is the *Dechoker* [52] which is a commercially available FDA Class I medical device. To use the device, the operator inserts a plastic tube inside the mouth and places the mask on the face. When tested on cadavers, this device did not cause injuries but it also did not remove the foreign object in all cases. It is noted that this device may damage the soft tissues of the mouth, lodge the foreign object deeper in the airway, cause mucosal injury and or negative pressure pulmonary edema [53]. While this device could be helpful in choking emergencies, there is not enough published data to understand the risks.

First aid skill retention is a known problem as many necessary skills are often forgotten shortly after training [92, 60, 129]. Anderson et al. [7] determined how rapidly the trained skills and knowledge decayed. They conducted a large study in which they tested the

choking first aid skills of first responders in an industrial setting. They found that the higher level an individual has been trained at, the less their knowledge and skills decay over time. They also found that during this study choking skills were performed poorly regardless of how long it had been since the participant was trained. To combat the skill and knowledge decay, they recommend shortening the time between training sessions. It is possible that our system can help with skill and knowledge decay. When needed in an emergency situation, BreathEZ and BBAid can refresh user knowledge and help improve the quality of the skill being performed. From this study [64], we see that bystander first aid performance can be greatly improved when audio instructions are given through a personal digital assistant (PDA). Their results show that the first group performed significantly better than the second when giving emergency care. Similarly, in our research work, we provide emergency care instruction but we take it a step further and provide live feedback to the user on their performance of that care as well. Deploying our BreathEZ and BBAid applications on a smartwatch instead of a handheld mobile device also allows for hands-free use by the user.

Chapter 3

Magneto: Joint Motion Analysis Using an Electromagnet-Based Sensing Method

3.1 Introduction

Joint angle analysis has been a major research focus in the field of body motion tracking and modeling because knowledge of joint angles can be used for preventing injuries, decreasing rehabilitation time after injury, and accurate activity monitoring. Wearable sensors are commonly used for monitoring body motion and joint angles due to the advantages provided by direct bodily contact. These sensors are often used to monitor patient adherence to rehabilitation programs and assess patient recovery progress both inside and outside of a medical facility. Any proposed sensor for joint monitoring must be unobtrusive, accurate, and capable of accurately monitoring dynamic, fast-paced motions in order to have effective healthcare applications.

Magnetic field sensors are affordable, low power sensors that are incorporated into many of the devices we use today including smartphones, smartwatches, and smart home devices. They allow large scale sensing of the Earth’s magnetic field, magnetic anomalies, orientation, and distance. They can also be combined with magnets to allow smaller scale sensing, and have even been incorporated into wearable devices to track joint angles [162], body motions [99], and gestures [127]. A drawback of these sensors is that they fall victim to magnetic interference from the Earth’s magnetic field, the environment, and nearby ferrous objects. Approaches used to protect a sensor from this magnetic interference include but are not limited to: using a hardware shield, using a magnet that is strong enough to eclipse all other fields, or using multiple magnetic sensors. In this work, we address this drawback to improve upon joint angle tracking using this sensor.

In this chapter, we address the following research questions:

RQ1: How can we eliminate environmental interference from a magnetic field reading?

RQ2: How can we localize an electromagnet given a purified magnetic field reading?

RQ3: How do we use electromagnet localization to determine joint motion?

To answer our first research question, we developed a method to remove environmental interference. First, we designed a small electromagnet that could produce a strong electromagnetic field. Then, we cycled the electromagnet between on and off states, and recorded the magnetic field strength in both states via a magnetometer. While the reading in both states have environmental interference, the on state reading has the environment with the magnetic field from the electromagnet, the off state reading only has just the environment. Comparing these two readings removes environmental interference, and provides a purified magnetic field reading of the electromagnet.

To answer our second research question, we localized the electromagnet given the purified magnetic field reading. For any purified reading, there is a set of location and orientation pairs that represent the possible locations of the electromagnet. To calculate

these, we first discuss the relationship between the magnetometer reading and the orientation of the magnet. Then, we explain how to calculate a single location and orientation pair for the electromagnet. Finally, we discuss the entirety of the set of location and orientation pairs for the electromagnet.

To answer our third research question, we conducted two pilot studies on human joint angles and explored other applications in which Magneto can be used. First, we conducted a user study consisting of 13 participants in which we examined 12 different elbow angles for a total data set of 650 measured angles. We processed the data and calculated the angles using a triangular representation and polynomial regression model. Second, we modeled shoulder motion and applied Magneto to calculate three dimensional shoulder positions. Finally, we discussed further applications for which Magneto can be used.

Research has been done into using magnets to measure body motion [162, 99, 126, 127, 148]. While these works have successfully measured body motion, they did not account for the influence of environmental interference. This suggests that any change in the magnetic field reading would be interpreted as a change in body motion. With Magneto, we are able to remove the environmental interference and purify the electromagnetic signal so that any change in the magnetic field reading results from a change in the localization of the electromagnet. Additionally, magnetic field sensors have been used to sense motion in a environment [25, 146, 131]. These sensors use the magnetic field of the Earth as a reference point and are also susceptible to electromagnetic interference from nearby ferrous objects. Magneto is also able to remove electromagnetic interference produced by such objects.

Our contributions are summarized as follows:

1. We developed a method that removes environmental interference from a magnetic field reading. We evaluated this method to show its performance when removing the interference in three movement dimensions, in six environments, and with six different cycling rates.

2. We designed an algorithm that allows us to localize a magnet with respect to a magnetic field reader. Our algorithm calculated orientation of the magnet with an average error of 3.43° and distance from the reader to the magnet with an average error of 2.34%.
3. We conducted two pilot studies to evaluate Magneto: elbow angles and shoulder position. We conducted a user study where we recorded 650 elbow angles from 13 participants in which we examined 12 different elbow angles for a total data set of 650 angles. Overall, our method saw an accuracy of 93.82% when classifying elbow angles to the nearest 15° angle and an average error of 2.52° . We modelled the motion of the shoulder in two and three dimensional space. We calculated the correct shoulder position (within 2.5 millimeters) in 96.87% of test cases in two dimensional space and in 75.79% of test cases in three dimensional space.

The remainder of this chapter is structured as follows: First, we introduce our Magneto Hardware Design by explaining the components the construction of our electromagnet. Second, we describe the method that we used to eliminate environmental interference. Third, we explain the process that we use to localize the electromagnet with respect to our magnetic field reader. Fourth, we describe the application scenarios that Magneto can be used in and conduct two pilot studies. Finally, we discuss our Future Work and we wrap up with our Conclusion.

3.2 Magneto Hardware Design

We designed our circuit for Magneto with two goals in mind. First, the device should be small so that it can be used in many different scenarios including as an on-body wearable. Second, the device should be capable of creating a strong and stable magnetic field so that it can be measures at a distance. To accomplish these two goals we created the circuit shown in Figure [3.1](#) with the following components:

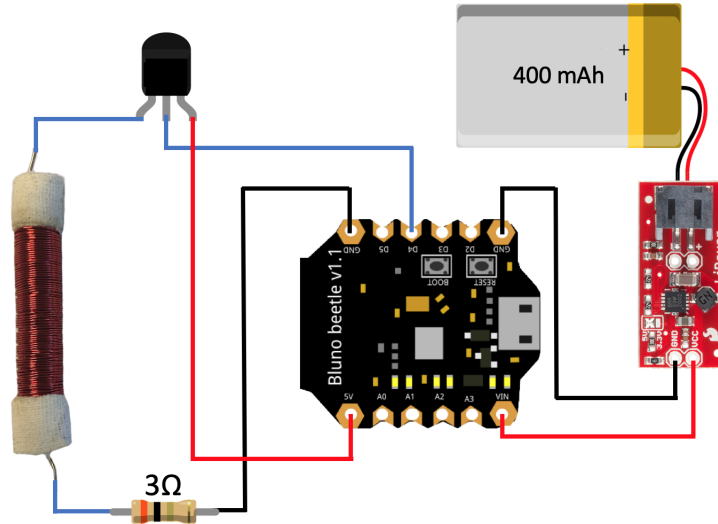


Figure 3.1: Circuit Diagram for Magneto

Electromagnet: We built our own electromagnet as the commercially available ones were large and weak. To build this electromagnet, we used the core of a 3.5 cm ferrite RF choke [163] and 28 gauge magnet wire [166]. Ferrite cores provide electromagnets with an increase in magnetic field strength, and our magnet wire has a very thin insulation coating allowing us to wrap the wire around the RF choke more times in a smaller area. This makes our electromagnet stronger while preserving the small surface area. To build our electromagnet, we wound the magnet wire around the RF choke for many turns; a "turn" is defined as one full wrap of magnet wire around the core. Our resulting electromagnet shown in Figure 3.1 has three layers where the first, second, and third layers have 74, 72, and 70 turns, respectively. The resulting electromagnet has 216 total turns and a measured resistance of 1.3 ohms. In Section 4, we explain how we use these values to calculate the strength of our electromagnet.

Microcontroller and Bluetooth Chip: To control our circuit, we chose the Bluno Beetle [24]. This device is currently the smallest bluetooth enabled Arduino on the market. This allows us to save space while providing all of the functionality that we need for our circuit. It outputs five volts which is important for the strength of the magnetic field of our

electromagnet. This chip uses an ATmega328P processor and a CC2540 Bluetooth chip.

Power Supply: Our electromagnet requires at least a 5 volt power supply to create a magnetic field strong enough to be read by our magnetometer. The Bluno Beetle requires 5 to 8 volts to function properly. We used a 400mAh lithium ion battery that only outputs 3.7 volts. To boost the 3.7 volts to 5 volts, we used a LiPower Boost Converter [181].

Resistor: We tailored the resistance in our circuit to accomplish two goals: protect the Bluno microcontroller and prevent battery drain. We used a resistance of 3 ohms combined with our electromagnet at 1.3 ohms. This gives us a total of 4.3 ohms. We then measured our current to be .317 Amps which is tolerable for the Bluno microcontroller. On a single charge, our battery would last for approximately one hour.

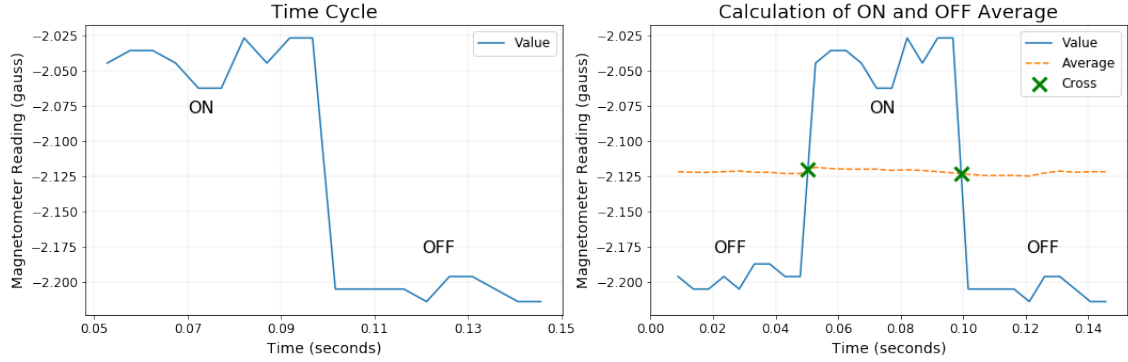
Transistor: We use a transistor as a switch in our circuit. This facilitates our ability to turn the electromagnet on and off at a specified rate while still powering the electromagnet from the 5 volts. We could not use a digital pin from the Bluno as these output 3.3 volts.

These components are connected via wires and solder as shown in Figure 3.1. The device is then put into small and flexible fabric pouch so that the wires are protected and the electromagnet's signal is not restricted. This allows for an unobstructed magnetic field which will provide for a high quality reading as shown in the later sections of this chapter.

3.3 Elimination of Environmental Interference

A problem with using a magnet and magnetometer combination as a sensor is the susceptibility to outside magnetic fields [37]. These magnetic fields include but are not limited to the magnetic field of the earth [95], ferrous metal objects [120], and other magnetized objects. These extraneous magnetic fields create a noisy signal that can make it hard to distinguish the movement of a magnet from the change in surrounding magnetic fields. To deal with this problem, we propose a method to eliminate the surrounding environment's magnetic field from the reading of the magnet. First, we will explain our time cycle and cycling rate. Then, we will discuss the method we use to remove the

magnetic field of the environment.



(a) Time Cycle of the Electromagnet

(b) Average Calculation

Figure 3.2: Calculation of Time Cycle Features

Our signal is characterized by two states: ON and OFF. When the electromagnet is ON, we read the combination of the magnetic field of the electromagnet and the magnetic field of the surrounding environment. When the electromagnet is OFF, we only read the magnetic field of the surrounding environment. These states are shown in Figure [3.2a](#). Next, we define a time cycle, t_{cycle} , that is the total time of a single ON state followed by a single OFF state, as shown in Figure [3.2a](#). The total time spent in the ON state equal to the total time spent in the OFF state within each t_{cycle} . Then, we define the electromagnet’s cycling rate to be the number of t_{cycle} per second.

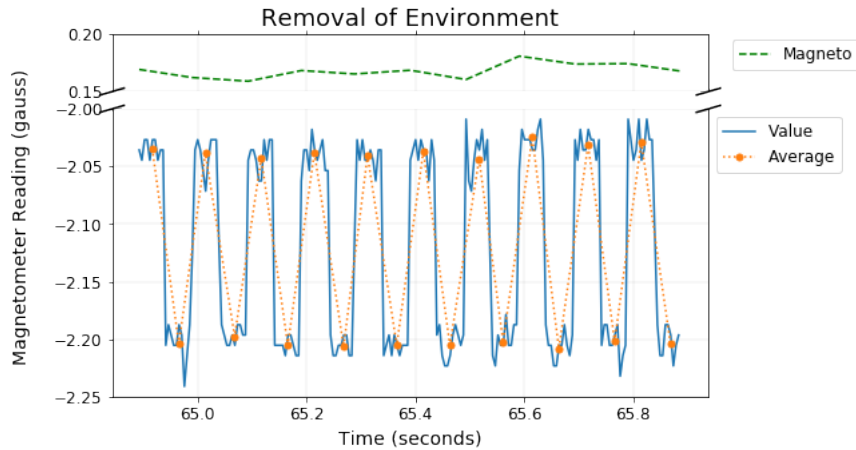


Figure 3.3: Averages and Environmental Noise Removal

Then for every ON and OFF state there is a beginning and end. To find these points, we calculate an average line as shown in Figure 3.2b. This average consists of the data points in one time cycle. These data points are consecutive and evenly surround our targeted average value. Next, we mark each time the magnetometer reading crosses the average. The crosses are shown in Figure 3.2b. Then, we label the point before the cross to be an end and the point after the cross to be a beginning. If the point is less than the value of cross, we mark it as OFF. If the point is greater than the value of the cross, we mark it as ON. Once, we have the beginning and end to each ON and OFF state, we calculate the average to be our reading for that state. This is shown in Figure 3.3

Then we proceed to eliminate the environmental reading from our signal. To do this we take the average of the two OFF states that surround an ON state and subtract that from the ON state. We will call this calculation M . It is shown in Figure 3.3. This is done for all three axes: x, y, and z. In some cases, the magnetic field shows up in only one or two of the axes. In these cases, we use the signal where the on and off switches are visible to set the ON and OFF starts and ends for the other axes.

3.3.1 Evaluation

We evaluate Magneto’s ability to remove the environmental magnetic field readings by testing the following dimensions: orientation, movement, magnetic field interference, and multiple environments. For these experiments, we set the electromagnet’s cycling rate to 10Hz. We attached the electromagnet and the magnetometer to a board with eight centimeters between them as this is within the range of magnetic field of our electromagnet. This ensures that the distance and orientation of the electromagnet and magnetometer are constant with respect to each other, so any changes in readings must come from the manipulation of the board. So, any reading that the magnetometer picks up should be filtered out by our environmental elimination algorithm.

Orientation Experiment: Each direction a magnetometer faces causes a different reading. This is because the magnetometer reads the static but directional magnetic field

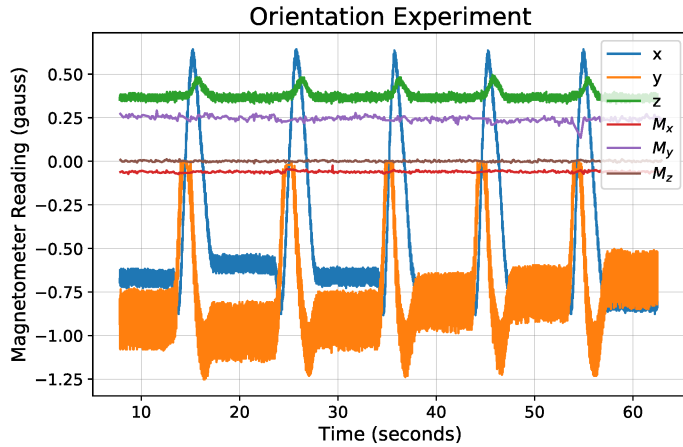


Figure 3.4: Orientation Experiment

of the earth. To test this dimension, we placed the board containing the electromagnet and magnetometer on an office chair. Then, we spun the office chair 360° . A single spin takes about five seconds to complete and we stop the chair between spins. We repeated this experiment five times and the results are shown in Figure 3.4. As you can see in this figure, the magnetometer reads the spin of the chair. Since our electromagnet is not moving in respect to the magnetometer, we can effectively remove the spin read by the magnetometer. This is shown by the M_x , M_y , and M_z readings that are all relatively flat, showing no motion.

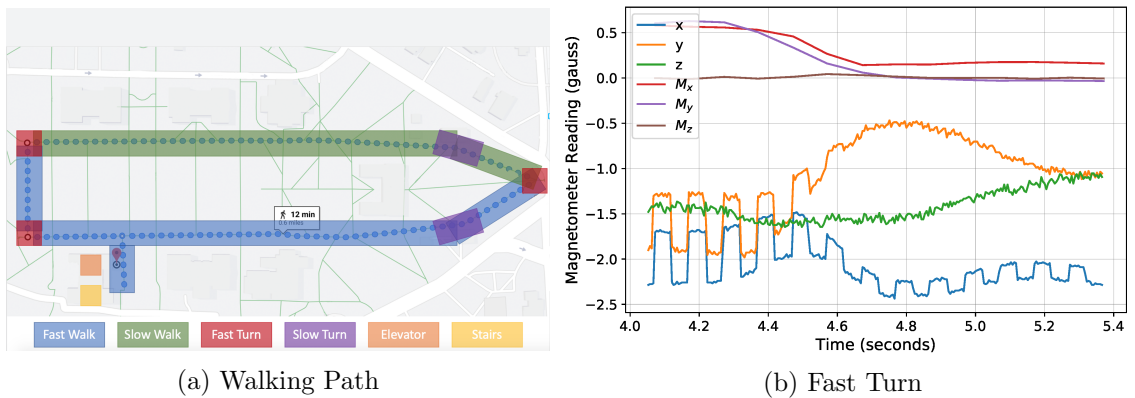


Figure 3.5: Movement Experiment

Movement Experiment: First, we tested how our sensor would react if it was facing dif-

ferent direction in a single environment. Next, it is important to move the sensor around in an environment. In this experiment, we vary the vertical and horizontal locations of the magnet in an environment. We also vary the speed at which we move through the environment. To test this dimension, we took our sensor attached to the board on a walk outside. The path we took is shown in Figure 3.5a. We did this twice: once counter-clockwise and once clockwise. Overall, it took approximately 25 minutes to complete both loops. On this walk, we completed several tasks: fast walk, slow walk, fast turn, slow turn, elevator, and stairs. We tested horizontal location and varying speeds with the fast walk, slow walk, fast turn and slow turn. The fast walk averaged 5.6 miles per hour and the slow walk averaged 3.4 miles per hour. We define a fast turn to be a sharp turn lasting approximately two seconds while the slow turn was more gradual and occurred over nearly 20 seconds. We varied vertical locations and speeds by walking up stairs and riding in an elevator.

Out of all of these tasks, we only saw a change in our Magneto reading during a fast turn. During these turns saw a slope in the reading of on and off state of the time cycle as shown in Figure 3.5b. In the following sections, we see that increasing the cycling rate will solve this problem. When more samples are taking the slope through the on and off states will diminish so the reading can be more accurate. We also saw that the periodic motions associated with walking were removed since they did not cause a motion between our electromagnet and magnetometer. In all of the other tasks, we saw no change in our Magneto reading once the environment was removed.

Magnetic Interference Experiment: Magnetic interference is a common problem that effects magnetometers. This interference causes the readings of the magnetometer to be inconsistent and inaccurate. Most interference is caused by iron present in the surrounding environment as it is a metal that can be magnetized. This interference can range from small static magnetic fields to distortions in the Earth's magnetic field. These distortions can warp the magnetic field in that area. This means that as a magnetometer moves through this field, we will read changes with our magnetometer. Because of this, the

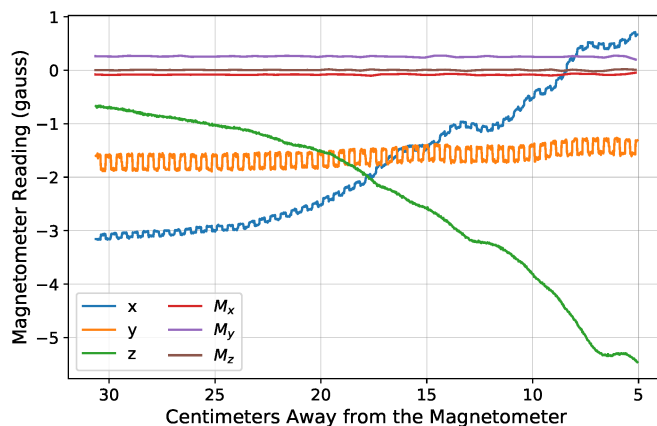


Figure 3.6: Magnetic Interference Experiment

distortion cannot be removed with a single calibration.

To test the removal of these distortions, we introduce a strong outside magnetic field to our sensor. For this, we introduced a stack of neodymium magnets. Neodymium magnets [110] are the strongest permanent magnets and are made from rare earth elements. We start these magnets 30 cm away from the magnetometer. We then move these magnets towards the magnetometer. The magnetometer reading is much larger than in the previous experiment due to the neodymium magnets. Inside of 5 cm the magnetometer saturates and it outputs error values. Even with the stronger magnetic field, we still see the on and off cycle of our electromagnet. This allows us to remove the reading of this magnet. We show this by the M_x , M_y , and M_z readings in Figure 3.6. These readings are comparable to what we see when there are not strong magnetic interferences. This shows that our device continues to function for its intended purpose even in the presence of strong and varied electromagnetic fields.

Multiple Environments: To ensure that our sensor could work in multiple types of environments, in the experiments above, we chose a different locations. The orientation experiment was completed in our research lab. Our lab is next to the geology lab which produces a strong and static magnetic field. Our magnetometer reads the direction of the lab as North when it is in fact Southeast. There is also a higher reading in our lab than

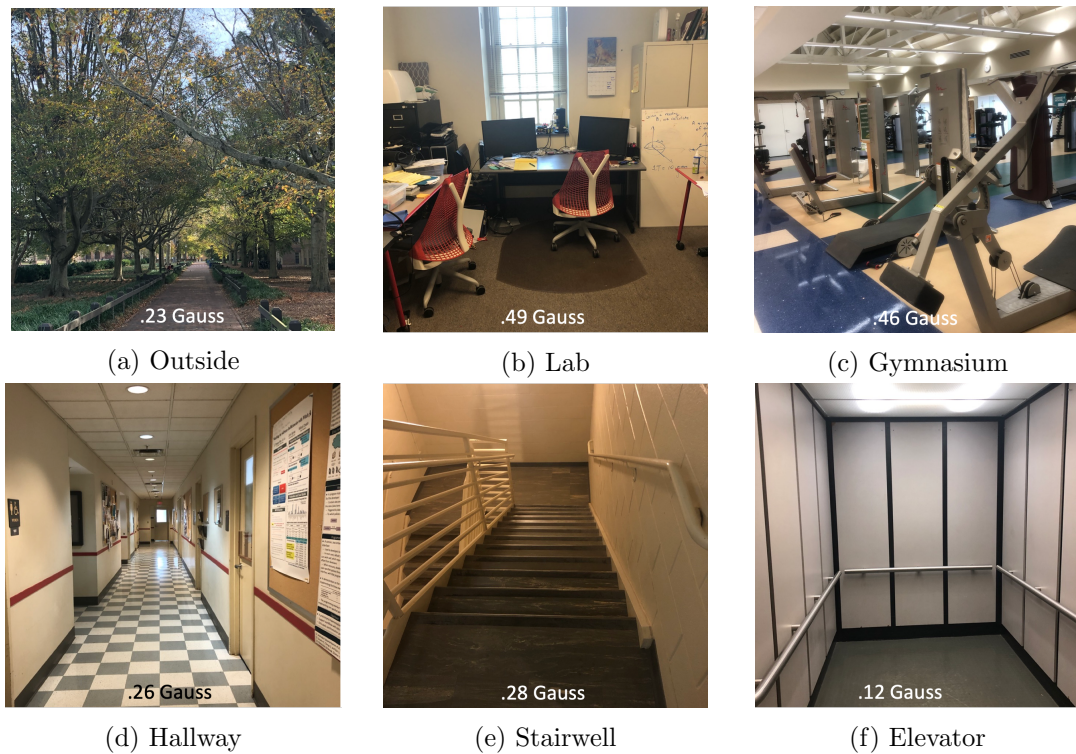


Figure 3.7: Environments Tested

what is expected from the Earth's magnetic field. We completed our movement experiment outside, in the elevator and in the stairwell and the Magnetic Interference experiment inside of a gymnasium. The gymnasium provides a large amount of environmental interference as many of the objects contained in a gym are made from ferrous materials. For example, many free weights are made from iron. These environments as well as their Gauss readings are shown in Figure 3.7. We noticed no difference in the final reading among all of the environments even though each environment had a different static magnetic field.

Cycling Rate: In the experiments above, we used a cycling rate of 10 Hz. This is due to the fact that it is very clear to see the ON and OFF states with the human eye when we graphed our readings. To use our device in high speed dynamic movements we must increase the cycling rate to get a clean reading on the movement. We tested the following cycling rates: 10 Hz, 20 Hz, 30 Hz, 40 Hz, 50 Hz, 100 Hz. We only tested up to a 100 Hz cycling rate as our magnetometer samples at 220 Hz and that gave us approximately one

Cycling Rate	Mean	Std Dev
10 Hz	0.0000	0.0121
20 Hz	0.0056	0.0157
30 HZ	0.0081	0.0183
40 HZ	0.0109	0.0211
50 HZ	0.0149	0.0372
100 HZ	0.0167	0.0533

Table 3.1: Cycling Rate Analysis

sample in each On and Off state. To understand if there is a degradation in the quality of our reading we did two studies. First, we compared the calculation of the means of the On and Off states using different cycling rates. Second, we looked at standard deviation in the raw signal in the On and Off states using different cycling rates.

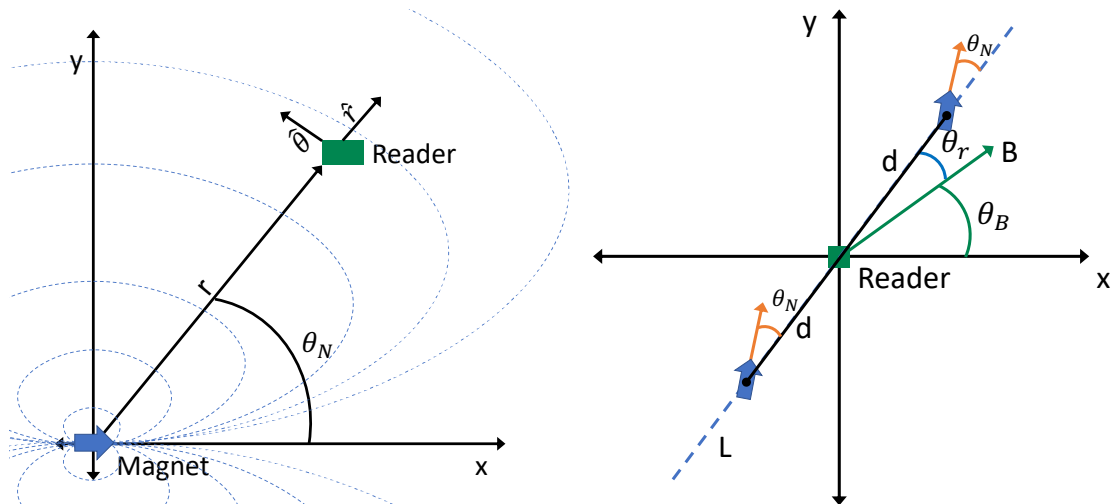
To compare the calculation of the means of the On and Off states using different cycling rates, we recorded 100 time cycles at 10 Hz. We then calculated the means of the On and Off periods using the number of expected data points in faster cycling rates. Then, we calculated the difference from the original mean. We show the average of the differences in the mean for all 100 time cycles in Table 3.1. As you can see, there is a small but steady degradation in the signal as the cycling rate increases. Next, we ensured that a faster cycling rate did not affect edges of the On and Off states. To do this, we calculated the standard deviation in the raw signal in the On and Off states using different cycling rates. We recorded 100 cycles at each cycling rate. We show the results of this in Table, 3.1. We saw that the standard deviation steadily increased as the cycling rate increased. With further analysis into this data, we saw spikes in the beginning of the On and Off states. We will discuss techniques to remove these spikes and to further increase the cycling rates in the Future Work Section.

3.4 Localization of the Electromagnet

For any reading recorded by the magnetometer, there is a set of location and orientation pairs for the electromagnet. To calculate these, we first discuss the relationship between the reading and the orientation. Then, we explain how to calculate a single location and orientation pair of the electromagnet. Finally, we discuss the entirety of the set of location and orientation pairs for the electromagnet.

3.4.1 Magnetic Field

Magnets are described as dipoles, with one end of a magnet being a north pole and the other being a south pole. The opposite poles attract one another, and identical poles repel each other. Electromagnets are magnets with adjustable strength that can be turned on and off. A two dimensional representation of the magnetic field surrounding our magnet is shown by the dotted blue lines in Figure 3.8a. The three dimensional representation would show this same magnetic field rotated around the magnet. This means that rotating the magnet would not change the magnetic field reading.



(a) Magnetic Field from the Perspective of the Magnet (b) Magnet Position from the Perspective of the Reader

Figure 3.8: The Relationship Between the Magnet and the Reader

Magnetic fields around a magnet can be modeled given a magnet's strength with the assumption that a magnet is a perfect dipole. For any location around a magnet, we will read a magnetic field (B) that will reflect the distance (r) and angle (θ_N) from the north pole of the magnet. We show this in Figure 3.8a. Since magnetic fields depend heavily on the angle θ_N , we will use polar coordinates to describe the magnetic field reading. We will represent the direction from the magnet to the reader as \hat{r} and the direction perpendicular to that as $\hat{\theta}$ [49]. So, given a distance (r) and angle (θ_N), we can calculate the magnetic field (B) at the location (r, θ_N). $\frac{\mu_0|m|}{4\pi}$ is a constant that depends on the materials and construction of the electromagnet. We can represent this with the following polar equation:

$$B(r, \theta_N) = \frac{\mu_0|m|}{4\pi r^3} \left(2 \cos \theta_N \hat{r} + \sin \theta_N \hat{\theta} \right) \quad (3.1)$$

The description of the variables used in Equation 3.1 are shown in the following Table:

Variable	Definition
B	Magnetic field strength at the center of the core in Teslas
r	Distance from the reader to the magnet
θ_N	Angle of the north of the magnet
μ_0	Constant of magnetic permeability of free space: $4\pi * 10^{-7}$
$ m $	Magnetic moment: current * area of a single turn * number of turns
\hat{r}	Direction from the magnet to the reader
$\hat{\theta}$	Direction perpendicular to \hat{r}

Table 3.2: Equation 3.1 Variable Definitions

For our purposes, we are given a magnetic field reading and want to calculate the distance (r) and orientation (θ_N) of the magnet. We will explain these calculations with the aid of Figure 3.8b. First, we put the reader at the origin of the coordinate system of the reader. The reader reads a vector, B . Given this reading, we can calculate θ_B which is the angle between vector B and the x axis. Then we assume the electromagnet is somewhere on a line that goes through the origin. This is represented by line L in Figure 3.8b. θ_r will be the angle between line L and vector B which can be calculated by finding

the angle between two vectors. Since we know that θ_r is the angle between B and \hat{r} in Figure 3.8a we can calculate the direction of the electromagnet's north with the following equation:

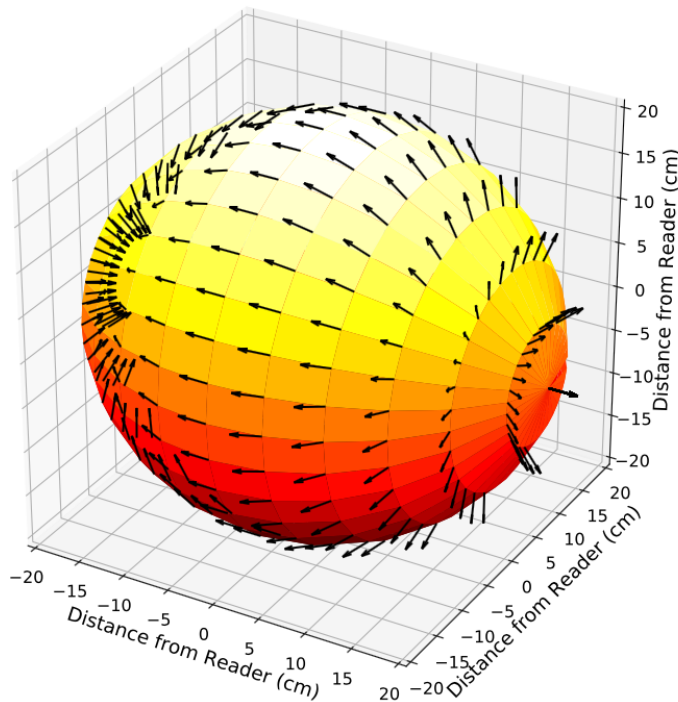


Figure 3.9: Ellipsoid of Location and Orientation Pairs

$$\theta_N = \arctan(2\tan\theta_r) \quad (3.2)$$

θ_N is the north for a magnet located anywhere on line l . Now that we know θ_N , we calculate the electromagnet's north with respect to the x axis. This will be represented by θ_X , where

$$\theta_X = \theta_N + \theta_r + \theta_B \quad (3.3)$$

Then, we calculate the distance (r), via a derivation of Equation 3.1

$$r = \sqrt[3]{\frac{\mu_0|m|}{4\pi|B|}(4\cos^2\theta_N + \sin^2\theta_N)^{\frac{1}{2}}} \quad (3.4)$$

This gives us the distance away from the origin on line L where the magnet is located. So, our magnet can be located in two locations denoted by the points on line L as shown in Figure 3.8b. Then we repeat this for every possible line through the origin. This will give us a set of location and orientation pairs around the reader in the shape of an ellipsoid as shown in Figure 3.9. In this example, we show the ellipsoid given by magnetic field pointed in the positive x direction on the same coordinate system as the reader. We will discuss how to use this in the Application Scenarios Section.


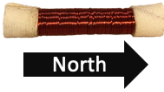
$-0.5\text{ cm}, 10\text{ cm}$ $\theta_N = 92.9^\circ$ $r = 10.0\text{ cm}$	$4.5\text{ cm}, 10\text{ cm}$ $\theta_N = 65.8^\circ$ $r = 11.0\text{ cm}$	$9.5\text{ cm}, 10\text{ cm}$ $\theta_N = 46.5^\circ$ $r = 13.8\text{ cm}$
$-0.5\text{ cm}, 5\text{ cm}$ $\theta_N = 95.7^\circ$ $r = 5.0\text{ cm}$	 $4.5\text{ cm}, 5\text{ cm}$ $\theta_N = 48.0^\circ$ $r = 6.7\text{ cm}$	$9.5\text{ cm}, 5\text{ cm}$ $\theta_N = 27.8^\circ$ $r = 10.7\text{ cm}$
		$9.5\text{ cm}, 0\text{ cm}$ $\theta_N = 0^\circ$ $r = 5.4\text{ cm}$

Figure 3.10: Experimental Setup

3.4.2 Evaluation

We calculated two variables to localize our electromagnet with respect to a magnetometer: distance and orientation. In this evaluation, we will evaluate the accuracy of the calculation of these variables. We setup our experiment with the magnet and the magnetometer in a grid, as shown in Figure 3.10. We left the electromagnet in a single location since the Shimmer Sensor is easier to move since it is housed in a case. This setup is in the same pattern as Figure 3.8a where the reader moves around the electromagnet. To perform this experiment, we created a grid in 5 cm by 5 cm blocks as shown in Figure

3.10 The distance measurements are offset in the x axis by a half centimeter as the magnetometer location in the Shimmer Sensor is not directly in the center of the device. We move the Shimmer Sensor to the center of each box for 30 seconds. We then randomly selected ten individual samples from each 30 seconds for analysis. We also record the ground truth values for our distance and orientation for that reading. These ground truth values are shown in each box in Figure **3.10**. We do not test the other three quadrants around the magnet in this experiment as the distance calculations reflect over the x and y axis and the angles reflect over the x.

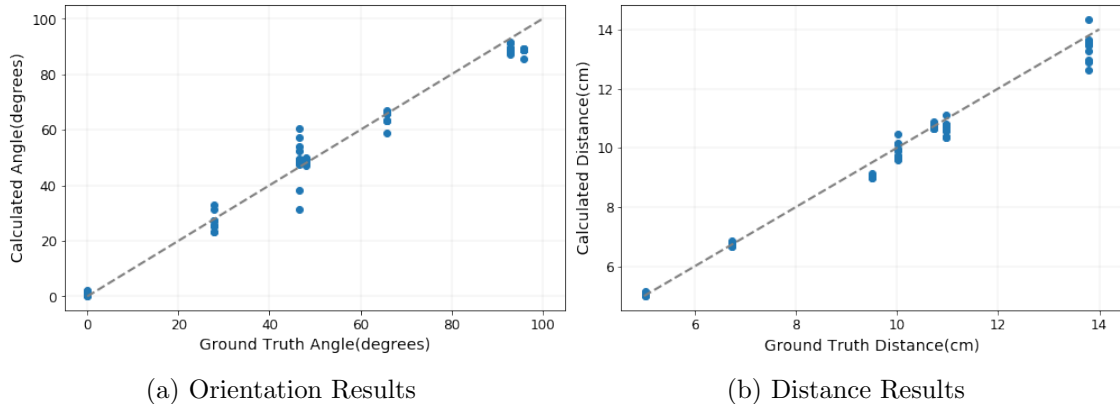


Figure 3.11: Distance and Orientation Results

In this experiment, we process the data by removing the environment and the calculating the distance and orientation. As before, this gives us a set of data points in the shape of an ellipsoid. When we compare our calculated distance and orientation to our actual values, we assume we know the the line L that the magnet is on. This comparison provides allows us to evaluate the accuracy of the set of distance and orientation pairs in the ellipsoid. Due to the limitations of our sensor, if we do not know how the electromagnet and reader move in relations to each other, then we do not know the actual location of the sensor. But for these instances, we do have a range of distances for which the electromagnet can be located in. First, we evaluated the calculation of the orientation of the electromagnet. Overall, we have an average error per orientation calculation of 3.43° with a standard deviation of 3.28° . We further evaluate this with the use of Figure **3.11a**.

The orientations with the biggest difference in calculated value are the positions at which the magnetometer is the furthest away from the electromagnet. Second, we examined the distance between the electromagnet and the reader. We calculated the relative error of the distance to be 2.34% with a standard deviation of 2.03%. As we can see in Figure 3.11b, the distance calculations are more accurate the closer the magnetometer is to the magnet. This means that the stronger our electromagnet, the more accurate our distance and orientation calculations will be at a distance. We will discuss ways to increase the strength of our electromagnet in the Future Work Section.

3.5 Application Scenarios

Magneto can be used in many different application scenarios. The key metrics that we compute are distance and orientation of the magnet, but to fully localize the magnet, we must know how the magnet and reader move in respect to one another. This setup lends itself to body motion application scenarios as we can set up our magnet and magnetometer equidistant from a joint. Then, because we know the biomechanics of the joint, we can calculate the exact localization of the magnet. This will allow us to monitor, joint angles, speed of motion and even gestures.

In situations where there is not a central joint, we can still localize the magnet if there is a restricted range of motion between the magnet and the reader. For example, over the life time of a spring, it will stretch out until it is no longer useful. Magneto can be used to determine the length of the spring as its length would change over time. This would also hold true for strain sensors since in general these sensors stretch out. Magneto could be used to sense the distance changed as the item wears out. Something of note is that while our magnet or reader would need to be on the device, nothing would need to physically connect them. So there would be free space so the Magneto would not interfere with mechanisms of the device being measured.

To demonstrate how Magneto can be used in application scenarios, we conducted two

pilot studies: elbow angles and shoulder position. Elbow angles occur in one degree of motion while shoulder position occurs in three. First, we evaluated our calculation of elbow angles in a user study with thirteen participants. Second, we examined the movement of the shoulder and Magneto’s ability to calculate its position.

3.5.1 Elbow Angle Pilot Study

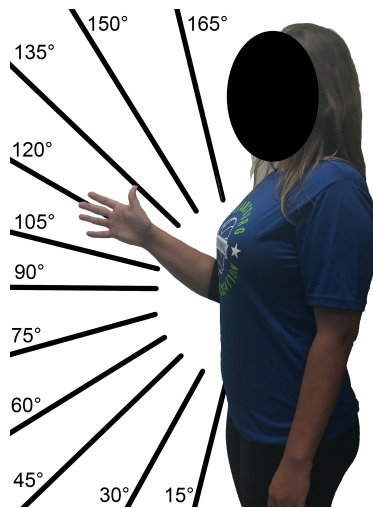


Figure 3.12: Elbow User Study Setup

We evaluated Magneto in an on-body scenario: elbow angles. In this scenario, we calculated elbow angles from the distance between the electromagnet and the magnetometer. First, we will describe the equipment that we use. Second, we will detail the parameters of our study and the demographics of our participants. Then we will explain the process used to calculate elbow angles from a magnetometer reading. Finally, we will evaluate our elbow angle calculation results.

Equipment: To perform our user study, we collected data on participants’ elbow angles. To do this, we collected magnetometer data that was influenced by our electromagnet’s signal and ground truth angles. We used a Shimmer Sensor’s [33](#) magnetometer in conjunction with their data collection application to record data. This application was run on a Google Pixel 3 smartphone connected to the Shimmer Sensor via Bluetooth. We used a

Medigauge digital goniometer [133], which is commonly used to measure joint angles and is accurate to the nearest 0.5° , to measure our ground truth angles. We marked these angles on a poster board to simplify the data recording process as shown in Figure 3.12. This means that our participants only needed to touch the line on the board for each angle instead of measuring each angle individually.

Parameters: When a participant arrived, we asked them to fill out a questionnaire. In this questionnaire, we asked for the following statistics: age, gender, height, weight, and for any details of past elbow injuries or surgeries. Then we asked the participants to put on an elbow sleeve that contains our device and a Shimmer Sensor as shown in Figure 3.12. We positioned the sleeve so that the electromagnet is five centimeters below the elbow crease and the Shimmer Sensor is five centimeters above. The magnet is positioned lengthwise on the arm and the north is pointing towards the hand. Then, we positioned the participant in front of the poster board with marked angles as shown in Figure 3.12. We asked the participant to touch each of the marks with the outside of their hand for five seconds. They repeated this five times on that arm and then did the same on the other arm. The normal range of motion for an elbow is 0° at full extension and 130° at full flexion [100]. We measured angles at 15° increments within the normal range of motion.

Demographics: In this study, we had seven female and six male participants for a total of 13 participants. On average, the participants were 22.5 years of age with an age range of 18 to 33 years. All participants were in the range of normal for their body mass index (BMI). Everyone who participated in the study was free of elbow surgeries or recent injuries.

Elbow Angle Calculation: Next, we processed the data to calculate an elbow angle, θ . We started with raw magnetometer values. First, we removed the environmental signal by using the method in Subsection 3.3 as shown in Figure 3.14a. Then, we averaged the data for the five seconds that the participants held each elbow angle so that we had one reading per angle. Next, we calculated ellipsoid of distance and orientation pairs between the electromagnet and the magnetometer by using the approach outlined in Subsection

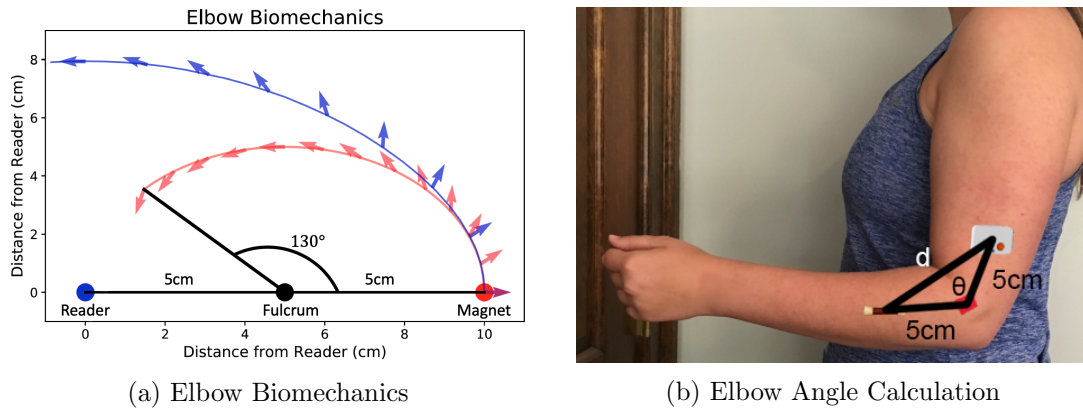


Figure 3.13: Elbow Angles

3.4. To reduce the possible outcomes we leverage the biomechanics of the elbow. We limited the elbow to a single degree of motion. This means that the elbow will move within a single plane. So we show the single plane from the ellipsoid in Figure 3.13a as the blue arc with arrows. As the elbow bends, the electromagnet will move through the distance and orientation pairs shown by the red arc and arrows in Figure 3.13a. In this Figure, the arrows represent the orientation of the north of the electromagnet and the arcs represents the strength of the magnetic field at that location. To calculate the exact orientation and direction of the magnet, we look to see where the red and blue arcs and arrows are identical. This gives us our location of the magnet. In our figure, this is shown by the purple arrow coming from the magnet.

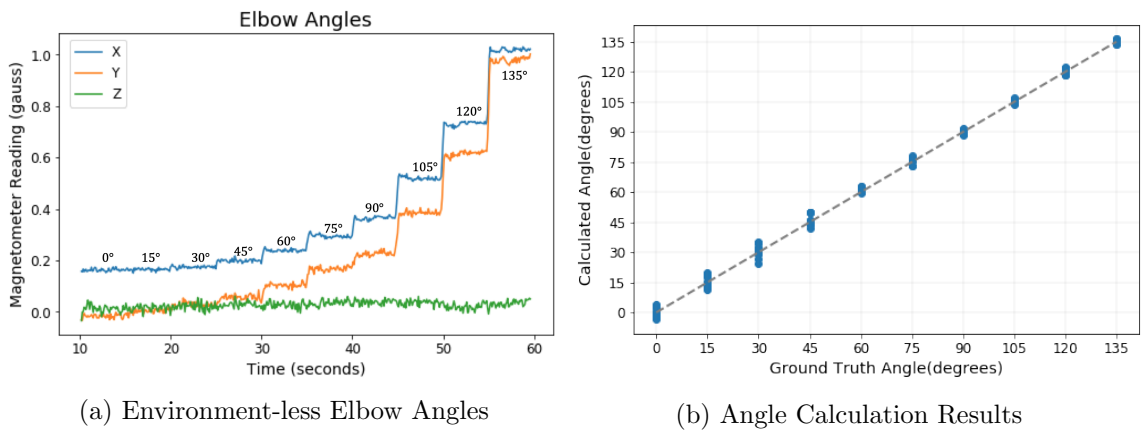


Figure 3.14: Elbow Angles Results

Next, we calculated the distance from the magnet to the magnetometer in the method that we described in Section 3.2. From this distance, we calculated the elbow angle using the law of cosines on a triangle. We know the distance between the magnetometer and the elbow crease; and the electromagnet and the elbow crease as we set these to five centimeters on each side of the elbow crease. Since we know all three sides of the triangle, we can calculate angle theta.

Results: We evaluated our elbow angle calculations on the 650 angles that we collected in our user study. Overall, we saw a 93.82% accuracy when classifying elbows to the nearest 15° and an average error of 2.52°. We show our results in Figure 3.14b. In this figure, we see that our angle calculations are much more accurate at the higher angles and that the first three angles have a much lower accuracy. To understand why, we look to Figure 3.13b and see that there is not much difference in the readings for angle 0°, 15°, and 30°. This is due to the fact that biomechanically there is more change in distance at the in the larger angles. If we remove these three angles from our overall accuracy, we see a 97.07% accuracy and an average error of 1.95°.

3.5.2 Shoulder Position Pilot Study

In our Elbow Angle Application Scenario, we worked with one degree of motion. Now, we will apply Magneto to the shoulder as it is the most mobile joint on the body. When dealing with shoulder position, we work with three degrees of motion. This makes this shoulder position more difficult to determine. First, we will model the range of motion of the shoulder. Second, we will combine that with the magnetometer's position and the magnetic field produced by the magnet on the shoulder. This allows us to localize the magnet to identify the position of the shoulder joint. Finally, we will evaluate our calculations.

Shoulder Motion: In Figure 3.15 we show the three degrees of motion that we will examine. First, the arm can move side to side as shown in Figure 3.15a. We will define this as Yaw. Second, the arm can be raised and lowered, as shown by Figure 3.15b. We

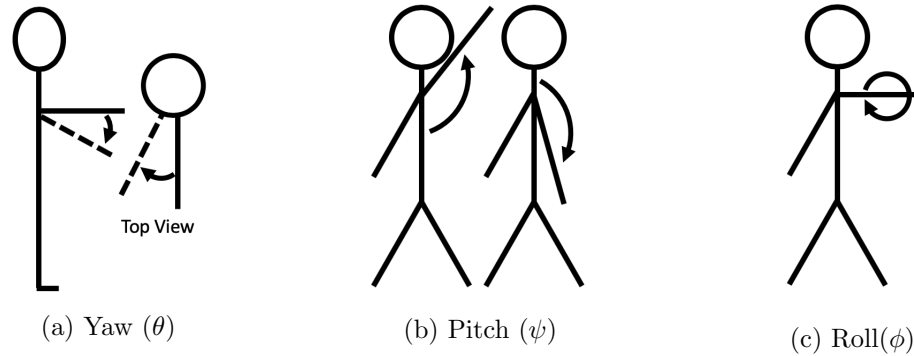


Figure 3.15: Shoulder Movements

will define this as pitch. Finally, the arm can twist, as shown in Figure 3.15c. We will define this as roll. All three degrees of motion can be combined, for example an arm can roll backwards, move forwards, and be raised all at the same time.

Next, we will place the magnet and reader on the shoulder. We will define the origin as the center of the rotator cuff, so that when the arm moves, the origin is the center of rotation in the shoulder. A person will face in the positive Y direction. The Z axis will be the vertical. The X axis will run in parallel with the shoulders with the positive x direction being away from the shoulder. This is shown in Figure 3.16. We will place the magnet on the humerus, right below the deltoid, and define the position of the magnet as m with m' being the unit vector in the magnet's direction, and d being the distance between the magnet and the center of the rotator cuff. For our model, we will assume that the magnet is always facing perpendicular to the humerus, and that it is always equidistant from the center of the rotator cuff. While these assumptions may not hold true due to differences in soft tissue, the model can be adjusted later to correct for any errors [201].

Shoulder Motion Model: In order to model the shoulder, we will use a rotational coordinate system as pictured in the Figure 3.16 as it expresses both the rotation and the location of the arm in relation to the shoulder. Yaw, the rotation around the Z axis will be denoted as Ψ which measures the movement of the arm side to side. $\Psi = 0$ is in the direction of the positive x axis, with a positive Ψ in the forward direction. Pitch, the

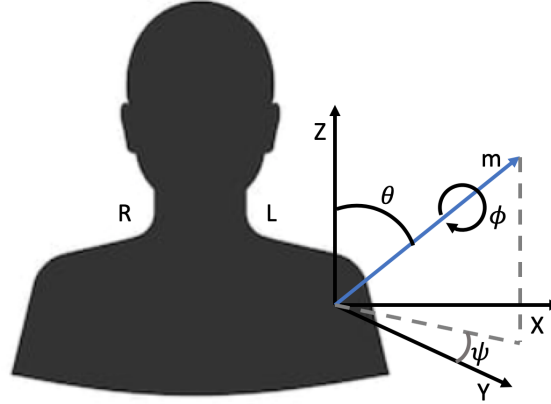


Figure 3.16: Shoulder Motion

angle formed by the arm and the positive Z axis, measures movement of the arm up and down. This will be denoted by θ . Roll is the action of twisting your arm, which will be denoted by ϕ . When $\phi = 0$ the palm faces down. Positive ϕ is a forward rotation. We can model the magnet's location by the following equations of a sphere of radius d , where m_x , m_y , and m_z are the x , y , and z coordinates of the magnet respectively because of the assumption that the magnet is always equidistant from the center of the rotator cuff. So, we define m_x , m_y , and m_z as the following:

$$m_x = d \cdot \cos \Psi \cdot \sin \theta \quad m_y = d \cdot \sin \Psi \cdot \sin \theta \quad m_z = d \cdot \cos \theta \quad (3.5)$$

Next, we will model θ_N , the direction that the magnet is pointing at any possible shoulder movement location. We will begin by modelling shoulder motion without roll, we will call this θ_{N0} . During this model, we will set $\phi = 0$. Then we will add the motion of roll, to have a full model of shoulder motion, which will be know as θ_N . On this model, we will change ϕ . This means that at each location, there are multiple directions of θ_N as opposed to the elbow application scenario where there is only one direction at each location, as shown in Figure [3.13a](#)

Since we know the magnet's north is perpendicular to the position vector, we can calculate the magnets north by rotating the position vector 90° ($\frac{\pi}{2}$ radians) in the upwards

direction. So, we know that θ_{N0} is the same as the position vector at $\theta - \frac{\pi}{2}$ because the magnet is rotated $\frac{\pi}{2}$ radians in the θ direction from the position vector. Thus, the following equations indicate the magnet's direction such that $\phi = 0$, where θ_{N0x} , θ_{N0y} , and θ_{N0z} are the vector components of θ_{N0} , in the x , y , and z directions respectively.

$$\begin{aligned}\theta_{N0x} &= \cos \Psi \cdot \sin\left(\theta - \frac{\pi}{2}\right) = -\cos \Psi \cdot \cos \theta \\ \theta_{N0y} &= \sin \Psi \cdot \sin\left(\theta - \frac{\pi}{2}\right) = -\sin \Psi \cdot \cos \theta \\ \theta_{N0z} &= \cos\left(\theta - \frac{\pi}{2}\right) = \sin \theta\end{aligned}\tag{3.6}$$

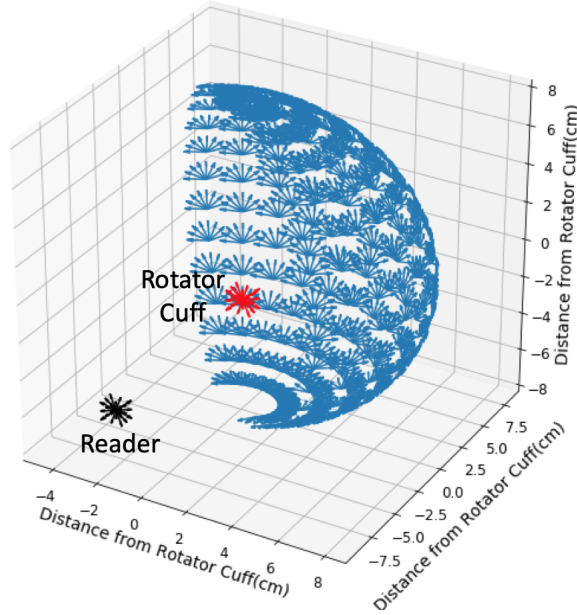


Figure 3.17: Direction of θ_N at Different Shoulder Locations

Next, to rotate θ_N in the ϕ direction, we need to rotate it around the position vector. Based on Rodrigues' Rotation Formula [132], we can express $\theta_N = \theta_{N0} \cdot \cos \phi + (\theta_{N0} \times \hat{m}) \cdot \sin \phi$. The following equations indicate the magnet's direction after being rotated ϕ radians, where θ_{Nx} , θ_{Ny} , and θ_{Nz} are the vector components of θ_N in the x , y , and z directions respectively. This is shown in Figure 3.17

$$\theta_{Nx} = -\cos \Psi \cdot \cos \theta \cdot \cos \phi + \sin \Psi \cdot \sin \phi \quad (3.7)$$

$$\theta_{Ny} = -\sin \Psi \cdot \cos \theta \cdot \cos \phi - \cos \Psi \cdot \sin \phi$$

$$\theta_{Nz} = \sin \theta \cdot \cos \phi$$

Modeling Magnetic Readings: Now that we have modeled the magnet's position and orientation on the shoulder, we can model its effect on the magnetometer at any shoulder location. The coordinate system will remain the same for modeling the magnetic field as for modeling the position and orientation of the magnet. The magnetometer will be located on the shoulder blade, right below the spine of the scapula. Using the magnetometer's readin-

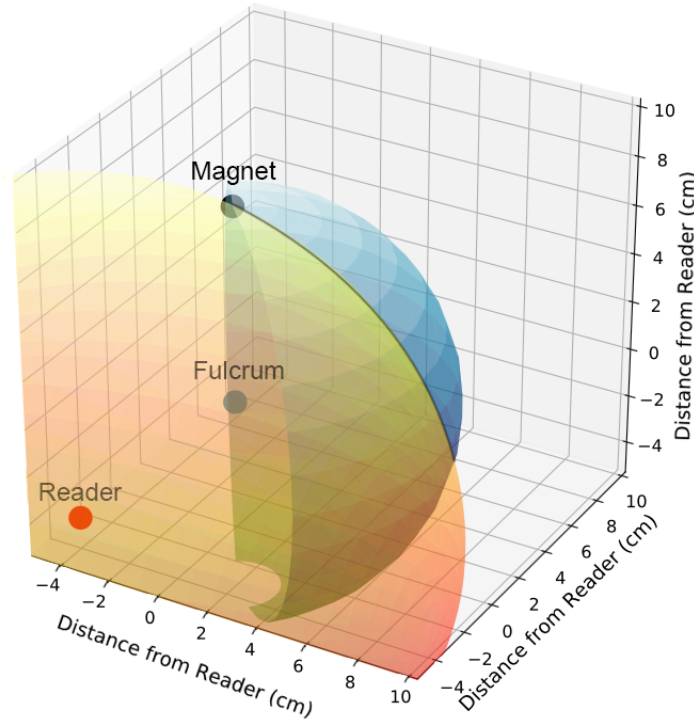


Figure 3.18: Intersection of Localization and Shoulder Motion Distance

gs as input, we can find the Ψ , θ , and ϕ , such that the calculated B equals the magnetic

field read by the magnetometer. We show the intersection of the calculated location of the magnet given a magnetometer reading and the shoulder motion model in Figure 3.18. The shoulder motion is represented by the blue half sphere and the locations of the magnet give a reading are shown by the red ellipsoid. The intersection is in the shape of an ellipse as shown by the black line in Figure 3.18. Then, we checked to see where the orientations of the magnet align to determine the location of the magnet. This is similar to what was done in Figure 3.13a except now we are in three dimension space with the arrows from Figure 3.17. In this Figure, we see two possible orientation matches. While this allows us to identify the position of the arm, we calculate more than a single solution.

One issue that arises with this model is that for some magnetic fields, there exists two locations that will produce the same magnetometer reading. If we fix ϕ to equal zero, such that the shoulder does not rotate, then we only get one solution, however, this limits the model significantly. On the other hand, if we know a previous position of the shoulder and the motion of the arm, we would be able to determine a path of locations that would allow us to distinguish between the two solutions.

Experimental Results: To put Magneto on the shoulder in a real world scenario, we would need a stronger electromagnet, so we modelled the biomechanical angle data instead. These results are used to analyze the number of positions that can be appropriate for a single reading. Given a magnetometer reading that is within the motion of the shoulder. From that reading, we calculated a shoulder location given the method outlined above. We then calculated the ground truth angle of that reading. We then compared the ground truth to the calculated angle to determine its accuracy.

We tested our model with and without roll. When we didn't include roll, we accurately computed the distance and direction given a magnetometer reading 96.87% of the time on 256 shoulder positions. We considered our computation to be an accurate calculation if it was within 2.5 millimeters from the ground truth location. The errors in our model were due to two biomechanical points creating a similar magnetic field. These similarities occurred when the Yaw was near 0° . While the magnetic fields at these two points were

not exactly the same, they were close enough to confuse our algorithm. Enhancements can be made in the future to produce better results at these points. When we included roll, we accurately computed the distance and direction given a magnetometer reading 75.79% of the time on 512 shoulder positions. In many of the situations where we calculated the wrong location, we calculate the correct set of locations but chose the the wrong one. Our algorithm chose the wrong location. In the future, modifications to our algorithm can be made to increase this accuracy.

3.6 Discussion and Future Work

There are many things that can be explored in future work. New algorithms can be examined for the elimination of the environment as well as for localizing the electromagnet. In this section, we focus on the ways that we can expand the sensing capabilities of our current electromagnet. First, we discuss how the strength of the electromagnet can be increased so that we can expand the working area of our device. Second, we discuss methods that can be used to increase the cycling rate. Third, we examined how we could use multiple electromagnets with a single magnetometer.

3.6.1 Increasing the Strength of the Electromagnet

We created our own electromagnet in our lab using a choke and magnet wire. Our magnet has a working range of up approximately 15 cm away from our magnetometer. While this worked for our applications, it would be helpful to have a stronger magnet with a larger range. To increase an electromagnets strength, you can increase the voltage to the magnet or change the materials the magnet is created with. Our electromagnet runs off of five volts so it would be easy to increase the voltage by using a larger battery and different microcontroller. We can also change out the material that we use to make the electromagnet; for example, a ferrite core could replace the choke.

When the strength of the electromagnet is increased it become susceptible to oversaturation of the core. We experienced this when working with much higher voltage batteries. This causes a peak in the beginning of each ON and OFF state. This would need to be accounted for. A better core could also prevent oversaturation. A stronger magnet could saturate the magnetometer causing error values to be given. In our lab, we experimented with running our electromagnet off of up to 24 volts. We saw oversaturation of the electromagnet and the magnetometer. While these factors can be accounted for, we did not address them in this work.

3.6.2 Increasing the Cycling Rate

In this work, we were limited by our electromagnets sampling rate of 220 Hz. This limited us to testing our magnetometer up to a cycling rate of 100 Hz. While we believe that we can run our sensor with a higher cycling rate, this will need to be tested with a different magnetometer. To increase the electromagnets cycling rate, we believe there are other ways to cycle the electromagnet. In this chapter, we cycled the electromagnets through on and off. Another method that could be used is flipping the polarity of the electromagnet. This means that you switch the North and South poles of the magnet. When you flip the polarity of the electromagnet, it demagnetizes at a faster rate than just turning it off. This is a potential method that could be explored to increase the cycling rate.

3.6.3 Multiple Electromagnets

Electromagnets of different strengths and frequencies can be investigated. This should provide the ability to record data from multiple electromagnets using only one magnetometer. This will allow for the sensing of multiple joints at once. For example, we could sense the motion of the shoulder and the elbow simultaneously with a strong enough electromagnet. Multiple electromagnets could even be used to sense parts of the body with many small joints such as the hands and fingers.

3.7 Conclusion

In this work, we presented Magneto: a sensing system for joint motion analysis. Magneto uses the combination of an electromagnet and magnetometer to remove environmental interference from magnetic field readings in a dynamically changing environment. Given this purified reading, we localized the electromagnet with respect to the magnetic field reader which allowed us to apply Magneto in two pilot studies: elbow angle and shoulder position. We calculated elbow angles to the nearest 15° with 93.8% accuracy, calculated shoulder positions in two-degrees of freedom with 96.9% accuracy, and calculated shoulder positions in three-degrees of freedom with 75.8% accuracy.

Chapter 4

TrackKnee: Knee Angle Measurement Using Stretchable Conductive Fabric Sensors

4.1 Introduction

Knee injuries are prevalent among all demographics of the population and the treatment of these injuries can be costly in recovery time and monetarily [124]. From 1999 to 2011, a study of more than 6.5 million knee injuries in the United States revealed that nearly 50% of the knee injuries were sports-related with adolescents making up an estimated 2.5 million sports-related knee injuries annually [70]. In the senior population, knee injuries are common due to falling and diseases such as osteoarthritis. More than 14 million individuals suffered from osteoarthritis of the knee in 2007 and 2008 in the United States [55]. Regardless of age and type of injury, a patient's recovery from a knee injury is based on their adherence to their assigned rehabilitation protocols [32, 31].

Technologies such as wearable devices can be used to help monitor the patients' adherence to their rehabilitation protocols. It can be used inside and outside of a clinical setting to enhance a patient's treatment plan [193, 104]. It can also be used to enhance and in-

dividually tailor each patient’s protocol to best suit their needs [172]. Proper monitoring and adherence to the prescribed protocols can be used to help decrease a patient’s recovery time, their overall pain, and the cost of their treatment. Further, soft wearable flexible sensors have been created to non-invasively record biometric data on patients [155].

Joint angle estimation is an important part of monitoring knee injury recovery [96]. Wearable sensors are frequently used for monitoring of joint angles. Many different sensors have been used to accomplish this task including IMU’s [113, 41, 117], ultrasonic sensors [161, 159, 160], optical sensors [183, 176, 109], liquid metal sensors [135, 136], potentiometers [54], acoustic sensors [188], force sensitive resistors [177], retractable string sensors [119], galvanic coupling systems [39], and flex sensors [197, 17]. Soft, flexible, wearable E-Textile sensors have also been used to monitor joint angles [175, 19, 150, 72].

In this chapter, we address the following research questions:

RQ1: How can we measure knee angles using stretchable conductive fabric?

RQ2: How can we design and fabricate a wearable device that tracks knee angles using conductive stretchable fabric and is comfortable to wear?

RQ3: How accurately can we measure knee angles with our wearable device?

To answer our first research question, we develop three models to be used in succession. First, we developed a model to calculate knee angles from the change of length across the front of the knee. To do this, we run an experiment with ten individuals of varying height in which we record the values for the change in length across the front of each of their knees at four different angles. Then we develop an Ordinary Least Squared (OLS) regression model that uses height and change in length across the front of the knee to calculate knee angles. Second, we developed a model to calculate the change in the length of conductive fabric from the resistance of the conductive fabric. To do this, we performed an experiment in which we repeatedly stretched our conductive fabric to specific lengths and recorded the resistance at each length. We then modeled this data with a third-degree

polynomial regression. Third, we modeled voltage to the resistance of our fabric using a voltage divider. Overall, using these models allowed us to measure knee angles using our stretchable conductive fabric.

To answer our second research question, we designed and fabricated our TracKnee device. Our TracKnee device had the following requirements: (1) It should be able to collect data from the conductive fabric sensor and wirelessly send it to a collection location. (2) It should be comfortable to wear and be easy to put on and take off. (3) It should be washable and be able to be cleaned as needed. Our device consisted of two main parts a control patch and the sensor sleeve. The control patch houses all the non-washable electronic components needed to control the device and wirelessly connect to a smartphone to send data. The sensor sleeve houses the conductive fabric sensor and conductive fabric wiring allowing it to be washable.

To answer the third research question, we conducted a user study to collect TracKnee sensor data and ground truth angles and used that data to evaluate our models. Our user study consisted of ten participants and 240 knee angles. We collected TracKnee sensor data and ground truth angles. Then we used our models to calculate the angle of the knee from our TracKnee sensor data. We compared that angle to the ground truth angle to evaluate. Overall, we saw an accuracy of 94.86% to classify our knee angles to the nearest 15th degree. The average error from the calculated angle to the ground truth is 3.69°. Following this, we evaluated our prototypes battery life. The battery life was 18 minutes and 50 seconds for a 40 mAh battery. Since the battery is removable, it can be replaced when it is fully discharged or a larger battery can be used.

Measuring human body joint angles is receiving an increasing amount of attention from the medical science and computing disciplines [174, 144, 47]. Since there is a growing movement to collect human motion data outside of a lab setting [193, 155] researchers have begun looking to more comfortable This enables researchers to collect more data in the real world which is essential when treating diseases. Soft, flexible, wearable E-Textile sensors allow for the comfort of the wearer while allowing still enabling the collection of critical

biometric data. Our TracKnee prototype utilizes a soft conductive fabric to measure the joint angle of the knee allowing for comfort during long term use.

Our contributions are summarized as follows:

- We propose three models that can be used in series to calculate knee angles from voltage. First, we model change in length across the front of the knee to the knee angle with respect to the height of an individual. Second, we model resistance of the fabric to change in length of the conductive fabric. Third, we model voltage to the resistance of the fabric.
- We designed and fabricated a wireless sensing knee sleeve to unobtrusively measure knee angles called TracKnee. TracKnee utilizes a soft and stretchable conductive fabric sensor to monitor knee angles. We designed it to be washable by making any non-washable electronic components removable. We also designed to be easy to put on and take off so that it would be as easy for the user to wear as a non-sensing knee sleeve.
- We conducted a user study with six participants where we collected ground truth angles and sensor data from our TracKnee device. To do this, we developed a data collection application on an Android smartphone to collect and store the data.
- We evaluated our models on the user study data. Our results show that our model is 94.86% accurate to the nearest 15th degree angle and that our average error per angle is 3.69°.

The remainder of our chapter is organized as follows. First, in Section [4.2](#) we discuss the three models that we propose to calculate knee angles. Next, in Section [4.3](#) we explain how we designed our TracKnee prototype to be comfortable, washable, and unobtrusive. Following that, we describe the data we collected and our methods for collection in Section [4.4](#). Then, in Section [4.5](#) Experimental Results, we evaluate models described in Section [4.2](#) with the data recorded in the [4.4](#). Finally, we draw our conclusions in our final section.

4.2 Modeling

Overall, we show that we can model knee angles based on the stretch of our conductive fabric. To do this, we need three models. First, we model the length across the front of the knee to the angle of the knee with respect to different human heights. Second, we model the length across the front of the knee to the resistance of our conductive fabric. Third, we model the resistance to the voltage that we read as an output of our voltage divider. These models can be used in a linear progression to calculate knee angles from voltage.

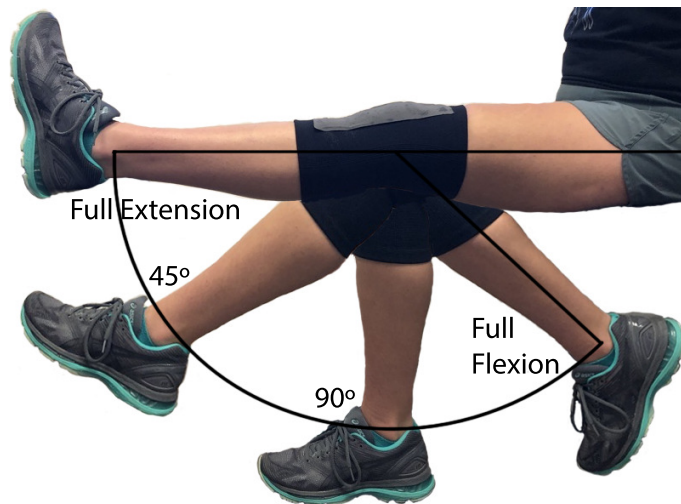


Figure 4.1: Measured Knee Angles

4.2.1 Change in Length to Angle Model

From medicine, we know that the normal range of knee motion is -10° to 130° [2]. Extension of the knee is defined as the straightening motion of the knee that results in an increase of the angle. Flexion of the knee is defined as the bending of the knee that results in a decrease of the angle. Full extension and full flexion are the max values of these motions. We illustrate these values in Figure 4.1. Between the full extension and the full flexion, there are many angles. To modeling the change in the length across the front of the knee and the angle of the knee, we measure the angle of the knee from full

flexion to full extension in increments of 45° . To collect these values across individuals of varying height, we do the following experiment:

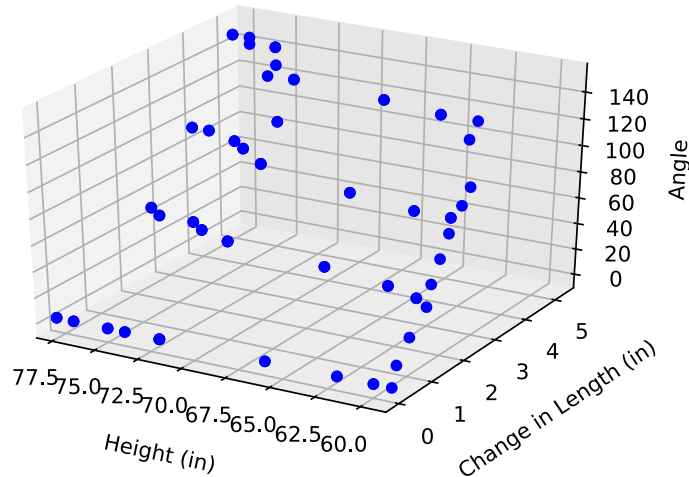


Figure 4.2: Change in Length for Knee Angles Adjusted for Height

Our experiment comprised of ten individuals recruited from the College of William and Mary and the surrounding area. Their data is shown in Table [4.1](#). Their ages ranged from 18 to 30 with a mean of 24.5. 5 males and 5 females participated in the study. They all had healthy BMI's with an average of 23.5. Our participants' heights ranged from 4'11" to 6'6" with an average height of 5'9". Two participants had had surgeries in the past but they were more than ten years prior to this study. We started the study with a questionnaire to determine the user's age, gender, height, weight, and assessment of any knee injuries or surgeries. Following this, we collected data on their knees. For each knee, we collected their patella width, knee circumference, the max flexion angle, the max extension angle, and the change in length across the front of the knee for the following angles: max extension, 45° , 90° , max flexion. The angles of the knee that we measure are shown in Figure [4.1](#). Patella width and knee circumference were measured with a cloth tape measure while the max flexion angle and max extension angle were measured with a digital goniometer. A goniometer is an instrument used to measure angles of joints on the body. We show a goniometer in Figure [4.12](#). Change in length across the front of the

knee for various knee angles was recorded using the goniometer and the tape measure. All participants in our study were able to extend their knee to a full 180°.

Height	Change in Length					Angle of Max Flex	
	0°	45°	90°	Full Flex R	Full Flex L	Right	Left
4'11"	0"	1"	1.625"	2.5"	2.25"	125°	119°
5'0"	0"	1.5"	2.25"	2.75"	3"	142°	148°
5'2"	0"	1.5"	2.25"	3"	3"	145°	143°
5'6"	0"	1.75"	2.5"	2.5"	3.5"	148°	146°
6'0"	0"	2"	3"	3.5"	3.5"	113°	115°
6'0"	0"	2"	3"	4"	4"	139°	137°
6'2"	0"	2.25"	3.5"	4.25"	4.5"	135°	140°
6'3"	0"	2.5"	3.75"	5"	5"	148°	148°
6'5"	0"	2.5"	4"	5.25"	5"	145°	140°
6'6"	0"	2.75"	4"	5.25"	5.25"	148°	145°

Table 4.1: Participant Knee Motion Statistics

From our data, we derived the following insight. The change in length across the front of the knee is influenced by the height of the user. This can be explained by the underlying skeletal structure for the taller participants naturally being larger. We examined this insight by creating a graph, shown in Figure [4.2](#), that compares the height, knee angle, and change in the length across the front of the knee of all of our participants. From this graph, we conclude that the greater the height and knee angle, the greater the change in the length. This is highlighted by looking at the change in the length for the max flexion of our shortest and tallest participant. Our shortest participant is 59 inches tall with a change in the length across the front of their knee of 2.4 for the right knee and 2.25" for the left knee. Our tallest participant is 78 inches tall with a change in the length of 5.25" for both knees. The difference between their change in length at max flexion was 2.75" for the right knee and 3" for the left. Looking further into their data, we see that the max flexion for the change in length the length across the front of the knee for our shortest participant was not even a 45° angle for our tallest participant.

To model this data, we created an Ordinary Least Squared (OLS) Regression using

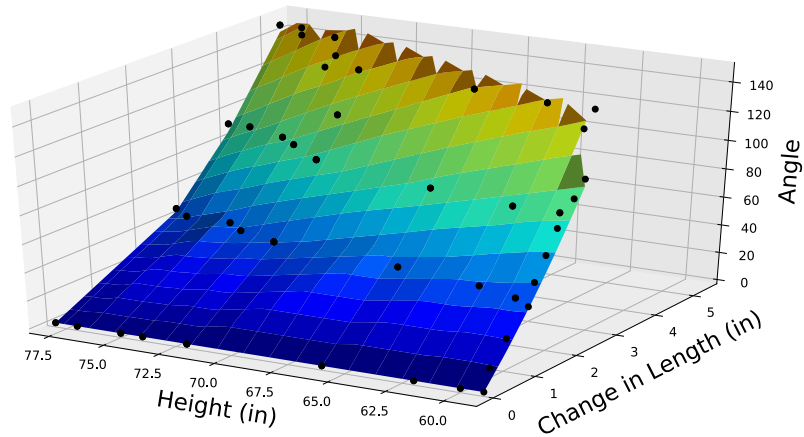


Figure 4.3: Change in Length to Angle model Adjusted for Height

Statsmodel [170]. We use height and change in length as parameters for the model. To start, we have eight coefficients and an intercept. We then train the model by removing the coefficient or intercept with the highest P value greater than the absolute value of its t-statistic while checking that the Adjusted R-squared value is not drastically decreasing. Once fully trained, the model has just three coefficients. The model has an R-Squared value of 99.3%. We graph this model in Figure 4.3. The model is as follows:

For $L = \text{Change in Length}$, $H = \text{Height}$, and $A = \text{Angle}$,

$$A = 148.948L + 4.428L^2 - 1.8651LH \quad (4.1)$$

4.2.2 Resistance to Change in Length Model

In this project, we use Eonyx Conductive Stretchable Fabric [63]. This fabric shows a change in resistance when it is stretched. In our project, we use an 8.5” by 2.25” piece of fabric. To model the change in resistance as it is stretched, we performed the following experiment. We connected a digital multimeter to each end of the fabric. We then stretched the fabric four inches in total and recorded the resistance at each half of an inch. We repeated this process ten times. The results of this are shown in Figure 4.4.

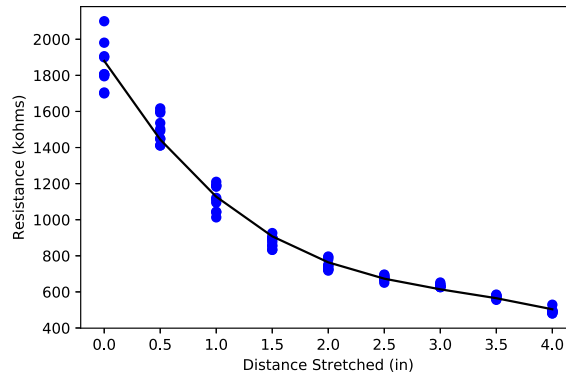


Figure 4.4: Fabric Resistance to Stretch Distance

We used this data to create a third-degree polynomial regression model in Scikit-learn: Machine Learning in Python [157]. This model has a Mean Absolute Error of 0.131, a Mean Squared Error of 0.026, and a Root Mean Squared Error of 0.162. The model is shown in Figure 4.4. The regression is as follows:

For $R = Resistance$ and $L = Change\ in\ Length$,

$$L = -29.184 * R^3 + 282.126 * R^2 - 1005.642 * R + 1880.047 \quad (4.2)$$

4.2.3 Voltage to Resistance Model

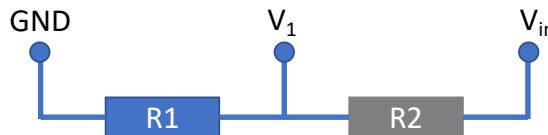


Figure 4.5: Voltage Divider

Finally, we model the voltage to resistance. In our circuit, which will be discussed in more detail in the following section: TracKnee Prototype Design, we use a voltage divider. The voltage divider allowed us to read the resistance variation of the conductive fabric sensor. In Figure 4.5, we show the setup of the circuit that we have employed in our



Figure 4.6: TracKnee Prototype

device. We define, $R_1 = \textit{Fixed Resistor}$ and $R_2 = \textit{Conductive Fabric}$. From this, we can compute the resistance from the following equation:

$$R_2 = \frac{V_1 * R_1}{V_{in} - V_1} \quad (4.3)$$

As this inverse function equation presents, the larger the resistance of the conductive fabric is, the smaller the voltage of V_1 . Similarly, the smaller the resistance of the conductive fabric, the larger the voltage of V_1 . The fixed resistor that is chosen to be in the middle of the variation of the resistance of conductive fabric. This allows us to calculate the resistance of the conductive fabric sensor from the voltage read on the device.

4.3 TracKnee Prototype Design

There are two main parts to our TracKnee prototype. The first is the control patch, which houses all of the non-washable electronic components. The second is the sensor sleeve, which houses our fabric sensor. When the two parts are connected, we have a full TracKnee prototype as shown in Figure 4.6a. As we were developing the TracKnee

prototype, we kept the following requirements in mind: (1) The prototype should be able to collect data from the sensor and wirelessly send it to a collection location. (2) The prototype should be comfortable when worn and be easy to put on and take off. (3) The prototype should be washable so that it can be cleaned when it gets dirty or sweaty. In this section, we discuss the control patch, the sensor sleeve, how they come together to form our TracKnee prototype, and the lessons we learned during development.

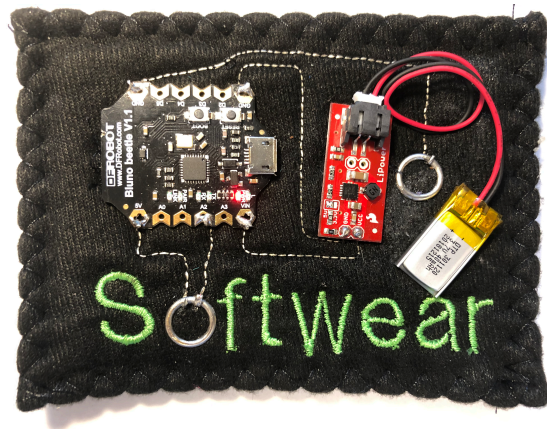


Figure 4.7: TracKnee Control Patch

4.3.1 Control Patch

The control patch houses all of our rigid electronic components. During the development of the control patch, we addressed the following: (1) The control patch should be as small as possible so that it goes unnoticed by the user. (2) Some of the components contained in the control patch are not washable, so the control patch must be detachable from the knee sleeve. In total, the patch is 3.5 inches wide by 2.5 inches tall. The control patch is shown in Figure [4.7](#). In this subsection, we discuss the components used and the process we used to fabricate the control patch.

4.3.1.1 Components

The components contained in the control patch are the microcontroller and Bluetooth chip combination, power supply, conductive thread wires, resistor, and snaps. We sewed all of our components to a layer of headliner foam. This gives anyone wearing the device some cushion from the rigid electronic components. In the following, we describe each of the components:

Microcontroller and Bluetooth Chip: The microcontroller that we chose is a Bluno Beetle [24]. We chose this because it is currently the smallest Arduino [10] based microcontroller with Bluetooth Low Energy. The Bluno Beetle features an ATmega328P processor and a CC2540 Bluetooth chip. It also contains four analog pins which surpasses our requirement of one analog pin.

Power Supply: The circuit is powered by a rechargeable 40 mAh lithium-ion battery. This battery outputs 3.7 volts. Since the Bluno Beetle operates in the range of five to eight volts, we use a LiPower Boost Converter [181] to boost the voltage of the battery from 3.7 volts to five volts. This battery last for about 40 minutes.

Conductive Thread: We use Syscom Advanced Materials' Amberstrand [185], a conductive thread, instead of traditional wires to connect the electronic components of our control patch. We chose this thread because it has a resistance of one ohm/foot and is solderable. It is also soft and flexible, making it a good choice for wearable devices worn on the body. Amberstrand fibers are made from Zylon which has very high in tensile strength and is resistant to heat [191]. This makes it a good choice for conductive thread wiring. The thread is coated in a combination of silver, copper, and nickel to make it conductive.

resistor: We chose a 470 ohm resistor because it is in the middle of the range of resistance values for the conductive fabric. This enhances the resolution of the data that we read from the conductive fabric sensor.

Snaps: To make the TracKnee device washable, the control patch must be removable

while allowing for easy reconnection to the sensors on the shirt. To accomplish this, we used conductive nickel snaps to connect the control patch to the knee sleeve.

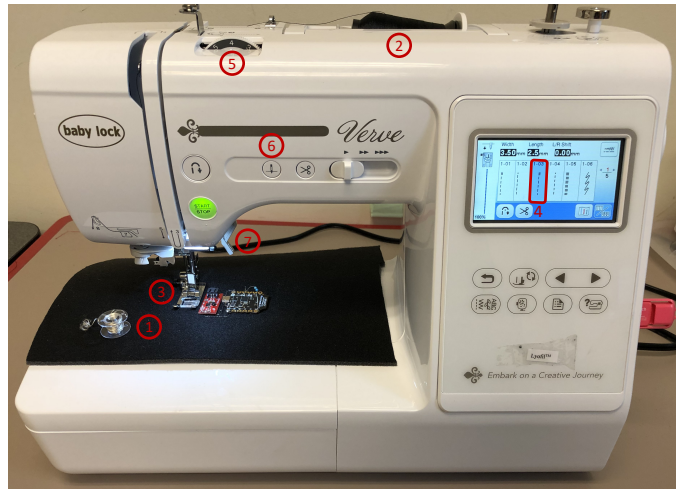


Figure 4.8: Baby Lock Verve Sewing and Embroidery Machine

4.3.1.2 Fabrication

When fabricating the control patch, we designed it as small as possible. To accomplish this, we used a sewing machine to sew the conductive thread into the control patch. This allowed us to get our conductive thread wires closer to each other, decreasing the space being used. We describe our sewing machine setup and then the entire procedure used to fabricate our control patch.

Our sewing machine is a Baby Lock Verve Sewing and Embroidery Machine [14]. We show it in Figure 4.8. To sew conductive thread with our sewing machine, we chose installed a Schemtez Metallic embroidery needle [168]. This needle has a longer eye that gives us more room for it move around as we are sewing. This helps to prevent snags in the thread. We found that it is easier to sew our conductive thread when it is wound into a bobbin ①. When we used a spool of conductive thread on the spool pin ②, we found that it came off of the spool too fast and this would cause loose stitches to be sewn. For our prototype, we found that it was best to use the standard zig-zag foot ③ that came

with the machine. We chose the 1-03 stitch for the control patch as it is small and it sews in a straight line ④. We set the tension to four ⑤. When sewing conductive thread we go as slow as possible so that we can check the thread for potential snags. To do this, we use the needle position button ⑥. This button moves the needle into the up or down position. Pushing this button twice is one stitch. For our circuit, we also need to be able to sew sharp 90° corners. To do this, once you have reached the position in which you would like to make a corner, you put the needle in the down position so that it is all the way through the foam, lift the foot with the lever ⑦, and turn the foam around the needle until you reach the desired angle. We also embroidered a logo onto our control patch. Because embroidery requires hooping the fabrics, this is done first.

Since our control patch has many different components, the procedure that we used to fully fabricate it is as follows:

- (1) Layout the circuit on the back of the headliner foam. Since the conductive thread is in the bobbin we sewed with the bottom of the headliner foam facing upwards
- (2) Draw out exactly where you want the wires to be. Once the circuit is live, the conductive thread is live so there cannot be any overlap in the conductive thread. This causes shorts in the circuit.
- (3) Sew the conductive thread into the foam with the settings for the sewing machine as described above. At the end of each conductive thread wire, you should leave about an inch of thread. This makes it easier to attach and solder in later steps.
- (4) Attach the snaps to the control patch making sure that there is contact between the conductive thread and the snap. The thread can be secured with solder or tied around the edge of the snap.
- (5) Put the microchips in place. Pull the conductive thread through the correct pins on the microchip. A needle threader helps with this.
- (6) Solder the conductive thread to the microchips.

- (7) Cut off the remaining conductive thread.
- (8) Finish the edges of the conductive foam and cut off any excess material.

4.3.2 Sensor Sleeve

The sensor sleeve contains only components that are washable so that it may be washed in the case that it gets sweaty or dirty. The sensor sleeve should accomplish the following: (1) The sleeve should not impede knee normal knee motion. (2) It should be comfortable to wear and be easy to put on and take off. (3) It should only contain components that can be washed. In this subsection, we discuss the components used and the process we used to fabricate the control patch.

4.3.2.1 Components

The components contained in the sensor sleeve are the knee sleeve, conductive fabric, conductive thread, and snaps. All of these components are washable in a washing machine. We describe the components in the following:

Knee Sleeve: We chose the Crucial Compression Premium Knee Compression Sleeve [\[46\]](#) as a base for our sensor sleeve. We chose this sleeve as it is easy to put on and have a good reputation for not sliding down when worn.

Conductive Fabric: We used Eonyx Conductive Stretchable Fabric [\[63\]](#) for the development of our knee sensor. We chose this fabric for the following reasons. It is coated in a conductive polymer that gives it piezoresistive properties. This allows us to see a change in resistance as the fabric is stretched. Additionally, the composition of the fabric is similar to that of many athletic fabrics. It is made of 72% nylon and 28% spandex. Nylon is soft and silky to the touch, quick drying, and mildew resistant. Spandex is breathable, quick drying, and moisture wicking but it additionally provides an unrestricted range of motion as it stretches with the motion of the user.

Conductive Thread: Again, we use Syscom Advanced Materials' Amberstrand [185] in place of wires. This time, the thread is hand sewn.

Snaps: We also use snaps on the sensor sleeve. The snaps from the control patch connect to these snaps when in use.

4.3.2.2 Fabrication

We could not use our sewing machine to assist with the fabrication of the sensing sleeve as we cannot lay the knee sleeve flat to sew through it. Because of this, we hand sew our conductive thread into the knee sleeve. To fabricate the sensor sleeve, we follow the following steps.

- (1) Attach the conductive fabric to the knee sleeve so that it is positioned down the vertical midline of the kneecap. Secure it with spray adhesive.
- (2) Attach the snaps so that they line up with the snaps on the control patch.
- (3) Hand sew conductive thread in a zig-zag pattern from the top of the fabric to a snap. Then sew from the bottom of the fabric to the second snap. To connect the thread to the fabric, put a stitch through the fabric and tie it off. To connect to the snap, feed the thread between the top and bottom of the snap and secure it with solder.

4.3.3 TracKnee Prototype

When we connect the control patch to the sensor sleeve, we have a full TracKnee device. The circuit diagram for this device is shown in Figure 4.9. Our circuit utilizes a voltage divider to incorporate our conductive fabric sensor. The voltage divider requires two resistors: our conductive fabric sensor and the 470 ohm resistor. We connect the resistor to ground and our fabric sensor to power. We read the voltage via analog pin A2 on the Bluno Beetle. So, when the conductive fabric sensor stretches, the resistance

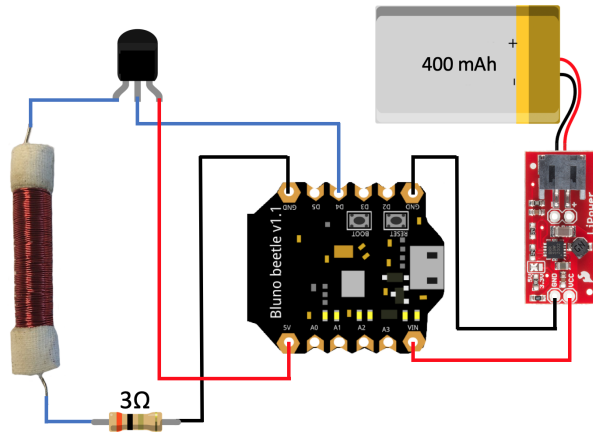


Figure 4.9: Circuit diagram of TracKnee

decreases and the voltage read on A2 increases. As the fabric sensor returns to its original length, the resistance increases and thus the voltage on A2 decreases.

4.3.4 Lessons Learned

Through the design process for our TracKnee prototype, we learned a few lessons. The most important were the using fabric adhesives, choices of conductive thread and using different stitch patterns in different fabrics.

We tried using 505 temporary fabric adhesive to help attach our conductive fabric to our knee sleeve. This adhesive changes the resistance of the conductive fabric. When applied lightly, we saw our resistance change from being near 100 kohms to almost 600 kohms. When applied heavily, the resistance jumped again to about 1100 kohms. While there was still a readable change in resistance, we did not model nor study how this adhesive affects our conductive fabric sensor.

Initially, we chose a commonly used stainless steel conductive thread [180]. It had a resistance of twenty-seven ohms/meter. While this thread was very smooth and did not have issues with fraying, we were not able to accurately read the data coming from the elbow sensor. To fix this, we replaced this thread with the Syscom Advanced Materials' Amberstrand that had a lower resistance of one ohm/foot.

Many stitch patterns can be used when sewing conductive thread. We tested two main stitch patterns for sewing on stretchy material. The first is a straight stitch and the second is a zig-zag stitch. When the fabric the stitches are sewn into is stretched, each stitch reacts differently. From these tests, we know that the straight stitch bunches in two places while the zig-zag stitch stays in place. Thus, we learned to use a zig-zag stitch when sewing into stretchy fabrics like our knee sleeve.

4.4 Data Collection

In this section, we evaluate our knee angle model by collecting data from human subjects. This data collected consists of ground truth knee angles measured by a goniometer and the data collected from our TracKnee device. Our target participants were between 18 and 35 years of age and were healthy without any major knee injuries or surgeries. In this section, we discuss the equipment used in our study, the parameters, and the demographics of our participants.

4.4.1 Equipment

To perform our data collection study, we need to collect statistics on each participant's knees, record the TracKnee device data, and record the ground truth angles. We used a Medigauge digital goniometer [133] and a fabric tape measure to collect statistics on each participant's knee. We developed an android application and implemented it on a Google Pixel 2 to record our TracKnee device data. We used a goniometer to measure the angles and a camera to record the time in our application to measure the ground truth angles and label them in our TracKnee data. Next, we discuss our application.

We developed an application to collect data from our TracKnee device. This application is shown in Figure 4.10. Our application has four states: *Initial State*, *BLE Scan State*, *BLE Connected State*, and *Data Collection State*. The states are shown in Figure 4.11. Next, we describe the application states.

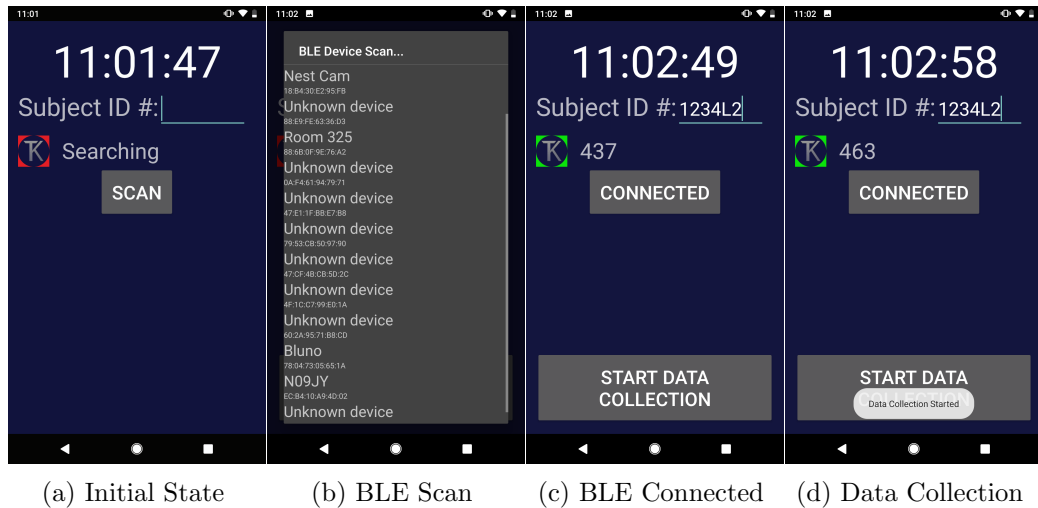


Figure 4.10: TrackKnee Application

Initial State: When the application is launched, the user is shown the *Initial State* (Figure 4.10a). This state has two main components: timestamp and *Subject ID #*. The timestamp is displayed throughout the entire application. This is essential, as during our user study, we recorded with the timestamp in view of the camera so that we can label the ground truth. The *Subject ID #* is a field where the user can input the number that is assigned to each subject participating in our study. Once this field has been completed, the user can press the scan button to move the application into the second state: *BLE Scan State*.

BLE Scan State: Once in the *BLE Scan State*, the application opens the activity that scans for and displays nearby Bluetooth Low Energy devices as shown in Figure 4.10b. The user should select *Bluno* from the displayed list of devices. Once a device has been selected, the application displays either the *BLE Connected State* or the *Initial State*. If the Bluetooth device is correctly connected and the application is receiving data, the application moves to the third state: *BLE Connected State*. If the application does not connect to the device, it returns to the *Initial State*.

We based our Bluetooth connection to our Bluno device off of the BlunoBasicDemo [35] from DFRobot. This demo connects a Bluno device to an Android application and fa-

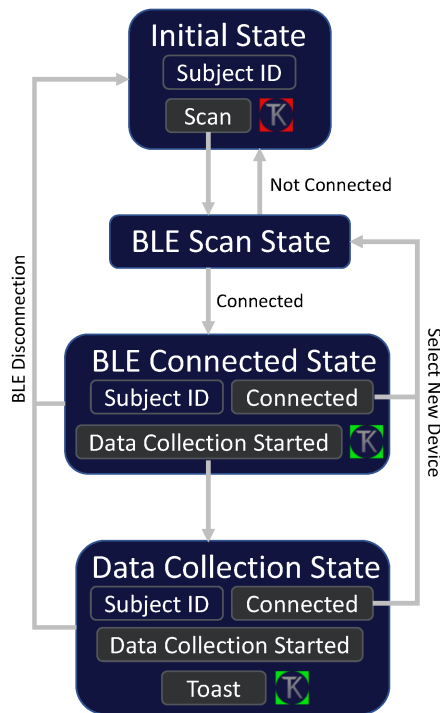


Figure 4.11: TracKnee Application States

facilitates the transmission of data between the two. The android application scans for Bluetooth devices, allows the user to select a Bluetooth device, connects to that device, and then allows the user to send and receive data. The Bluetooth is coded via Arduino to receive data and send a copy of the received data back to the application.

BLE Connected State: In the *BLE Connected State*, shown in Figure 4.10c, the background of the TracKnee logo changes to green and the *Scan* button is renamed *Connected*. During this state, if the Bluetooth device disconnects, the application returns to the *Initial State*. If the wrong device was connected, the application still proceeds to the third state. If the application connects to the wrong device, the user can press the *Connected* button and the user is once again presented with the *BLE Device Scan State* where they can select the correct device. At this point, the application displays the *Start Data Collection* button. This button is used in the final state.

Data Collection State: Once the device is correctly connected and the user is ready to begin logging data, the *Start Data Collection* button is displayed. To start collecting

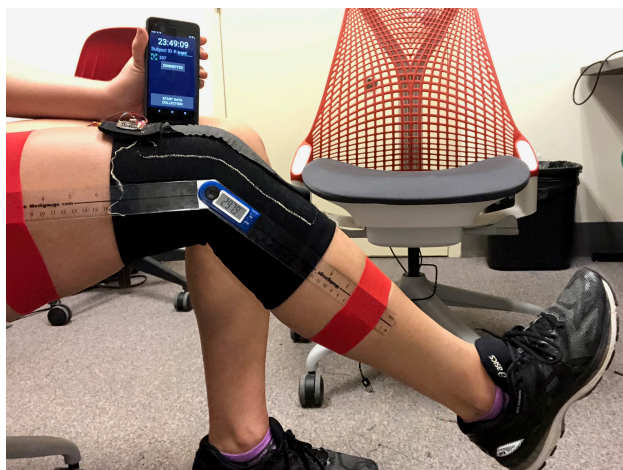


Figure 4.12: User Study Setup

data, the user should press the *Start Data Collection* button. Once the button has been pressed, the application proceeds to the fourth state and pop up a toast message to let you know that data collection has started as shown in Figure [4.10d](#). The application logs data to a .csv file. This file is named with the *Subject ID #* and the corresponding time. The .csv consists of two values: timestamp and sensor.

4.4.2 Parameters

At the beginning of the study, we administered a pre-user study questionnaire. On the questionnaire, we asked for the following statistics: age, gender, height, weight, and information pertaining to previous knee injuries or surgeries. Next, we recorded the following statistics about each of their knees: width of patella, circumference of their knee (taken mid-patella), maximum flexion of their knee, maximum extension of their knee, change in length from maximum extension to maximum flexion (CLEF value), distance from top of kneecap to top of TracKnee device, and distance from bottom of kneecap to bottom of TracKnee device. Following that, we asked the participants to put the device on their right knee. Then, we connected the device to the data collection application and set up the camera to record the study. Following this, we asked the participant to position their knee to the following angles: 0° , 15° , 30° , 45° , 60° , 75° , 90° , 105° , 120° , and 135° . We

used a goniometer to confirm the ground truth measurement of the angle of their knee. We repeated this process once on the right knee and then twice on the left knee. Overall, we recorded data for 240 knee angles.

Participant #	Height	CLEF		Max Extension		Max Flexion	
		Right	Left	Right	Left	Right	Left
1	4'11"	2.5"	2.25"	123°	120°	-1°	0°
2	5'5"	3"	2.75"	147°	145°	0°	0°
3	5'6"	2.75"	2.5"	136°	126°	-2°	-4°
4	5'7"	3"	3.25"	123°	130°	0°	-1°
5	6'0"	3.25"	3.25"	113°	116°	-10°	-8°
6	6'0"	4"	4.25"	139°	137°	0°	0°

Table 4.2: Participant Knee Range of Motion Statistics

4.4.3 Demographics

We recruited the participants in our study from the College of William and Mary and the surrounding area. In total, we had six participants: three male and three female. On average, our participants were 25.3 years of age with the youngest being 18 and the oldest being 32. All participants were in the normal range for BMI with an average of 21.86. The normal range for BMI is 18.5 to 25. Our participants were also free of major knee surgeries and injuries.

We show the height, CLEF value, maximum flexion, and minimum flexion for each participant in Table [4.2](#). In this table, we see that each participant's height, maximum flexion, and minimum flexion affect the CLEF value of each knee. In general, the taller the participant the higher the CLEF value but it is also affected by how flexible each individual is. The lower the maximum flexion angle, the higher the CLEF value. For example, we had two 6'0" participants. The participant with the lower maximum flexion angle had a higher CLEF value.

4.5 Experiment Results

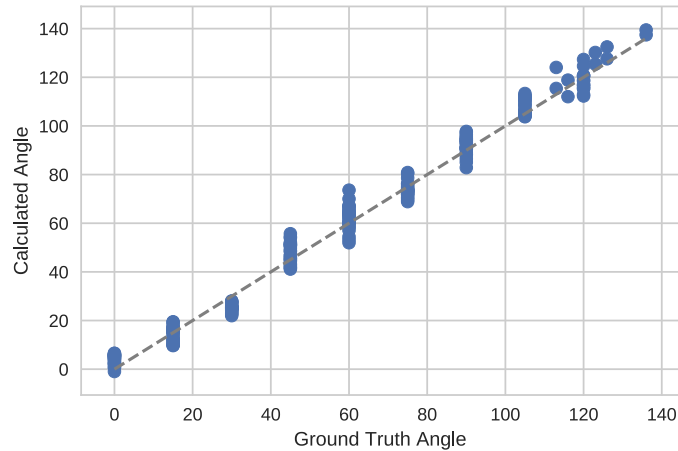


Figure 4.13: Comparison of Ground Truth Angle and Calculated Angle

We evaluate the model that we created in Section 4.2 on the data collected in Section 4.4. We removed three outliers from our dataset as the angle calculated by the model was off by over 30° . We show our ground truth angle and our calculated angle in Figure 4.13. We evaluate the accuracy of the model that we created. To do this, we evaluated our model’s ability to classify an angle correctly to the nearest 15, 12.5, 10, 7.5, and 5-degree angle. Our results are shown in Table 4.3. Respectively, we see a 94.86% accuracy at the nearest 15^{th} degree, 84.11% at the nearest 12.5 degree, 70.09% at the nearest 10^{th} degree, 53.27% at the nearest 7.5, and 38.79% at the nearest 5^{th} degree. On average, overall, our model experiences an error of 3.69° . These results are shown in Table 4.3. We further analyzed our data by breaking down the accuracy by each participant. This can be seen in Table 4.3. From this table, we can see that the shorter participants’ angles were more accurate. In terms of average error, the shorter the participant the smaller the error.

In our study, we used a goniometer to collect ground truth angles. When used by inexperienced individuals to measure elbow angles, goniometer readings can be off by 8° to 18° [23]. This can cause variability in the actual value of the ground truth angles that we record. It is possible that this is the reason for the low accuracy of the nearest 5th

and 7.5-degree angle. In future work, a more accurate ground truth measurement should be acquired. This can be done by using a device such as Pasport Goniometer Sensor [154] which achieves an accuracy of 2° before calibration. This sensor uses a cuff on the upper arm and forearm with the sensor positioned at the hinge of the elbow.

Participant #	Height	Accuracy					Average Error
		15	12.5	10	7.5	5	
1	4'11"	94.44	86.11	80.56	63.89	41.67	3.29°
2	5'5"	94.29	88.57	77.14	60.00	40.00	3.34°
3	5'6"	100.00	80.55	66.67	58.33	50.00	3.35°
4	5'7"	91.67	83.33	72.22	52.78	41.66	3.79°
5	6'0"	94.44	83.33	69.44	47.22	33.33	3.99°
6	6'0"	94.29	82.86	54.29	37.14	25.71	4.42°
Overall		94.86	84.11	70.09	53.27	38.79	3.69°

Table 4.3: Model Accuracy by Participant

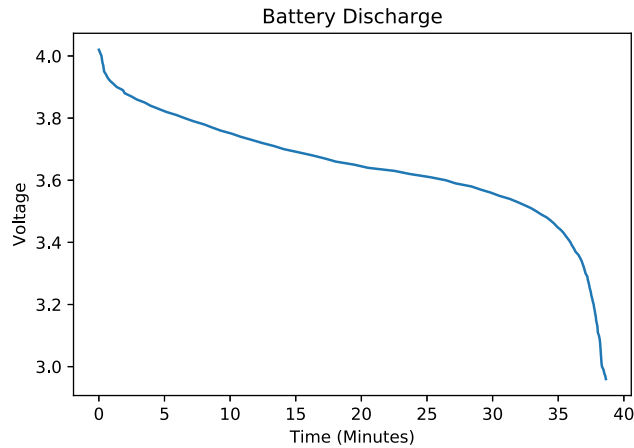


Figure 4.14: Voltage of Battery Over Time

We recorded the voltage while discharging the rechargeable 40 mAh lithium battery. Figure 4.14 shows the discharging curve for the voltage change from 4.02 volts to 2.96 volts in 38 minutes and 38 seconds. In this figure, we can see that the voltage decreased quickly in the beginning and then stabilized from 3.90 volts to 3.40 volts. The average current of the main circuit can be calculated by dividing the recorded discharging time and the

power, 40 mAh. The average current is 62.45 mA. The current is within the tolerance of our circuits and the microchip. We also calculated the charging time. To do this, we recorded the time it took to charge the battery fully three times. The average time for charging for the 40 mAh battery is 18 minutes and 50 seconds, which is less than the half time of discharging. Since our battery disconnects from our device, we can adjust the capacity. For example, other options that are compatible with our device are 110 mAh, 400 mAh, and 850 mAh. The drawback with increasing the capacity is that the size of the battery also increases. While the 110 mAh battery is only marginally larger than the 40 mAh, the 400 mAh and 850 mAh are more than double the size.

4.6 Conclusion

In this chapter, we proposed three models that can be used in succession to calculate knee angles given a voltage reading. Given a voltage reading, we first calculate the change in resistance of our conductive fabric, then its change in length, and finally the knee angle. We present TracKnee a sensing knee sleeve made with a conductive fabric sensor that unobtrusively measures knee angles. We created TracKnee device while keeping in mind the comfort of the user. Because of this, we made sure the device was comfortable, unobtrusive, and washable. We ran a user study in which we collected data on 240 knee angles from six individuals. We used this data to calculate knee angles using our models. Our results show that our model is 94.86% accurate to the nearest 15th degree angle and that our average error per angle is 3.69°.

Chapter 5

ServesUp: Using Wearables to Improve the Volleyball Serve

5.1 Introduction

Watching and analyzing film is a key way to help a volleyball player improve their skills. Video analysis for just one player during one game can take several hours [77]. With a minimum of six players on an indoor court, it quickly becomes very time consuming for a coach to watch film with all of their players. As teams get more competitive, they generally carry more players. Many college level teams carry upwards of fifteen athletes at the time. On average, ten players play per game. Work towards fully automatic analysis can decrease the need to watch game film and allow the athlete to spend more time actually improving their skills.

In volleyball, the serve is one of the most important skills. It is the first move of the game and players or teams that cannot serve well do not find success in the sport. As players become more skilled, their serve becomes more varied and specialized. The main progressions of the volleyball serve are the float serve and the top spin serve which can be

combined with a jump. This makes classification and evaluation of serves more difficult.

In this chapter, we answer the following research questions:

RQ1: How can we accurately classify the volleyball serve using a wearable device?

RQ2: How do we design a wearable device that is comfortable and unobtrusive to wear when playing volleyball?

To determine how accurately we can classify serves with our wearable device, we perform a user study in which 1000 serves are performed. Then, we extract features to describe a single serve from each of the sensors attached to the sensing shirt. Finally, we feed these features in various classifiers. From this, we see a classification accuracy of 89%.

To understand how to design and create a comfortable and unobtrusive wearable device that can be worn during volleyball play, we created a device that we call the sensing shirt. This shirt can be worn as a normal athletic shirt would be worn. All the sensors are made from fabric and all the wires are made of thread. Because there are no rigid sensing devices on joints of the body it does not impede the movement of the athlete. The shirt is as washable as all non-water soluble components are removable.

Sensing research into the sport of volleyball has just begun to be explored [106, 48, 103]. Research into volleyball has been focused on injury prevention and distinguishing the professional players from the amateurs [16, 68]. Human activity recognition has been well explored in sports and daily life [18, 114, 164, 88, 112]. Wearable and E-textile sensors have made great advancement in recent years [74, 98, 76]. In this chapter, we combine the advancements made in wearables with the research done into volleyball.

Our contributions are summarized as follows:

- We designed and implemented a wearable device, called the sensing shirt, with sensors embedded into the fabric of a shirt to recognize volleyball serve in real time.

- We collected data using our shirt on 1000 serves collected from 10 volleyball players. We developed a classifier that achieves 89% serve classification accuracy.

The remainder of this chapter is structured as follows. First, we will discuss the design of our sensing shirt prototype. Then, we will discuss our user study and results from it. Finally, we will wrap up with a discussion of future work and summarize with a conclusion.



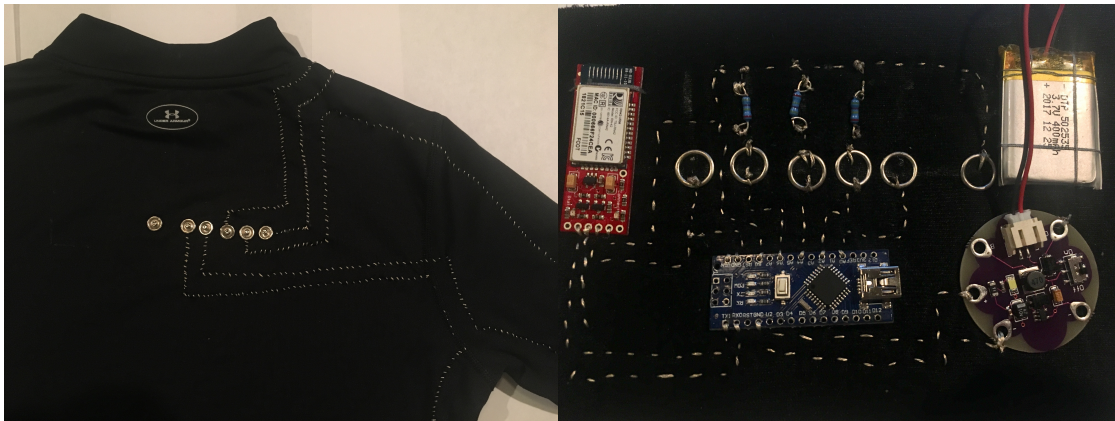
Figure 5.1: Sensing Shirt

5.2 Prototype Design: Sensing Shirt

We designed our sensing shirt such that it does not impede the player's serve, is comfortable to wear while playing volleyball, has enough battery life to make it through a three-hour volleyball practice, and is durable enough to last through common volleyball movements such as diving. The sensing shirt must also be washable as we expect the players to sweat during practice. To make our shirt washable, we designed our shirt in two parts: the control swatch and the sensor shirt. This allows separation so that the rigid non-water soluble components are easily removed from the shirt.

5.2.1 Control Switch

The control switch holds all of the rigid electronic components. It is not washable so it is made to be detachable from the main shirt. In total, it is four inches long by five inches wide and is attached in the upper middle back.



(a) The control switch is attached to the upper back by the six snaps. (b) Non-washable components that is attached by snaps to the upper back to the shirt.

Figure 5.2: Control Switch and its Attachment Location

5.2.1.1 Components

The components are the microcontroller, Bluetooth chip, resistors, power supply booster, and battery as shown in figure 5.2b. The controller is an Arduino Nano development board [11] featuring an ATmega328P processor. Sensor readings are collected at 100 hz and then transmitted to a mobile device by a SparkFun BlueSMiRF Silver [179]. The sensing shirt is powered by a rechargeable 400 mA lithium battery. This battery outputs 3.7 volts. Since the Arduino Nano operates at five volts, we use a Lilypad LiPower microchip [181] to boost the voltage of the battery from 3.7 volts to five volts. This battery last through a three-hour practice. All of the components are sewn onto a thin layer of foam to give the user some cushion from the rigid electronic components. Because the stitches go through both sides of foam, an insulating layer is attached to the back for the control switch to prevent any shorts from occurring.

5.2.1.2 Connection

To make the sensing shirt washable, the control swatch must be removable while allowing for easy reconnection to the sensors on the shirt. To accomplish this we used conductive nickel snaps to connect the control swatch to the shirt and the sensors to the microcontroller. For each sensor, we have a connection to ground and its analog pin. We do this with the use of six snaps as shown in figure [5.2a](#). On the control swatch, we also have a resistor for each sensor. These resistors connect to power and a corresponding analog pin. We chose resistors that are between the minimum and maximum resistance for each sensor. All four resistors used are 470 kohms.

5.2.1.3 Conductive Thread Wiring

We use Syscom Advanced Materials' Amberstrand, a conductive thread [\[185\]](#), instead of traditional wires to connect the electronic components of our control swatch. We chose this thread because it has a resistance of one ohm/foot and is solderable. It is made from Zylon, which is very high in tensile strength and is resistant to heat [\[191\]](#). It is coated in a combination of silver, copper, and nickel to make it conductive. To connect the thread to the microcontroller and the Bluetooth chip, we knotted the thread around the pin and then solder it in place. To connect the thread to the resistors, we shaped the end of the resistors into a loop and cut off the remaining portion. Then we sewed through the loop, wrapped the conductive thread around the loop and tied it off. To connect the thread to the snaps, we sewed a star pattern under where the snap would be connected. We then popped the snap on over top of the conductive thread star. Any fraying of the thread can be secured by solder.

5.2.2 Sensor Shirt

The sensor shirt contains only components that can be washed. Overall, it contains the conductive fabric bend sensors, conductive thread wiring, and snaps to connect the

control panel. We chose an Underarmour Coldgear shirt [192] as the base for our project as it is skin tight and will stretch as elbow and shoulder move.



Figure 5.3: Sensor Placement Inside of Sensing Shirt

5.2.2.1 Conductive Fabric Bend Sensors

In our design, we wanted a shirt that monitors a volleyball player's serve without impeding the athlete in any way. To do this, we created our sensors from conductive fabric. When the conductive fabric stretches, there is a change in the resistance of the conductive fabric. We chose EeonTex Conductive Stretchable Fabric [63] as it is made of a blend of nylon and spandex, is coated with a conductive polymer, and has a resistance of $10E4$ to $10E7$ Ohm/sq ft. This fabric blend is similar to common athletic fabrics giving it a similar feel and movement to athletic clothing. This fabric is also washable and does not show any noticeable resistivity increase after thirty wash cycles. We attach the conductive fabric on the inside of the shirt with a non-conductive fabric adhesive [57].

Our sensing shirt was designed to model two joints: the elbow and the shoulder. To monitor the motions of these joints we must place the conductive fabric sensor in locations

where it will be stretched. When the fabric is stretched a drop in resistance is observed. We adjusted the length and width of each fabric sensor by its location in the shirt, resistance change when stretched, and warp recovery. We will start by discussing the elbow sensor and then we will discuss the shoulder sensors.



(a) Elbow Measurement Markings

(b) Experimental Setup

Figure 5.4: Elbow Sensor Design

Elbow: The elbow is a hinge joint with a single degree of motion. To monitor this joint we attach a single fabric sensor to the shirt on the back of the elbow. To size the sensor correctly we consider the following factors: the size of the elbow and the warp recovery and resistance change of the fabric at different lengths.

Fabric Length (inches)	Number of Stretches
4	2
5	4
6	100
7	100
8	100

Table 5.1: Fabric Warping

To size the width of the sensor, we measured the author’s elbow. Their elbow was two inches wide. This influences our length and width sizes for the fabric. For this sensor, we do not exceed the width of the elbow. The sensor should also be wide enough that it will

always cover the smallest point on the elbow, also known as the olecranon. Our author's olecranon measured one inch wide. To allow for some sensor movement, we set the fabric width to one and a half inches.

To determine the length of the fabric, we first found a minimum and maximum length for the elbow sensor. To determine the minimum, we measured the end of the author's elbow when bent and then added an inch to each side so that the sensor could be attached to the arm. The end of the author's elbow measure two inches in length and with the added inch on each side, we had a minimum of four inches for the sensor. To determine the maximum length of the sensor, we measured the original size of the piece of conductive fabric. Because it was eight inches long at its longest, our maximum length for the sensor was eight inches. To set the length from here, we looked at two factors: the warp recovery and the change in resistance.

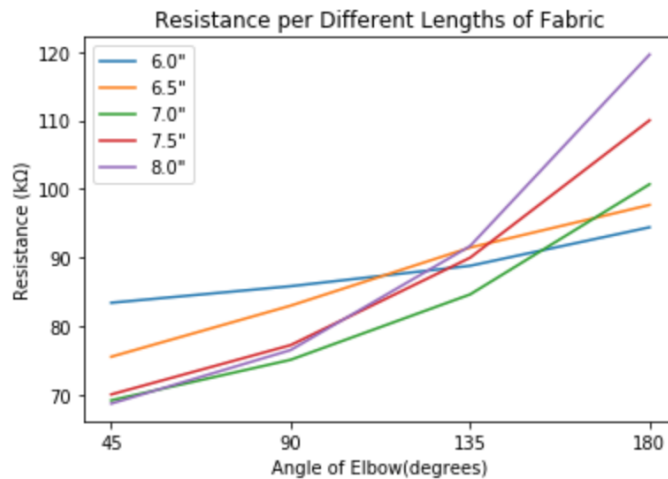


Figure 5.5: Resistance Change of Conductive Fabric for Elbow

To test the warp recovery, we must first know how far the fabric will need to be stretched. To do this, we put two points of reference on the arm as shown in figure [5.4a](#). Then, we straighten the arm and measure the distance between the points with a cloth ruler. Next, we bend the elbow all the way and measure again. The difference in the two measurements was 2.125 inches. To test the warp recovery, we will repeatedly stretch our

fabric 2.125 inches and measure the size it returns to. Once the fabric no longer returns to its original dimension, we will record the number of stretches completed. If a piece of fabric can be stretch one hundred times without warping, we will record one hundred stretches and end the test there. We tested fabrics between the already determined minimum and maximum length at one inch intervals. The results of this are shown in table [5.1](#). From this table, we can easily tell that the four and five inch pieces of fabric warped almost immediately while the six, seven, and eight inch pieces of fabrics could be stretched one hundred times without any warping.

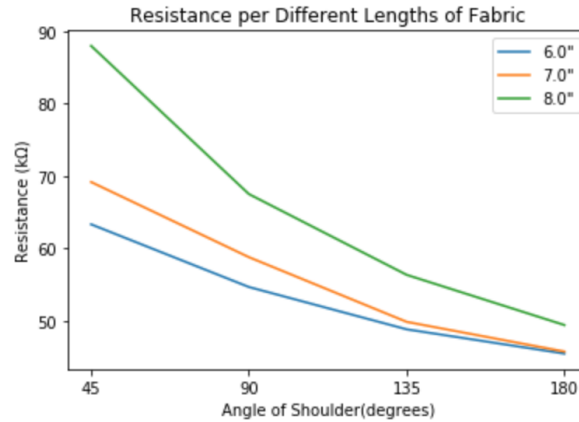


Figure 5.6: Resistance Change of Conductive Fabric for Shoulder

Following this, we tested the change in resistance of the different lengths of fabric. For our pieces of fabric, we used the preset width of 1.5 inches. To test the change in resistance, we tested fabrics between the already determined six inches and eight inches at half inch intervals. We test these pieces of fabric across four different angles of the elbow: 45 degrees, 90 degrees, 135 degrees, and 180 degrees. We calculate the distance the fabric will have to stretch when it is at each angle by once again marking two points of reference and measuring the distance with a fabric ruler. We measure the angle of the elbow using a Goniometer [133](#). We attached the leads from a multimeter to each end of the piece of fabric and recorded the resistance as we stretched the fabric to the lengths that correspond with our four tested angles. This is shown in figure [5.4b](#). We stretch each

piece of fabric to each angle five times. We averaged the resistance and displayed it in figure [5.5](#). From this graph, we can see that there is a smaller change in resistance for the six and 6.5 inch piece of fabric. All pieces of fabric above a length of 6.5 inches have a noticeable change in resistance. To maximize the comfortability of wearing the sensing shirt, we decided to keep the sensors as small as possible. Because of this, we set the length of our elbow sensor at seven inches. The final sensor is shown in figure [5.3c](#).

Shoulder: The shoulder, being a ball and socket joint has a more complicated movement profile. Because of this, we will need more than one sensor to monitor all of the motions. To place the sensors, we leveraged athletic training knowledge of the shoulder. Our sensor location choices are influenced by a common method of applying Kinesio tape to the shoulder [71](#). We follow the tape locations as shown and attached a sensor on the front and back of the shoulder. Since the sensors will be placed in close proximity, we must limit the width of these sensors. We also measured the distance from the underarm to the top of the shoulder on the author. This distance was 3.5 inches and since we needed space for wiring, we left an inch of space on each side of the sensor. The space in the middle would be shared by both sensors. These sensors are shown in figure [5.3a](#).

This allowed us to monitor the front and back movement of the shoulder joint but not the up and down. To do that, we placed a sensor on the underarm. We measured across the author's underarm and it was four inches wide. This gives us the ability to place a wider sensor than the elbow or the top of the shoulder. We chose a sensor width of 2.5 inches so that we would still have 0.75 inches for wiring on each side of the sensor. To determine the length of this sensor, we performed an experiment on the change in resistance in which we tested fabric lengths between the six inches and eight inches at inch intervals. We attached the leads from a multimeter to each end of the piece of fabric being tested and recorded the resistance as we stretched the fabric to the lengths that correspond with our four tested angles. The angles we tested were: 45 degrees, 90 degrees, 135 degrees, and 180 degrees. This is shown in figure [5.6](#). From this graph, we see that the eight inch long piece of fabric has more change in resistance so we chose that length.



(a) Straight and Zig-Zag Stitch

(b) Connection Point

Figure 5.7: Stitch Patterns and Connections Points

5.2.2.2 Conductive Thread Wiring

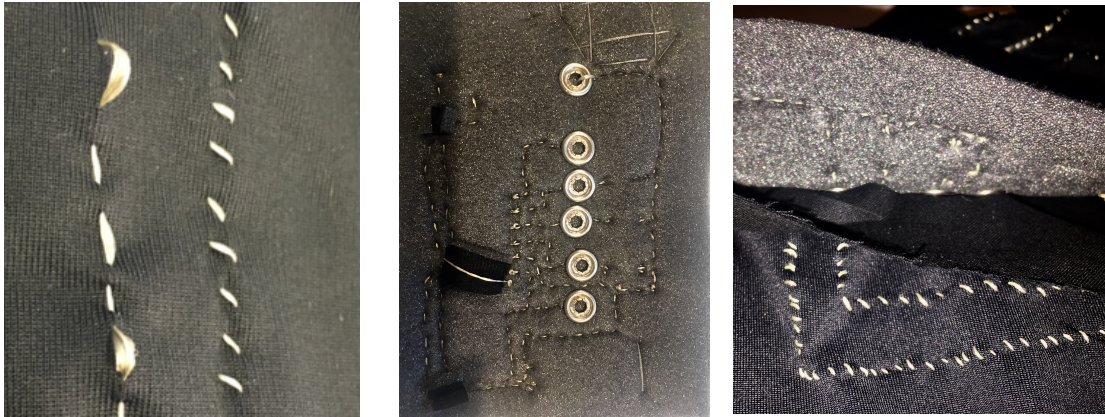
To keep the shirt washable, flexible, and comfortable for the players to use, we forgo wires in this project and instead use conductive thread. We chose Syscom Advanced Materials' Amberstrand as our conductive thread as it has a resistance of one ohm/foot and is solderable. This thread is made from Zylon and is coated in a combination of silver, copper, and nickel. To prevent the thread from breaking when stretched, we sew it into the fabric of the garment in a zig-zag pattern. When the thread is sewn into the seams of the garment, it can be sewn in a straight line. The patterns of the stitches are shown in figure [5.7a](#). To attach the thread to each sensor, we sew through the middle of the end of each sensor and knot the thread at the end. This is shown in figure [5.7b](#).

5.2.3 Lessons Learned

Through the process of designing the prototype for the sensing shirt, we learned some lessons. The most important were the choices of conductive thread, using different stitch patterns in different fabrics, and how to appropriately create bridges and barrier layers to prevent short circuits.

5.2.3.1 Conductive Thread Choices

Originally, we chose a commonly used stainless steel conductive thread [180]. It had a resistance of twenty-seven ohms/meter. While this thread was very smooth and did not have frayed hairs, we were not able to accurately read the data coming from the elbow sensor. To fix this, we replaced this thread with the Syscom Advanced Materials' Amberstrand that had a lower resistance of one ohm/foot.



(a) Straight and zig-zag stitch after being stretched. (b) Bridges are used to prevent short circuits. (c) Barrier layer to prevent short circuits.

Figure 5.8: Lessons Learned

5.2.3.2 Conductive Thread Stitch Patterns

There are many stitch patterns that can be used when sewing conductive thread. The two stitches we used in our prototype are a zig-zag pattern and a straight stitch. These stitches are shown in figure 5.7a. In different types of fabrics, different stitches should be used. In our project, we sewed through a thin foam and a stretchy shirt made of eighty-seven percent Polyester and thirteen percent Elastane [192]. In the non-stretchy foam, a straight stitch was used. In the stretchy shirt, we used a zig-zag pattern so that when the shirt was stretched, the seams would stretch with it. In the beginning, we tested a straight stitch in the shirt and individual stitches would pop up as shown in figure 5.8a. This allowed for more short circuits to occur. Further, we learned that the seams in the

Underarmour shirt were not a stretchy as the main fabric. Because of this, it was more effective to use a straight stitch when sewing through these.

5.2.3.3 Bridges and Barrier Layers

In some situations, crossing over an already made stitch is unavoidable. When this happened, we used bridges and barrier layers to prevent two different conductive thread wires from crossing and short circuits from happening. This happened repeatedly on the control swatch between the Arduino nano, the Bluetooth chip, and the power booster. We used three bridges to prevent short circuits as shown in figure [5.8b](#). To create a bridge, we took an additional piece of foam, cut it down to the size of the needed stitch. From there we stitched over the foam and pulled the stitch tight. This locked the bridge into place. Since the back of the control swatch contained exposed conductive thread that could create a short when attached to the sensing shirt, we added a barrier layer. The barrier layer is made of a non-conductive cotton. This prevents shorts from occurring when the control swatch is connected. This layer is shown in figure [5.8c](#). In the final prototype design, the layer of cotton fabric shown in the middle is sewn onto the back of the control swatch.

5.3 User Study

In this section, we discuss the setup of our user study. We will detail the equipment used, parameters followed, drills chosen, and the demographics of our subject.

5.3.1 Equipment

During our study, the participants wore the sensing shirt as they would normally wear an athletic shirt. Beyond the sensing shirt, the participants were asked to dress as they normally do when playing volleyball. We collected data from all four sensors in the shirt. We sent this data over Bluetooth to a Google Pixel 2 [79](#). During the data collection

process, we took video of the participant's serve for post analysis on an iPhone 6s [9] recording 1080p video at thirty frames per second. In the gym, we also provided a cart of volleyballs and a standard women's height volleyball net with pads and antennas.

5.3.2 Parameters

We conducted our study in various gyms in the area surrounding our college. When the participant arrived for the user study, they were handed a questionnaire. In this questionnaire, we asked for a basic set of demographics: age, gender, height, and weight. We also ask for statistics more specific to our wearable device: upper arm length, lower arm length, and the distance from control swatch to the participant's rotator cuff. Additionally, we ask the following free response questions:

1. For how many years have you played volleyball?
2. How frequently do you play?
3. What is the highest level of volleyball that you have played?
4. What position(s) do you play?
5. What kind of volleyball do you play? Grass, Beach, Indoor, Indoor Sand, Other
6. Which arm is your hitting arm? Right, Left, Ambidextrous
7. Do you own any smart fitness devices? Yes or No. If Yes, what devices?
8. Are there any smart fitness devices that you want to own? Yes or No. If Yes, what devices?

Then we ask the participants to participate in four common volleyball drills that will be discussed in the next subsection. Once the participant completes their volleyball drills, they are given the following questionnaire:

1. Does this device help you in any way? 1-very unhelpful 2 -unhelpful 3 -neutral 4-helpful 5-very helpful. Explain
2. How comfortable would you be wearing our device in a game or practice environment? 1-very unhelpful 2 -unhelpful 3 -neutral 4-helpful 5-very helpful. Explain
3. Any feedback on how to further improve this device?
4. Any other comments?

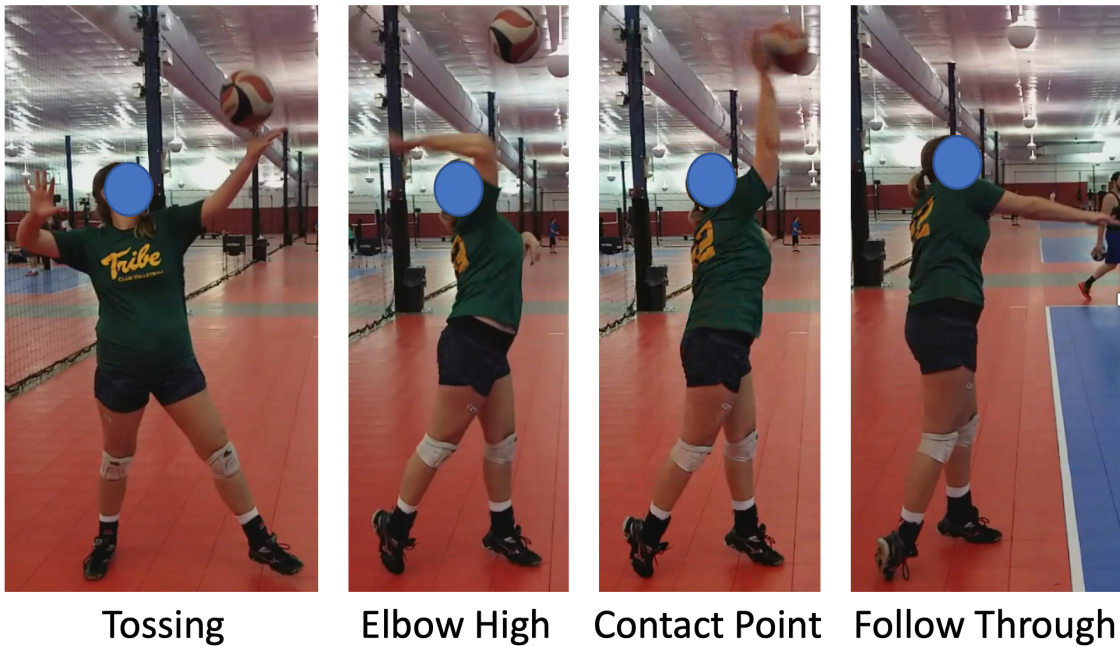


Figure 5.9: Progression of the Volleyball Serve

5.3.3 Demographics

We recruited our study participants from our college and surrounding volleyball communities. Our user study consisted of ten participants with an age range of 19-35 and an average age of 26.5 years. On average, the participants were 5'10" with a BMI of 18.5. All participants were female. They were all right hand dominant so that the current

shirt would record their data. The participants had between 8 and 23 years of volleyball experience and had played at the college to professional level.

5.4 Results

In our user study, we analyze a total of 1000 volleyball serves. The serves were recorded via video camera and sensing shirt while the athlete served a ball from the service line of an indoor court. The serve did not have to go over the net or in the court to count. We had a volleyball coach manually label the frames of video data that include the serve. We use the first serve on video and in the data to align the marked video ground truth with the sensor data.

5.4.1 Serve Classification

	Tossing	Elbow High	Contact Point	Follow Through
Underarm	Stretch	Stretch	Stretch	
Elbow	Stretch	Stretch		
Shoulder Front	Stretch	Stretch		
Shoulder Back		Stretch	Stretch	Stretch

Table 5.2: Sensor Stretch Progression During a Serve

When an serve is broken down into individual motions, it follows this process: First, the elbow bends. Then, the hand is lifted above the head while the hand faces out. At this point, an athlete’s form should look similar to the tossing portion of figure [5.9](#). Next, the athlete starts to swing forward. During this, the elbow straightens and moves from behind the athletes head to in front. Finally, the athlete finishes their serve during which their hand and elbow drop back below the shoulder. In table [5.2](#) we show which sensor stretches as an athlete progresses through the motions of the serve as shown in figure [5.9](#). As we can see in the figure, at the beginning of a serve, the underarm, elbow, and front of the shoulder sensor are stretched. As the arm swings forward, the back of the shoulder

stretches. When the ball is contacted, the elbow and front of the shoulder relax. As the serve is completed and the athlete goes back to a resting position, the underarm and then the shoulder back relax.

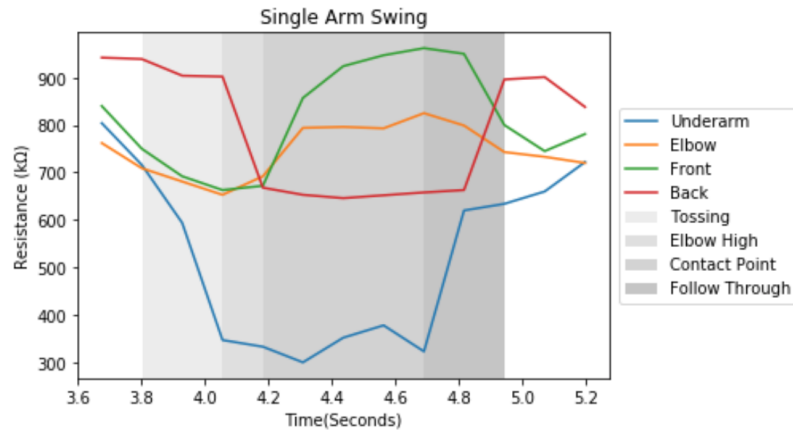


Figure 5.10: Sensing Shirt Readings for a Single Serve

We can compare these serve insights to the raw data read from our sensing shirt on a serve. This is shown in figure 5.10. As a sensor is stretched, the resistance decreases. As a sensor relaxes, its resistance increases. In figure 5.10, all sensors start in a relaxed state. We marked the different phases of the serve as discussed on this figure. From this, we can clearly see that the sensors that should intuitively be stretching in each phase are in fact stretching.

5.4.1.1 Naive Serve Classifier

We built this classifier such that it could run locally on the sensing shirt. To build our intuitive serve classifier, we need to know two pieces of information: when an serve begins and the maximum length. From the analysis above, we know that a serve begins with a stretch in the underarm, elbow, and shoulder front sensors. So, we will scan the incoming underarm data for a reading that crosses a set threshold. We calculated this threshold by taking the maximum value in kΩ for the initial stretch for the dataset where our participant was hitting against the wall. This threshold is set to 416 kΩ. Next,

we calculated the size of our window for classification. The maximum serve length was 1.66 seconds. To account for the possibility of longer serves we round up the maximum length to two seconds. To test this code on our dataset, we wrote a version in python and compared its results to the ground truth. Overall, our naive classifier was 87.25% accurate at classifying serves.

5.4.1.2 Weka Serve Classifiers

We classify serves using data from all four sensors on the sensing shirt. To do this, we use a sliding window with a size of 2000 milliseconds that moves right by 1000 milliseconds each time. We set the size to be 2000 milliseconds by calculating the maximum length of a serve from our user study data.

Classifier	Precision	Recall	F-Measure
Random Forest	84.5	84.5	84.5
Random Tree	86.9	86.7	86.8
SMO	87.5	87.9	87.1
Nearest Neighbor	89.1	89.3	89.0
Logistic	82.8	83.1	82.6

Table 5.3: Evaluation of Classifiers

We used the Weka Data Mining Software to create additional classifiers for serves. We evaluated these classifiers on three metrics: precision, recall, and f-measure. The results of the evaluation of these classifiers are shown in Table [7.1](#). From the results, we saw that the nearest neighbor model outperformed the rest in all the metrics.

5.4.2 Results from Questionnaires

We administered a questionnaire before the participant participated in our user study performed the requested volleyball skills. This questionnaire helped us to gauge the participant’s volleyball experience and familiarity with wearable fitness devices. Here are the results from that questionnaire. Our participant was very experienced and had played

volleyball for fifteen years. She played two to three times a week on average at a semi-professional level so her skills are still at a high level. She also plays four types of volleyball: grass, beach, indoor, and indoor sand. She is interested in smart fitness devices and owns a Polar Edge heart rate monitor and a Fitbit. She would like to own a VERT jump tracker.

After the participant performed the requested volleyball skills we gave her a second questionnaire. This questionnaire allowed us to gauge the user's experience with our sensing shirt. The results are as follows. On a scale of one to five for helpfulness, she rated the device as a four. Our participant was helped by the device because "knowing that I'm being monitored makes me think more about my form". On a scale of one to five for comfort with five being the most comfortable, our participant rated us a five stating that it "feels just like a normal athletic shirt". She also gave us feedback on how to further improve our sensing shirt. Her recommendation was to implement a version of the shirt in a more heat friendly fabric instead of Underarmour ColdGear.

5.5 Discussion and Future Work

5.5.1 Evaluating the System on Other Volleyball Players

Our user study focused on a single semi-professional volleyball player with fifteen years of experience playing volleyball. In future work, we plan to expand this study to multiple volleyball players of many different positions and genders. To do this, we would need to create sensing shirts in a range of sizes and in styles that suit both men and women. Another expansion of this study will be to create a shirt that can monitor left handed players and even ambidextrous players.

5.5.2 Sensing Shirt Upgrade

While we have a working prototype of the sensing shirt, we can still work to improve the design. The sensing shirt can be improved in two main ways. First, we can shrink the

size of the control swatch. Second, we can test out new kinds of fabric for more accurate stretch sensors.

The control swatch on our sensing shirt has three separate microchips and a battery. This can be reduced. The requirements for the swatch are Bluetooth connectivity, battery power, and four analog ports. To shrink the size of the control swatch, we will look to find microchips that combine functionality. One such microchip is the Bluno Beetle [24]. It is an Arduino based board that already incorporates Bluetooth technology and it has four analog pins. Switching to this microchip will allow us to remove all of the wiring between the Bluetooth chip and the Arduino Nano. This will remove about an inch and a half of space from the right side of the control swatch, as shown in figure 5.2b. This chip will also be replacing the Arduino Nano. The Nano is eighteen millimeters by forty-five millimeters while the Bluno Beetle is twenty-nine millimeters by thirty-three millimeters. Since these sizes are similar, and the Bluno has more functionality for our project, it is a natural upgrade to the sensing shirt.

We chose EeonTex Conductive Stretchable Fabric [63] because it was readily available and common to use with wearable technology projects. This fabric also feels similar to athletic fabric so it is an obvious choice to use in our sensing shirt. But as wearable technology advances, more stretchy conductive fabrics become available. In future work, we will be exploring different conductive fabrics that can be used to increase the accuracy of each sensor. It is even possible that we can use our stretch sensors to measure the angle of each joint. We also use a spray fabric adhesive to connect the fabric to the shirt. More secure connection methods should also be explored.

5.5.3 Other Applications for the Sensing Shirt

It is possible that our shirt could be used to monitor motions in other scenarios. The easiest scenarios to expand to are monitoring other volleyball skills and monitoring motions that are similar to the volleyball serves in other sports.

Our study focused on the volleyball serve but there are many other volleyball skills

that can be monitored. Some volleyball skills such as passing and setting require both hands/arms. To monitor these skills we would need to design a shirt that monitors both arms instead of one. Designing a shirt that monitors both arms will also allow us to improve our serve detector. We would be able to not only monitor the dominant hitting arm but also the lead/tossing arm.

Our sensing shirt can also be extended to be used in other sports. The motion of throwing is very similar to the volleyball serve. It should follow that we can use our sensing shirt to monitor that motion. To test the sensing shirt's capability of classifying throwing, we can run a study with football and baseball players. Football quarterbacks and baseball pitchers should be targeted for this study as they spend the most time perfecting their throwing motion.

5.6 Conclusion

In this chapter, we presented a new sensing device that can be used to collect data for volleyball serves. The sensing shirt is comfortable, unobtrusive, and washable. The sensors are made from fabric and instead of wires, we use conductive thread. This allows for the athlete to be able to perform as they would normally without being impeded by the sensors. This makes it ideal for athletes who want to improve their skills. With our sensing shirt, we collected data on 1000 volleyball serves from ten volleyball players. We created a classifier for these serves that achieved 89% accuracy.

Chapter 6

BreathEZ: Using Smartwatches to Improve Choking First Aid

6.1 Introduction

According to the National Safety Council, choking is the fourth most likely cause of unintentional injury death accounting for 4,800 deaths in 2015 [44]. Choking incidents cause a medical condition known as cerebral hypoxia and is characterized by a lack of oxygen to the brain and causes tissue damage and cell death in as little as four to six minute [142]. Since the average emergency medical service (EMS) response time in the US is 7.51 minutes, EMS services cannot be fully relied upon in choking incidents. The quickest possible response would be from a bystander that has been trained in choking first aid.

The rate of cardiopulmonary resuscitation (CPR) trained individuals in US counties ranges from zero to fifteen percent [8] and standard CPR courses often include choking first aid training. Even among those trained in CPR and choking first aid, many individuals will not attempt to intervene during a choking incident due to a phenomenon colloquially called the “bystander effect”. The bystander effect occurs when individuals in a group believe that another onlooker must be more qualified than themselves to offer aid and so

they refuse to intervene which often results in no aid being provided at all [50]. To help combat this effect, we hypothesize that many would be more comfortable and willing to perform a life saving first aid procedure if they were to receive real-time guidance and encouragement.

Ubiquitous computing devices such as the smartphone and smartwatch may provide an ideal medium for delivering real-time, life saving first aid coaching to improve bystander assistance. Current smart devices are equipped with an array of sensors (i.e. accelerometer, gyroscope, etc.) which can be exploited to determine the quality of a bystander's performance of a particular first aid technique in order to provide instant feedback to help and encourage them. Because smartwatches are unobtrusive, easy to use, and readily available on the wrist, they may be particularly effective tools to help bystanders perform choking first aid.

We answer the following research questions in this chapter:

- How accurately can we classify abdominal thrusts?
- Does the assistance of a smartwatch application that provides live feedback to the user increase the performance of the abdominal thrust portion of choking first aid?
- Does the assistance of a smartwatch application that provides live feedback to the user increase an individual's willingness to perform choking first aid?

To determine how accurately abdominal thrusts can be classified, we collected choking first aid data and used a random forest to classify each abdominal thrust. We collected data by performing three separate user studies, one of which consists of data collected from only those with formal training in choking first aid. We then analyzed the data using the Weka toolkit [91] and found that by using a random forest we could accurately classify abdominal thrusts at a rate of 94.6%.

To understand if a smartwatch application that provides live feedback to the user increases the performance of the abdominal thrust portion of choking first aid, we compared

the performance of our participants based on whether they were given a smartwatch application that provides feedback on choking first aid or shown a choking first aid tutorial prior to being asked to perform choking first aid. To accomplish this we develop BreathEZ, a smartwatch application that not only provides real time feedback to a user on choking first aid, but also attempts to combat the bystander effect and provide timely assistance to an individual who is choking. To begin we asked each participant to give their best effort performing choking first aid. Then we split the participants of our final user study into two groups, group 1 was given BreathEZ while group 2 was shown a video tutorial.

To quantify whether people are more willing to perform choking first aid with the use of a smartwatch and decrease their fear of injuring the choking victim, we add questionnaires to our user study. In these questionnaires we ask each participant to quantify their comfort and willingness on a scale of one to five by administering a questionnaire before and after they perform choking first aid. We compared how each group improved and found that while both groups improved, group 1 saw greater improvement in their comfort, willingness, and performance of choking first aid.

To date, a system that monitors and provides feedback on choking first aid has not been developed. Abdominal thrusts combined with back blows is the recommended treatment if someone is choking [3]. Zoll Medical corporation designed a handheld device for first aid training using several accelerometers to monitor abdominal thrusts [190]. To improve the performance of a CPR, Gruernerbl et al. [85] developed a smartwatch application that provides live user feedback. Our BreathEZ smartwatch application combines these two approaches by providing live feedback on the abdominal thrust portion of choking first aid. It also goes beyond and provides recommended instructions for choking first aid. Other types of first aid have also been improved with the use of smartwatches, smartphones, and newly developed devices [171, 101, 123, 149]. An approach of using games to help improve the performance of first aid has also been taken [34, 51].

Our contributions may be summarized as follows:

- We introduce BreathEZ, a smartwatch application that improves choking first aid by providing auditory and tactile feedback to the user and improves bystander performance of abdominal thrusts as part of choking first aid.
- We conduct two user studies with the first comprised of 135 abdominal thrusts from 13 individuals and the second comprised of 100 abdominal thrusts from 10 individuals. Short surveys were administered to gain insight on the viability of using BreathEZ in real world scenarios.
- We present a model describing abdominal thrust performance using number and quality of the abdominal thrusts which are used to coach the user while they are performing choking first aid.

The remainder of this chapter is divided into six sections. We begin with a background of choking first aid, a discussion of our pre-user study, and the feasibility of using a smartwatch to assist in the performance of choking first aid. Following that we detail our system design and the evaluation of that system, then continue on to our BreathEZ application and the results of a user study in which it was used. Finally we discuss future work and summarize with our conclusion.

6.2 Pre-User Study

To evaluate the usefulness and effectiveness of our application, we performed a pre-user study in which participants were asked to perform abdominal thrusts on a CPR training manikin while wearing a Motorola 360 smartwatch. The CPR training manikin known as the “Annie” training manikin [115], shown in Figure 6.1 is the standard training manikin used in First Aid Training courses.

6.2.1 Choking First Aid Background

To prevent complications from choking incidents such as cerebral hypoxia, choking first aid should be administered immediately after the victim is confirmed to be choking and consent to administer aid is given. From here we refer to the individual receiving choking first aid as the victim and the individual administering choking first aid as the first aid provider. The American Red Cross recommends this treatment [3], which we quoted in the following bullets, for choking victims who are conscious and either standing or sitting:

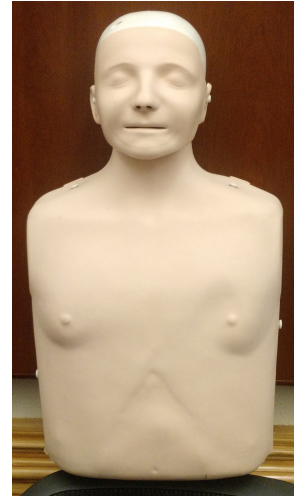


Figure 6.1: CPR Training Manikin

- “After checking the scene and the victim, have someone call 911 and get consent to perform first aid.”
- “Bend the victim forward at the waist and give five back blows between the shoulder blades with the heel of one hand.”
- “Place a fist with the thumb side against the middle of the victim’s abdomen, just above the navel. Cover your fist with your other hand. Give five quick, upward abdominal thrusts.”
- “Continue sets of five back blows and five abdominal thrusts until the, object is forced out, the victim can cough forcefully, breathe, or the person becomes unconscious.”

In this chapter, we focus on the abdominal thrust portion of choking first and discuss back blows in the future work section. Abdominal thrusts are also known to many as the “Heimlich Maneuver”. The “Heimlich Maneuver” was developed by Dr. Henry Heimlich and was first published in 1979 [93].

The above recommended choking treatment is for adults and children large enough that you can stand or kneel behind them. We do not address choking first aid for infants

in our solution. We discuss the recommended treatment for infants in the related work and how we can add this to our solution in discussion and future work.

6.2.2 Study Design

The study group participants were students recruited from the College of William and Mary. No incentives were garnered by our participants for their participation in our study. In total, we collected 105 recordings of abdominal thrusts from seven participants, three female and four male. The average participant age was 21 with a standard deviation of 6. Prior to this study, four participants had completed choking first aid training.

Pre-Study Questionnaire First, each user was asked to fill out a questionnaire with the following questions:

1. Have you had abdominal thrust or Heimlich maneuver training? Yes or No. If yes, why?
2. On a scale of 1-5, how comfortable are you performing abdominal thrusts?
3. Is the topic of the study (bystander abdominal thrusts) relevant for you personally? Yes or No. If yes, why?
4. On a scale of 1-5, how willing are you to perform abdominal thrusts?
5. On a scale of 1-5, how familiar are you with a smartwatch?

We asked these questions to assess each participant's previous experience with abdominal thrust training and their willingness to perform abdominal thrusts.

Three Scenarios for Abdominal Thrusts Next, each study participant was asked to perform abdominal thrust first aid in three different scenarios. We designed our scenarios to test our users basic knowledge of abdominal thrusts and determine if their performance and confidence improved when given instructions to follow. First we test their untrained

knowledge of abdominal thrusts. Following this, we show them a tutorial and test their performance again. Then we test their retention of the knowledge gained from the tutorial. It takes each participant no more than ten minutes to complete the three scenarios. Each participant performs five abdominal thrusts per scenario for a total of 15 abdominal thrusts per individual per study.

1. Without training: In the first scenario, each participant was asked to perform abdominal thrusts to the best of their ability without help from a video tutorial.
2. With the video tutorial: In the second scenario, each participant was shown a video tutorial on the correct way to perform abdominal thrusts and was then asked to perform abdominal thrusts.
3. With knowledge gained from training: In the third and final scenario, each participant was again asked to perform abdominal thrusts without the aid of the video tutorial.

Data Recording For our study, we chose to use a smartwatch as it is a consumer available device that allows the wearer to be hands free when performing first aid and will also provide us with the ability to convey feedback to the user through the screen. We recorded the accelerometer and gyroscope data from the smartwatch during the study using WristSensors [108], an Android smartwatch application. The data was written to a CSV file and stored on a connected Android smartphone. The average file size was 107 MB.

Post-Study Questionnaire Following these scenarios, the participant was asked to fill out the following questionnaire:

1. Did the smartwatch irritate you? Yes or No. If yes, why?

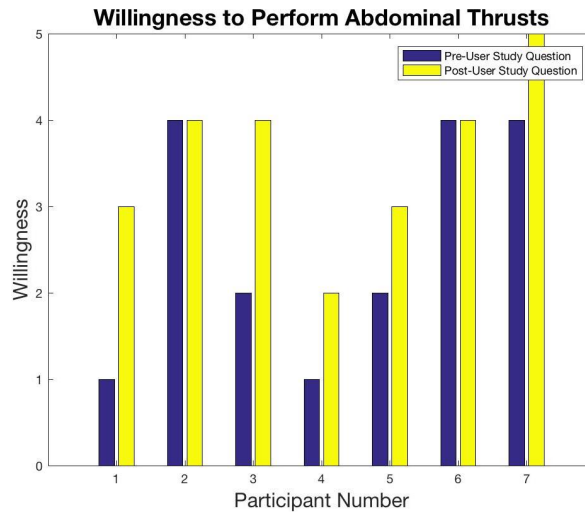


Figure 6.2: Participant Willingness

2. On a scale of 1-5, how willing are you to perform abdominal thrusts using a smartwatch with our app?
3. Did you feel that you performed abdominal thrusts better with the smartwatch? Yes or No. If yes, why?
4. Would using the smartwatch with our app reduce your fear of injuring the person you are performing abdominal thrust on? Yes or No. If yes, why?
5. If you had a smartwatch, would you install our app? Yes or No. If yes, why?

We use these questions to assess any changes in their comfort level and likelihood of performing first aid on choking victims as well as their familiarity with smartwatches.

6.2.3 Results

With this user study, we gauge the effectiveness of a smartwatch as a tool for assisting in the performance of abdominal thrusts, if a smartwatch application would combat the bystander effect, and finally if it will increase a participant’s willingness to perform choking first aid. Of our seven participants, six had no experience with smartwatches. After

performing abdominal thrusts we surveyed all participants to determine if the smartwatch was a cause for irritation. None of the participants reported irritation because of the smartwatch and six of the seven participants would install a smartwatch application that provided real time feedback during their performance of choking first aid if they owned a smartwatch.

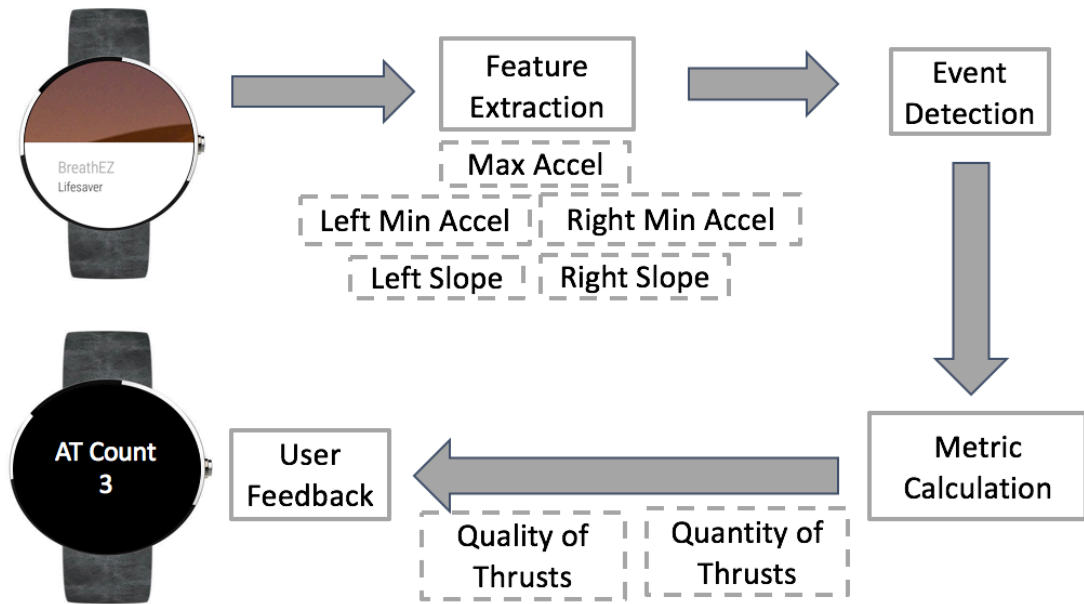


Figure 6.3: System Architecture for BreathEZ

We evaluated each participant’s comfort and willingness to perform abdominal thrusts both with and without the aid of an instructional video and show the results in Figure 6.2. Here we see that no matter what level of training the participant came in with, no participant was less willing to perform choking first aid and the mean level of willingness increased by one. From this user study, we see that our participants are not only comfortable with using a smartwatch while performing choking first aid but also are more willing to perform it. This shows that it is possible that a smartwatch application could help to combat the bystander effect and provide an individual with the knowledge and confidence required to help save a life.

6.3 System Design

In this section, we describe the design of BreathEZ. BreathEZ is a smartwatch application that assists users in the performance of choking first aid by providing instructions and feedback on abdominal thrusts. First, we discuss the System architecture. Then we discuss each of the features we extract to detect an abdominal thrust event. Following this we describe the metrics used to quantify how well our users performed each abdominal thrust.

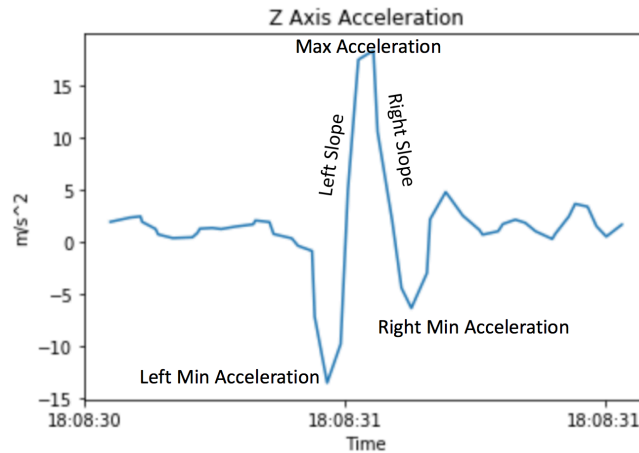


Figure 6.4: Abdominal Thrust Features

6.3.1 System Architecture

In order for BreathEZ to classify abdominal thrusts and provide feedback on choking first aid, it must perform several tasks. First, BreathEZ must acquire data from the smartwatch accelerometer. Next, the application extracts five features that will be used to detect an abdominal thrust event. To detect this event, the features will be fed into a random forest classifier and it will classify the event as either Abdominal Thrust (AT) or Not Abdominal Thrust (NAT). Following this, for events classified as AT we calculate two metrics: quality of thrusts and quantity of thrusts. These metrics allow us to provide

feedback to the user.

6.3.2 Feature Extraction

We classify abdominal thrusts using accelerometer data from the Y axis. To do this, we use a sliding window with a size of 1500 milliseconds that moves right by 750 milliseconds each time. We set the size to be 1500 milliseconds by calculating the maximum length of an abdominal thrust from our expert data to be 1000 millisecond and adding 50% to give our non-experts some buffer room. Abdominal thrusts have a very distinct shape due to the high maximum acceleration needed when performing a thrust. To model the abdominal thrust we focus on this. An example of a single abdominal thrust with our features labeled is shown in Figure [6.4](#).

To calculate our features, we define,

$$\mathit{arg}(x_i) \triangleq i \quad (6.1)$$

Then, on each sliding window, $\mathit{Input} = [x_1 \dots x_n]$, we calculate 5 features:

$$\mathit{MaxAccel} = \max_i(x_i) \quad (6.2)$$

$$\mathit{MinLeft} = \max_{x_i \in [x_1, \mathit{MaxAccel}]}(-x_i) \quad (6.3)$$

$$\mathit{MinRight} = \max_{x_i \in (\mathit{MaxAccel}, x_n]}(-x_i) \quad (6.4)$$

$$\mathit{SlopeLeft} = \frac{\mathit{MaxAccel} + \mathit{MinLeft}}{\mathit{arg}(\mathit{MaxAccel}) - \mathit{arg}(\mathit{MinLeft})} \quad (6.5)$$

$$\mathit{SlopeRight} = \frac{\mathit{MaxAccel} + \mathit{MinRight}}{\mathit{arg}(\mathit{MinRight}) - \mathit{arg}(\mathit{MaxAccel})} \quad (6.6)$$

6.3.3 Event Detection

We leveraged Weka Data Mining Software provided by the University of Waikato [\[91\]](#). We fed the five features described above into the five standard data mining classifiers. We

evaluated these classifiers on three metrics: precision, recall, and f-measure. The results of the evaluation of these classifiers are shown in Table 7.1. From the results, we saw that the random forest classifier outperformed the rest in all the metrics.

Classifier	Precision	Recall	F-Measure
Random Forest	94.5	94.5	94.5
Random Tree	92.9	92.7	92.8
SMO	87.5	87.9	87.1
Nearest Neighbor	91.2	91.4	91.2
Logistic	88.8	89.1	88.6

Table 6.1: Classifier Evaluation

We evaluated our classifier using a data set combining both the expert and the pre-user study data. Within this data set, we had a total of 105 abdominal thrust events. After we partitioned the data we had a total of 853 windows to be classified as AT or NAT. Since the data was partitioned into 1500 millisecond windows and we moved our sliding window by 750 milliseconds, it is possible that a single abdominal thrust could fall in two different windows. This caused some abdominal thrust events to be classified twice. Because of this, we had a total of 194 windows whose ground truth is AT even though there were only 105 abdominal thrust events recorded. We discuss how we handle the abdominal thrusts that are repeated in two windows in the Quantity of Thrusts portion of the Metric Calculation subsection.

6.3.4 Metric Calculation

To provide feedback to the user, we must calculate two metrics. First, we determined the quality of abdominal thrusts by calculating a maximum acceleration from expert data. Second, we counted the number of abdominal thrusts performed. This allowed us to provide feedback to the user on their maximum acceleration after five abdominal thrusts were performed.

6.3.4.1 Quality of Thrusts

To the best of our knowledge, there is no known standard for the maximum acceleration when performing abdominal thrusts. The goal of performing abdominal thrusts is to expel the foreign object from the victims airway while attempting to prevent further injury to the victim. Abdominal thrusts that have too low a maximum acceleration will not expel the foreign object while those that have too high a maximum can cause injuries including damage to internal organs and ribs [196, 67, 20]. Due to the lack of availability of a recommended maximum acceleration, it can be difficult for a first aid provider to gauge these metrics and so to combat this, we asked six experts to perform abdominal thrusts on the “Annie” [115] CPR manikin while we recorded their accelerometer data. The six experts consisted of four CPR certified lifeguards and two CPR certified trainers. We instructed each expert to perform five abdominal thrusts for a total training set of thirty abdominal thrusts. The mean maximum acceleration for expert abdominal thrusts was 11.302 m/s² with a standard deviation of 4.437 m/s².

6.3.4.2 Quantity of Thrusts

For each window, we classified if an abdominal thrust had occurred. In the Event Detection subsection, we discussed that a single abdominal thrust can appear in two adjoining windows. To ensure that we did not count the same abdominal thrust twice, we only count the abdominal thrusts such that

$$\max(AT_n) < \max(AT_{n-1}) \quad (6.7)$$

This allowed us to get an accurate count of abdominal thrusts so that we could provide feedback after each fifth abdominal thrust.

6.4 BreathEZ Application

We accomplish two goals with our BreathEZ application. First, we offer easy to follow instructions for choking first aid and second, we provide feedback to the user on their performance of the abdominal thrust portion of choking first aid. BreathEZ is implemented on Android 8.0 Oreo. The smartphone application is approximately 3.5 MB and the smartwatch application is about 9.5 MB. To make certain that feedback is provided to the user in a timely manner, the functions that run the display, data processing, and data logging are implemented in their own threads. When in use, BreathEZ samples the accelerometer at 5 Hz.

We displayed the instructions for choking first aid in a manner that is both user friendly and intuitive. We designed our smartwatch screens to show both a summary of the current screen's instruction and a more detailed explanation below that can be scrolled through. These screens are shown in Figure 7.5



Figure 6.5: Instructional Screens

Once the user gets to the “5 Abdominal Thrusts” screen as shown in Figure 7.5 we start to give the user feedback on their performance of abdominal thrusts. The user is given tactile and auditory feedback as the smartwatch counts five abdominal thrusts to let the user know that each abdominal thrust is classified and logged. Once the user has completed their 5 thrusts and they swipe to the following screen, the user is given feedback

on the performance of their abdominal thrusts by providing textual feedback and changing the background color of the screen. The different feedback screens are shown in Figure 7.6.

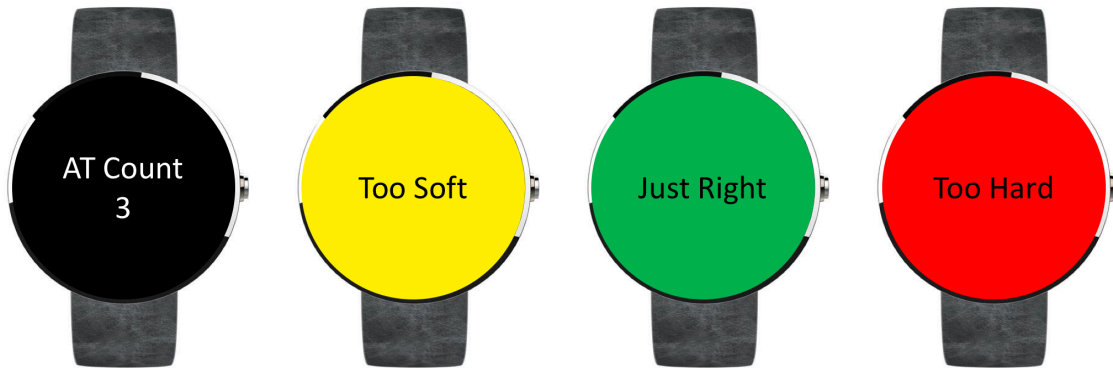


Figure 6.6: Feedback Screens

6.5 Post-User Study

In order to evaluate BreathEZ, we performed a post-user study in which participants were asked to answer two questionnaires and perform abdominal thrusts on a CPR training manikin [115], shown in Figure 6.1 while wearing a Motorola 360 smartwatch.

6.5.1 Study Design

The study group consisted of participants recruited from the College of William and Mary and surrounding area. No incentives were given for participation in our study. Overall, we collected 229 recordings of abdominal thrusts from ten total participants, eight female and two male. The average participant age was 35.4 with a standard deviation of 14.6. Prior to this study, four participants had completed choking first aid training.

Pre-Study Questionnaire First, we ask each participant to answer the following questions:

1. Have you had choking first aid and/or Heimlich maneuver training? Yes or No. If yes, why?
2. On a scale of 1-5, how comfortable are you performing the choking first aid?
3. Is the topic of the study (choking first aid) relevant for you personally? Yes or No. Why?
4. On a scale of 1-5, how willing are you to perform choking first aid?
5. On a scale of 1-5, how familiar are you with smartwatches?
6. Which is your dominant hand? Right, Left, Ambidextrous

Two Scenarios for Choking First Aid We designed our two post-user study scenarios to complement the pre-user study scenarios. These scenarios again tested the participants' basic knowledge of abdominal thrusts and determined if their performance and confidence improved. First, we tested their untrained knowledge of abdominal thrusts. We did not instruct them on any aspects of choking first aid, just handed them the CPR manikin and allowed them to give it their best effort. Following this, we divided the participants into two groups. Group 1 was shown a Red Cross tutorial video [5] and then asked to once again perform choking first aid. Group 2 was instructed to use BreathEZ app. It took each participant no more than ten minutes to complete the two scenarios. Each participant performed a minimum of five abdominal thrusts per scenario for a minimum of ten abdominal thrusts per individual per study.

1. Without training: In the first scenario, each participant was asked to perform abdominal thrusts to the best of their ability without any help.
2. With the video tutorial or BreathEZ: In the second scenario, each participant was either shown a Red Cross video tutorial [5] on the correct way to perform choking first aid or instructed to use the BreathEZ app. If the participant was shown the

Red Cross video tutorial, they were asked to once again perform choking first aid. If the user was instructed to use the BreathEZ app, they were asked to follow the in app instructions.

Data Recording We recorded the accelerometer and gyroscope data from the smartwatch during the study using our BreathEZ application. The data recording service was run in the background on the smartwatch and did not effect the performance of the user facing BreathEZ app. The data was written to a CSV file and stored on a connected Android smartphone. The average file size was 237 MB.

Post-Study Questionnaire

After performing abdominal thrusts, the participant was asked to answer the following questions:

1. Did the smartwatch irritate you? Yes or No. If yes, why?
2. (a) On a scale of 1-5, how willing are you to perform choking first aid using a smartwatch with our app?
(b) On a scale of 1-5, how willing are you to perform choking first aid after watching the Red Cross Video Tutorial?
3. (a) Did you feel that you performed choking first aid better with BreathEZ? Yes or No. Why?
(b) Did you feel that you performed choking first aid better after watching the Red Cross Tutorial Video? Yes or No. Why?
4. (a) Would using the smartwatch with our BreathEZ app reduce your fear of injuring the person you are performing choking first aid on? Yes or No. Why?
(b) Did watching the Red Cross video tutorial reduce your fear of injuring the person you are performing choking first aid on? Yes or No. Why?

5. If you had a smartwatch, would you install our app? Yes or No. Why?
6. Any other comments?

Questions two through four are modified depending on which group the participant is in. Group 1 received questions 2a, 3a, and 4a. Group 2 received questions 2b, 3b, and 4b. Question five is only given to group 1.

6.5.2 Results

In this subsection we discuss the results of the user study and the questionnaires. First we quantify the two main objectives of BreathEZ: to classify abdominal thrusts in real time and provide feedback to the user. Following that we discuss how our participants willingness and fear to perform choking first aid changed after using BreathEZ.

6.5.2.1 Classification of Abdominal Thrusts

The five participants in group 1 used the BreathEZ app in their user study. BreathEZ classified each participant's abdominal thrusts in real time and then gave them feedback on how well they performed them. Each abdominal thrust classification was monitored by the individual giving the study. On each possible classification of an abdominal thrust, the individual would mark whether or not the application correctly classified the abdominal thrust. Among the five participants there were 55 possible abdominal thrusts classifications and BreathEZ correctly classified 50 of them in real time. So BreathEZ correctly classifies abdominal thrusts in real time 90.9% of the time. When BreathEZ did not classify an abdominal thrust correctly, it did not register an abdominal thrust. When this happened, the participant had to perform an extra abdominal thrust to get to the feedback screen of the application. This is an issue that should be resolved in later versions of the BreathEZ app. We will discuss this more in the Discussion and Future Work Section.

6.5.2.2 Abdominal Thrust Performance Feedback

We recorded the feedback that each of our participants received after performing abdominal thrusts while using the BreathEZ app. We show this feedback in Table 6.2. From Table 6.2, we saw that four of the five participants improved from their first performance of abdominal thrusts to their second. Of the four participants that improved their performance, we saw three that received the feedback, “Too Soft”, after performing their first set of abdominal thrusts. Participants 4 and 5 were able to increase their feedback to “Just Right”. Participant 3 again received the feedback “Too Soft” but was able to raise their max acceleration and get closer to the “Just Right” feedback. The final participant who showed improvement was able to better his feedback from “Too Hard” to “Just Right”. From this study we saw that after being given feedback, most of our participants were able to improve their performance in abdominal thrusts.

The participant who did not improve their BreathEZ feedback, participant 5, began with a “Just Right” feedback and moved to “Too Soft”. It is worth noting that this participant was trained as an EMT-Basic and found the “CPR specific manakin is painful to do abdominal thrusts at the appropriate force”. We used the CPR specific manakin for our study, since after contacting two local fire stations, one hospital, and two CPR training facilities in the nearby area we found that they only used the CPR specific manakin.

Participant #	1st Feedback	2nd Feedback
1	Just Right	Too Soft
2	Too Hard	Just Right
3	Too Soft	Too Soft
4	Too Soft	Just Right
5	Too Soft	Just Right

Table 6.2: Group 1 Feedback

To understand how our users felt about their improvement in their performance we included a question in the questionnaire for all ten participants. Of the five participants

that were shown a tutorial video, we saw that three of five believe their performance improved after being shown the tutorial video. A summary of their comments showed that they found the instructions helpful but they still could not tell if they were performing choking first aid correctly. More specifically their comments consisted of “instructions helped, I had never heard of back blows”, “its good to know what to do”, and “I still don’t know if I’m doing it right”. Of the five participants that were allowed to use BreathEZ, we saw that all five found believed their performance improved. Their comments were centered around the feedback they received saying that it was “helpful to have feedback”, “it tells you what to do and that you are doing it right”, and “it helped to know how well I was doing”. One participant even commented on their personal improvement by saying “it told me to thrust harder and I was able to get a just right the second time”.

6.5.2.3 Willingness and Fear

To combat the bystander effect, we focus on two factors. The first is our participants’ perceived willingness to perform choking first aid. The second is the fear of injuring the victim of choking while performing choking first aid. To gauge this, we asked three questions relating to this in our pre and post questionnaires.

We began by asking all participants to rate their willingness to perform choking first aid on a scale of one to five before and after training was given. These results are shown in Figure [6.7](#). On average, before any training was given, the average willingness was 2.4 out of 5.0. After each participant performed choking first aid, we questioned them again to understand any changes. Those who were asked to watch a tutorial video, participants 2-6, had an average willingness of 2.8. Those who were asked to use BreathEZ, participants 1 and 7-10, had an average willingness of 4.2. From this we can clearly see that while each average willingness increased, those who were asked to use BreathEZ had a much higher increase in willingness.

After performing choking first aid, we asked participants if their fear of injuring a choking victim had decreased. Of those who were asked to watch a video tutorial, three

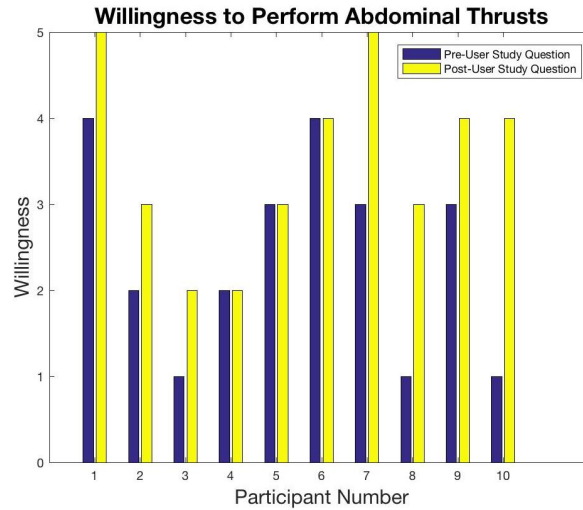


Figure 6.7: Post-User Study Willingness

of five said that their fear had not been reduced, citing that they were not sure that they could perform choking first aid correctly. More specifically the commented “I feel slightly better now that I know what I’m doing”, “I don’t want to hurt anyone”, and “What if I do it wrong”. Of those who were asked to use BreathEZ, all five participants responded that their fear had been lessened. A summary of their comments is as follows: “I would be less scared because it would tell me if I was thrusting too hard”, “it told me I was in the just right zone”, and “it made me more confident in my skills”.

6.6 Discussion and Future Work

6.6.1 Angle of Abdominal Thrusts

To create a better abdominal thrust feedback system for the user, the angle of the abdominal thrust can be measured. This is essential because the angle of the abdominal thrust contributes to the expulsion of the foreign object [87]. This feedback should be given before the user begins administering the abdominal thrusts to ensure that the best care is provided. The BreathEZ app should incorporate this by guiding the user to the correct angle with either verbal or tactile feedback. This will allow for a more complete

BreathEZ system.

6.6.2 Feedback After Each Abdominal Thrust

In the current implementation of the BreathEZ application, the user only receives feedback after all five abdominal thrusts are complete. For a more complete user experience, two factors should be considered. First, it can be beneficial to the user to receive feedback on their abdominal thrusts performance after each abdominal thrust. This can be implemented by developing a training mode and/or giving the user access to analytics after performing choking first aid. Second, it may not take all five abdominal thrusts to expel the foreign object. If this is the case the user should be able to either manually move on from the abdominal thrusts portion of BreathEZ and/or BreathEZ should time out after a set threshold of time if it has not registered the performance of any abdominal thrusts.

6.6.3 Back Blows

Choking first aid requires the first aid provider to be able to perform two maneuvers: back blows and abdominal thrusts. In our solution, we only address abdominal thrusts. "Back blows are given with the heel of your hand between the victim's shoulder blades" [3]. If the first aid provider wears a smartwatch on the wrist of the hand that they are delivering back blows, it is possible that we can also detect, classify, and give feedback on these motions. Kautz et al. [107] are able to detect sports motions based on sensing an impact between a sports ball and a hand or arm by having the subject wear an accelerometer on their wrist. Here we will be tackling a similar challenge by attempting to sense the impact between a subject's hand and the back of a manikin. To provide feedback on the back blows portion of choking first aid, we can measure the max acceleration to determine if the first aid provider is within a range of the average max acceleration data collected from experts.

6.6.4 Choking First Aid for Infants

We focus on choking first aid for adults but choking first aid procedures for infants should also be addressed. The American red cross recommends this treatment [4], which we quoted in the following bullets, for infants who cannot cough, cry, or breathe:

- “After checking the scene and the victim, have someone call 911 and get consent to perform first aid.”
- “Give firm back blows with the heel of one hand between the infant’s shoulder blades.”
- “Give five chest thrusts. Place two or three fingers in the center of the infant’s chest just below the nipple line and compress the breastbone about one and half inches. Make sure to support the head and neck securely when giving back blows and chest thrusts. Keep the head lower than the chest.”
- “Continue sets of five back blows and five chest thrusts until the object is forced out, infant can cough forcefully, cry or breathe, infant becomes unconscious.”

A complete choking first aid application should also address this scenario. At this point, our app does not address this scenario but the movements described can be monitored. Back blows can be monitored as described above but the max acceleration should be set by expert data where back blows are performed on an infant manakin. To monitor the chest thrusts, we look to Gruenerbl et al. [85] as chest thrusts for infants are similar to measuring the depth and frequency of CPR chest compression.

6.7 Conclusion

In this chapter we presented BreathEZ, the first smartwatch application that classifies and provides feedback in real time on choking first aid. BreathEZ identifies abdominal

thrusts, measures the peak acceleration, and provides feedback on the quality of the abdominal thrust to the user. This application is shown to not only increase the user's performance of choking first aid, but to also combat the bystander effect by increasing a user's willingness to perform choking first aid and decreasing their fear of injuring a choking victim. This is important because choking leads to nearly 5,000 deaths per year in the US. While EMS response is optimal for the victim, it does not always occur in less than six minutes and within that time frame brain damage can occur. Using BreathEZ to help combat the bystander effect and increase the quality of performance of choking first aid can help to bring the number deaths due to choking down.

Chapter 7

BBAid: Using Smartwatches to Improve Back Blows

7.1 Introduction

In the event of a choking emergency, the flow of oxygen must be restored to the body or hypoxia will begin to occur. Hypoxia is a condition in which the supply of oxygen in the body is insufficient to sustain normal bodily functions. Within a few minutes, this can cause irreparable damage to an individual's brain, vital organs, and nervous system [142]. Within six to eight minutes of the onset of hypoxia, it is likely that organ systems will fail and brain death will occur. In a study of the local choking incidents in the San Diego County Medical Examiner's database, there were 19 incidents that occurred in restaurants in adults over a ten year period. Of the 19 incidents, there was only one attempt by a bystander to perform choking first aid [56]. In the US, choking accounted for 4,800 deaths in 2015 and 5,051 deaths in 2017 making it the fourth leading cause of unintentional injury death according to the National Safety Council's 2015 and 2017 Injury Facts [43] [44].

Basic choking first aid training courses are readily available at community centers, hospitals, colleges, some workplaces, and even online. Many first aid training courses include a module on choking first aid and the percentage of trained individuals in US

counties varies between zero and fifteen [8]. This training prepares bystanders to react to and provide immediate treatment to a choking victim. When choking first aid is performed, there is a 66% chance the victim will survive [28]. One barrier to a choking victim receiving non-EMS aid is a psychological phenomenon known as the “bystander effect”. This effect presents itself when individuals who are in a group environment do not help someone in need of aid because of the belief that someone else in that group is more qualified than they are. In the end, it is likely that no one will intervene as the entire group believes that there is someone more qualified to help [50].

In this chapter, we answer the following research questions:

RQ1: How can we accurately classify back blows with a wearable device?

RQ2: What kind of feedback should we provide to enhance the performance of back blows?

RQ3: How do we combat the bystander effect?

To determine how accurately we can classify back blows with a wearable device we perform a user study in which 109 back blows were performed by ten participants. Then, we extract five features to describe a single back blow from the Z-Axis of smartwatch accelerometer data and feed it into a random forest classifier. From this, we see a classification accuracy of 93.5%.

To understand what kind of feedback we should provide to enhance back blows, we calculated two metrics, developed a smartwatch application called BBAid, and conducted a user study. First, we calculated two metrics: the quality and quantity of back blows. These metrics are then added to the feedback system in the BBAid application. BBAid not only provides instructions on how to perform choking first but also provides feedback to the user on how well they performed back blows. Then we perform a user study in which our participants filled out two questionnaires and performed choking first aid. In this user study, our participants were split into two groups: Group 1 was given a video tutorial and Group 2 was instructed to use the BBAid application.

To understand if BBAid can help to combat the bystander effect, we asked our participants to answer questions about willingness, comfort, and fear of performing choking first aid on a choking victim. We compared our participant’s responses to these questions based on their randomly selected group, previous knowledge, and choking first aid background. We found that all of our participants regardless of group, previous knowledge, or skill were more willing and comfortable with performing choking first aid after receiving training.

When someone is choking, the American Red Cross [3] recommends a series of back blows and abdominal thrusts. To the best of our knowledge, to date, a system for the back blow portion of choking first aid scenarios that provides instructions and feedback has not been developed. Watson and Zhou [199] developed an application for the abdominal thrust portion. Zoll Medical Corporation [190] and Dechoker LLC [52] developed devices that could be used in choking first aid scenarios. Zoll Medical Corporation solely focuses on the abdominal thrusts and does not consider back blows. Dechoker LLC takes a new approach to choking first aid that does not involve abdominal thrusts or back blows. CPR feedback on smartwatches and other devices has been developed and is being deployed into training facilities [182] [86] [1]. Frequently, choking first aid is taught in CPR first aid courses which gives us the opportunity to leverage the systems already in place in training facilities. First aid skill retention is a known problem [92] [60] [129] and it has also been shown that choking first aid skills decline more rapidly than others [7]. We address this decline in skills and knowledge by providing feedback and instructions at the time choking first aid would need to be performed.

Our contributions are summarized as follows:

- We are the first to extract features from smartwatch accelerometer data and use it to accurately classify back blows. We selected five features to describe a single back blow. We feed these five features into a random forest classifier and see a 93.5% accuracy.

- We are the first to provide insightful feedback to enhance back blow performance. We calculate two metrics: quality and quantity of back blows that are used to provide feedback. In our final user study, all of our participants experienced an increase in performance while using BBAid.
- We propose and develop the first smartwatch application that incorporates our features, classifier, and feedback to combat the bystander effect. All of our participants saw an increase in their willingness to perform choking first aid when using the given choking first aid instructions.

The remainder of this chapter is structured as follows. First, we will discuss our and preliminary study with a background on choking first aid. Second, we will discuss and evaluate our system design and BBAid. Then we will describe our Post-User Study and our results from it. Finally, we will wrap up with a discussion of future work and summarize with a conclusion.

7.2 Preliminary Study

We want to evaluate whether a smartwatch application that provides feedback will improve choking first aid. To do this, we performed a user study where we asked our participants to wear a smartwatch and to perform choking first aid on a CPR training manikin. Based on the above, we formulated the following study questions:

SQ1: What is the user awareness of proper choking first aid?

SQ2: How does user awareness improve with the addition of live feedback?

7.2.1 Study Setup

First, we will provide a background on choking first aid. We follow the method recommended by the American Red Cross. We continue by describing our user study in

terms of the equipment used, the parameters of the study, and the demographics of our participants.

Choking First Aid Background: The American Red Cross recommends the following quoted treatment for choking victims [3]:

- “After checking the scene and the victim, have someone call 911 and get consent to perform first aid.”
- “Bend the victim forward at the waist and give five back blows between the shoulder blades with the heel of one hand.”
- “Place a fist with the thumb side against the middle of the victim’s abdomen, just above the navel. Cover your fist with your other hand. Give five quick, upward abdominal thrusts.”
- “Continue sets of five back blows and five abdominal thrusts until the object is forced out, the victim can cough forcefully, breathe, or the person becomes unconscious.”

Equipment: The smartwatch application used to collect accelerometer data was implemented on a Motorola 360 smartwatch [140]. This application was connected to a Google Pixel smartphone [78] where the data files were stored. We tested a preliminary mechanism for choking first aid where we observed the participants’ response to real-time feedback during abdominal thrusts [199]. To provide feedback, we used a threshold based method on smartwatch accelerometer data to detect participant thrust strength. We provide no feedback for back blows.

Parameters: Our study began with a simple questionnaire in which we gauge each participant’s knowledge, willingness to perform choking first aid, and their familiarity with smartwatches. Then we asked each user to wear a Motorola 360 smartwatch and perform choking first aid on a CPR manikin [115], shown in Figure 6.1 that was shown in the previous Chapter. During this part of the study, we randomly split the participants into two groups. Group 1 was shown an educational video from the American Red Cross [5].

Group 2 was given a smartwatch application that provided choking first aid instructions and included our preliminary mechanism for real-time feedback on abdominal thrusts. Following this, we gave each participant a follow-up questionnaire to determine if their willingness to perform choking first aid and comfort with a smartwatch had changed as well as a free response question for any additional feedback they had. Ground truth for this study is collected by having a researcher who is observing the study log the time at which each back blow started. Ground truth labels were back blow and not back blow. In this study, motions that were classified as not back blows include abdominal thrusts, picking up and putting do the manikin, repositioning the manikin, any actions or adjustments made between back blows or abdominal thrusts.

Demographics: We recruited the participants in our study from the College of William and Mary and the surrounding area. In total, we had ten participants. Of our participants, eight were female and two were male. In terms of age, on average, the participants were 35.4 with a standard deviation of 14.6. Prior to this study, only four participants had some form of first aid training.

7.2.2 Study Results

We asked our participants two questions regarding smartwatches. The first question was “On a scale of 1-5, how familiar are you with smartwatches?”. The second question was “Did the smartwatch irritate you? Yes or No. If yes, why?”. We asked these questions to determine how familiar our users were with a smartwatch and if it could potentially irritate them when performing choking first aid maneuvers. On a scale of 1-5, our participants averaged a 1.8 in terms of smartwatch familiarity with a standard deviation of 1.3. Since our subjects are not highly familiar with smartwatches, it follows that if they do well with the application it should be easy for new adopters to use. Only one of our ten participants found the smartwatch to be irritating stating that “It was a bit big”. From this, we conclude that a smartwatch will make a good tool for choking first aid as it is not irritating to users.

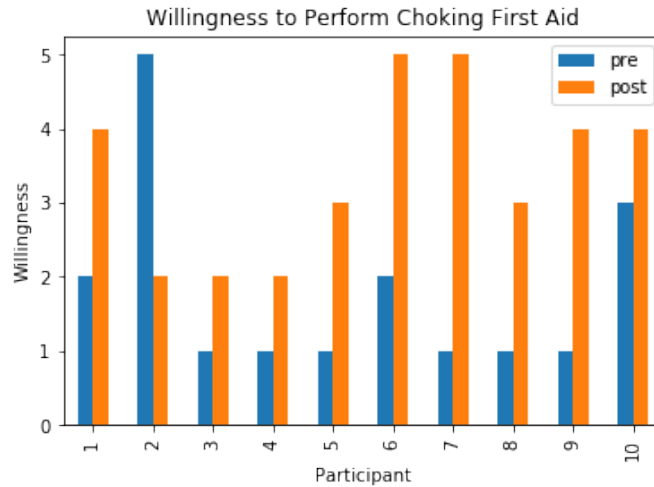


Figure 7.1: Willingness to Perform Choking First Aid

We compare our participants’ willingness to perform choking first aid before and after performing choking first aid. Before beginning, we asked our participants to rate their willingness to perform on a scale of one to five. We repeated this question after they had performed choking first aid and these results are shown in Figure [7.1](#). Participants one through five were shown the Red Cross video and participants six through ten were given the smartwatch app. From this figure, we clearly see that those who received the application had a greater increase in willingness to perform choking first aid. On average the participants who were shown the video had a willingness increase of 2.8 while those who were given the application had a feedback increase of 4.2.

Part of our study included a short survey in which the user could provide open-ended answers to questions. Of our ten participants, four mentioned back blows. More specifically, their comments were as follows:

- “The instructions helped. I had never heard of back blows.”
- “Please add feedback on the back blows as well.”
- “You should also tell me when I am doing back blows correctly.”

- “I only knew of the Heimlich maneuver before... thanks for informing me about back blows.”

These comments fall into two categories: a lack of knowledge about back blows and request for a feedback system similar to the one used for abdominal thrusts. The existence and combination of these two deficiencies demonstrates that the users feel the need for live feedback to help improve their performance.

We also look to see whether our participants’ performance of abdominal thrusts improved with the addition of feedback. All five participants saw improvements in the performance of abdominal thrusts. Feedback for back blows was not given in this study. Following our hypothesis that the addition of feedback improves performance, only one participant improved in the performance of back blows. The common issue in the performance of abdominal thrusts and back blows is that the participant does not provide enough force when performing the maneuvers. We saw that providing feedback helps the participant to increase the force provided for abdominal thrusts. It follows that this will also be the case for back blows.

7.3 System Design

In this section, we describe the design of BBAid, an Android smartwatch application that assists the user in their performance of choking first aid by providing them with instructions and feedback on their performance. We begin by describing the features used, then we explain how we use those features to detect a back blow event. Finally, we show how we calculate the metrics we use to provide feedback on the user’s performance of back blows.

7.3.1 System Architecture

Here, we describe the pipeline for the classification and quality metric calculation of the back blow portion of choking first aid. First, we must acquire accelerometer data from

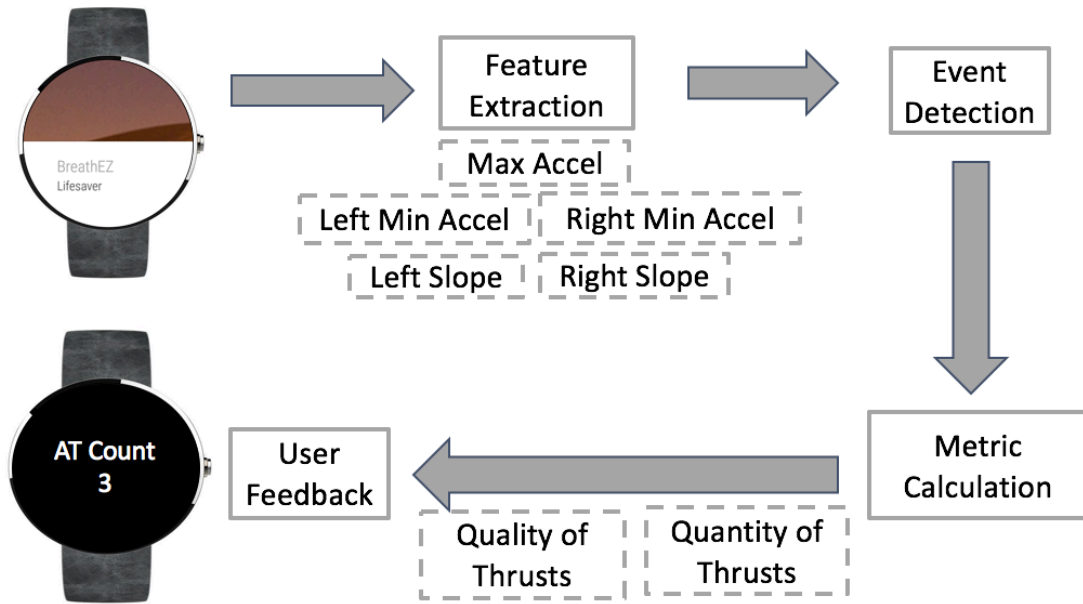


Figure 7.2: System Architecture of BBAid

a smartwatch accelerometer. Next, we extract 5 features that will be used in our classifier to classify an event as either a Back Blow (BB) or Not Back Blow (NBB). Finally, we define and calculate two metrics that are the basis for the feedback provided to the user.

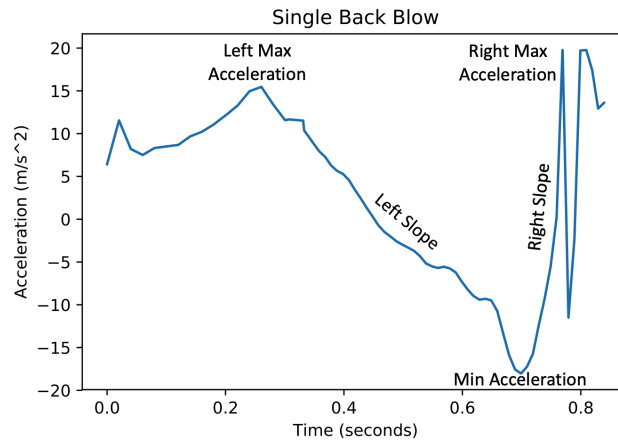


Figure 7.3: Back Blow Features

7.3.2 Feature Extraction

In Figure 7.3 we show an example of a single back blow event. As seen in the figure, back blows have a very distinct shape due to the nature of the change in direction of the acceleration. To classify back blows, we use accelerometer data in the Z-axis. If the Z-axis acceleration exceeded a threshold, $\mathcal{E}_{threshold}$, the next local minimum is sought. $\mathcal{E}_{threshold}$ is defined as the maximum of the acceleration peaks of the ground truth data collected in the Preliminary Study. The value of $\mathcal{E}_{threshold}$ is 3.083. We then draw a window of size .85 seconds equally spaced around the minimum. The size of the window is determined by the size of the longest back blow from the training data collected in the Preliminary Study with an additional 50% of that time added. In Figure 7.3 we label the features we calculate as follows:

First, we define:

$$arg(x_i) \triangleq i \quad (7.1)$$

Then, on each sliding window, $Input = [x_1 \dots x_n]$, we calculate 5 features:

$$MinAccel = \min_i(x_i) \quad (7.2)$$

$$MaxLeft = \min_{x_i \in [x_1, MinAccel]}(-x_i) \quad (7.3)$$

$$MaxRight = \min_{x_i \in (MinAccel, x_n]}(-x_i) \quad (7.4)$$

$$SlopeLeft = \frac{MinAccel + MaxLeft}{arg(MinAccel) - arg(MaxLeft)} \quad (7.5)$$

$$SlopeRight = \frac{MinAccel + MaxRight}{arg(MaxRight) - arg(MinAccel)} \quad (7.6)$$

7.3.3 Event Detection

To detect each back blow event we fed our five features that are described above into several classifiers that were successfully used in other sensing-based activity classification

Classifier	Precision	Recall	Effort
Random Forest	93.5	93.5	low
Random Tree	91.4	91.4	low
SMO	93.7	93.5	mid
K - Nearest Neighbor	93.5	93.5	high
Logistic	90.9	90.9	low

Table 7.1: Evaluation of Multiple Classifiers

research [30, 29, 45, 42]. These classifiers were random tree, random forest, SMO (Sequential minimal optimization), KNN (K-Nearest Neighbor), and Logistic Regression. To test these classifiers, we leveraged the Weka Data Mining Software provided by the University of Waikatao [91]. We evaluated these classifiers on three metrics: precision, recall, and the effort it takes to run the classifier and the results of our evaluation are shown in Table 7.1. From these results, three of the five classifiers outperformed the rest in terms of precision and recall: Random Forest, SMO, and KNN. These classifier exhibit high precision and high recall meaning that these algorithms return a high number of correctly classified back blow instances. Since we had high precision and recall for three algorithms, we also evaluated them on the amount of effort it takes to train and use each algorithm. This is shown in the effort column in figure 7.1. We chose random forest for use in BBAid because it exhibits the highest precision and recall while being in the low effort category. We evaluated our classifiers using the Preliminary Study data. In this data set, we have a total of 109 back blow events.

7.3.4 Metric Calculation

We calculate two metrics to gauge user performance of back blows: quantity of back blows and quality of back blows. First, we determine the quality of back blows by comparing the minimum acceleration of each user’s back blows to the average minimum acceleration of our expert data. Second, we calculate the number of back blows by keeping a running total of the number of back blows performed.

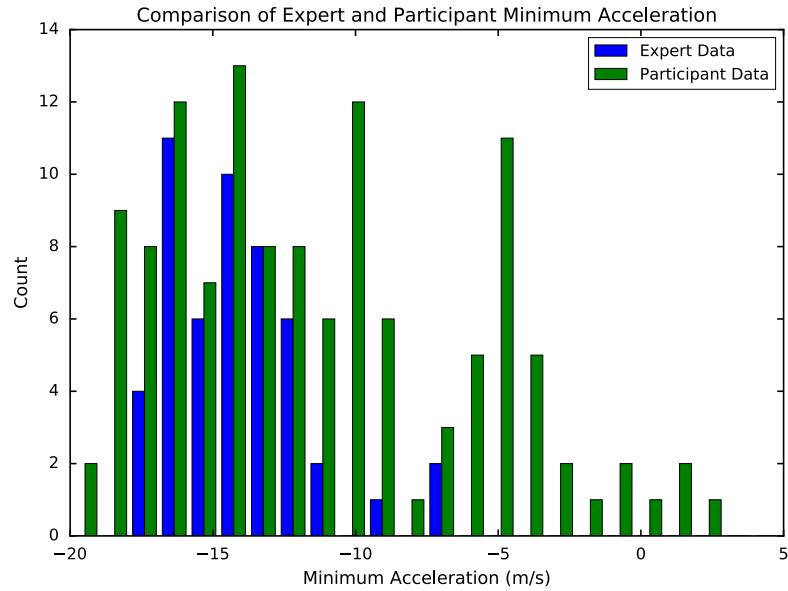


Figure 7.4: Comparison of Expert and Participant Back Blow Accelerations

When performing back blows it is important for the user to provide enough acceleration to effectively dislodge the object. Due to the lack of availability of a recommended acceleration for an individual back blow, we asked five experts to perform back blows on a provided “Annie” CPR manikin [115] while we recorded their accelerometer data. The five experts consisted of three CPR certified lifeguards and two emergency medical technicians (EMT). We instructed each expert to perform ten back blows for a total of fifty back blows. The mean minimum acceleration was -14.63 with a standard deviation of 2.591. There were three outliers in the data set that were removed. The minimum acceleration was -17.02 and the max acceleration was -12.32. We compare the expert data to the data collected in the preliminary user study and show this in a histogram in figure 7.4. In this figure, it is easy to see the difference between the expert and participant data. The expert data falls mostly between -12 and -18 while the participant data is further spread out from three to -20.

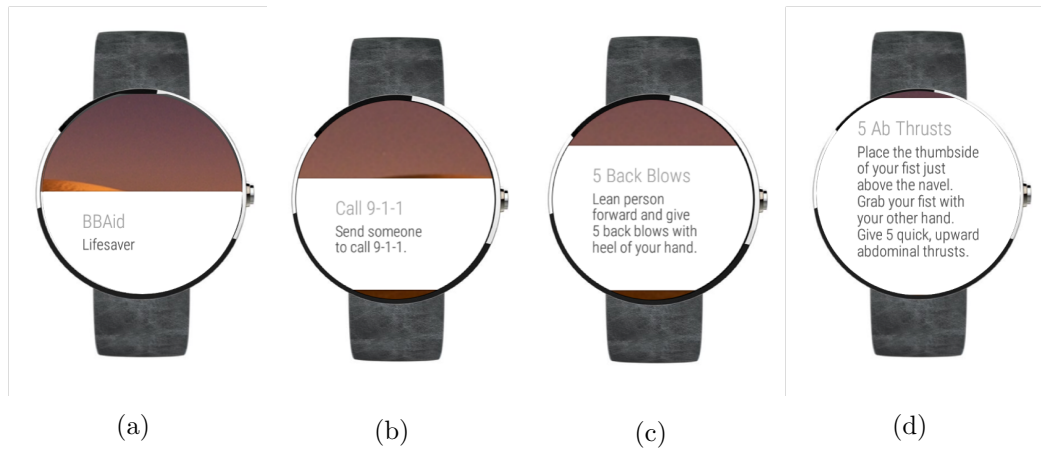


Figure 7.5: BBAid Instructional Screens

7.4 BBAid Application

BBAid provides two functions. First, it provides simple, clear, and concise easy instructions for choking first aid. Second, it provides feedback to the user on their performance of the back blows. BBAid is implemented on Android 8.0 Oreo. The smartphone application is approximately 4.3 MB and the smartwatch application is about 3.5 MB. BBAid samples the accelerometer and gyroscope at a rate of 5 Hz. The display, data processing, and data logging are implemented in their own threads so that feedback is provided to the user in real-time.

7.4.1 Instructions

Instructions for BBAid must be clear and concise because of the limited space available on smartwatch screens. Our instructions must also be simple and easy to understand for the user. Because of this, we designed our smartwatch screens to show both a title and description. The title is an overall summary of the current screen’s instruction. The description is a more detailed explanation. When a user first opens BBAid, they are greeted with a welcome screen shown in Figure [7.5a](#). Following this, the application gives instructions based on the Red Cross recommended choking first aid procedure [\[3\]](#). To

navigate through the pages, the user swipes left as they are finished with each screen to proceed.

The first step in the Red Cross procedure is to alert the EMS services. The first instructional screen in BBAid, shown in Figure 7.5b, titled “Call 9-1-1” reminds the user to “Send someone to call 9-1-1”. Next, it is important to begin first aid maneuvers. The Red Cross recommends beginning with 5 back blows, following with 5 abdominal thrusts, and then repeating that process until the foreign object is either expelled or the person becomes unconscious. Illustrating this, the next two screens shown in Figure 7.5c and Figure 7.5d give an overview of the maneuver to be performed along with a more detailed description. For back blows, BBAid displays “5 Back Blows” with a description of “Lean person forward and give 5 back blows with the heel of your hand”. For abdominal thrusts, it displayed “5 Ab Thrusts” with a description of “Place the thumb side of your fist just above the navel. Grab your fist with your other hand. Give 5 quick, upward abdominal thrusts”. Altogether these instructional screens give the user reminders for the correct way to perform choking first aid as a whole.

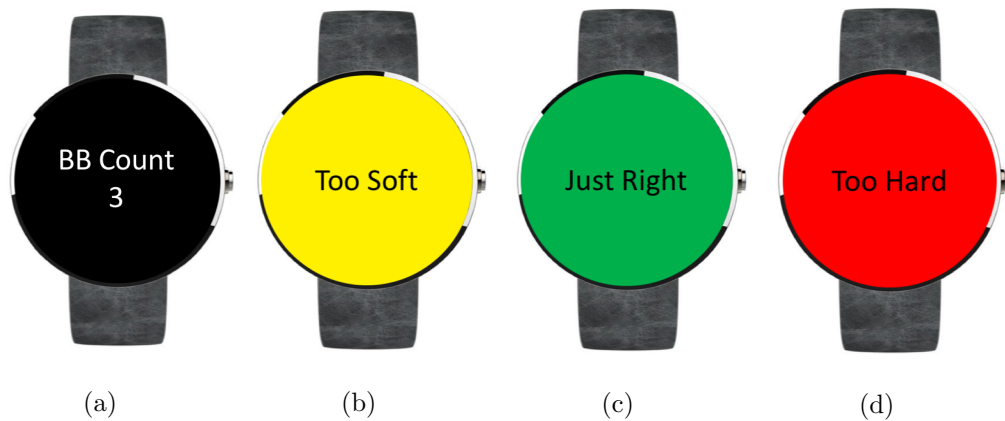


Figure 7.6: BBAid Feedback Screens

7.4.2 Feedback

BBAid utilizes three types of feedback that can be given through a smartwatch: tactile, auditory, and visual. When the user swipes left to move on from the back blow instructional screen, they are shown the first feedback screen. This screen is shown in Figure 7.6a and counts the number of back blows that the user has performed. For each logged back blow, the smartwatch provides tactile feedback in the form of a 150 millisecond vibration and a beep sound on smartwatch devices with a speaker. Once the user has completed and logged five back blows, BBAid averages the minimum acceleration of the five back blows and show the user one of three force feedback screens.

We break the feedback into three options: too soft, too hard, and just right. We based the colors used for each screen on the stoplight coding method [90]. The stoplight coding method has been shown to be effective at promoting understanding of the meaning of the information presented [12, 111, 165]. The stoplight coding method is a method that maps red to stop, yellow to caution, and green to go. We use this method in a similar mapping. When the back blow average is too soft we provide the user with the yellow screen shown in Figure 7.6b. When the back blow average is too hard we provide the user with the red screen shown in Figure 7.6d. When the back blow average is just right we provide the user with a green screen shown in Figure 7.6c.

We use the data collected from the experts to set the thresholds for each option. In this case, we removed the three outliers from the data set. This leaves us with a maximum of -12.329 and a minimum of -17.026. We used these values as the max and minimum for our just right option. All values lesser than -17.026 will be classified as too hard and all values greater than -12.329 will be classified as too soft.

7.5 User Study

In this section, we evaluate BBAid and its effects on our participants' performance of back blows and their willingness to perform choking first aid. To do this we performed a

user study in which we asked our participants to answer two questionnaires and perform choking first aid on a manikin. Given this, we formulate the following study questions:

SQ1: How does real-time feedback on back blows improve the user’s performance and technique?

SQ2: Can our application combat the bystander effect in relation to choking first aid?

7.5.1 Study Setup

In the study setup, we first give a background of choking first aid. Then, we describe the equipment we use in this user study. Next, we will discuss the parameters of the study. Finally, we will discuss the demographics of our participants.

Choking First Aid Background: We followed the same recommended treatment in this user study as we followed in the Preliminary Study. This is the American Red Cross recommended treatment for victims of choking [3]. We quote the method as follows:

- “After checking the scene and the victim, have someone call 911 and get consent to perform first aid.”
- “Bend the victim forward at the waist and give five back blows between the shoulder blades with the heel of one hand.”
- “Place a fist with the thumb side against the middle of the victim’s abdomen, just above the navel. Cover your fist with your other hand. Give five quick, upward abdominal thrusts.”
- “Continue sets of five back blows and five abdominal thrusts until the object is forced out, the victim can cough forcefully, breathe, or the person becomes unconscious.”

Equipment: During our study, participants wore an LG Urbane [121] Android smart-watch on the wrist of the hand that they would use to perform back blows. We collected

accelerometer and gyroscope data from the smartwatch and sent these measurements wirelessly over Bluetooth to a Google Pixel Android Smartphone [78]. Our study also required the user to perform choking first aid procedures on a first aid manikin. While there are many first aid manikins to choose from, we selected the “Annie” CPR manikin [115] as it is readily available at most first aid training facilities.

<p style="text-align: center;">Pre-Study Questionnaire</p> <ol style="list-style-type: none"> 1. Have you had choking first aid and/or Heimlich maneuver training? Yes or No If yes, why? 2. On a scale of 1-5, how comfortable are you performing the choking first aid? 1 2 3 4 5 3. Is the topic of the study (choking first aid) relevant for you personally? Yes or No Why? 4. On a scale of 1-5, how willing are you to perform choking first aid? 1 2 3 4 5 5. On a scale of 1-5, how familiar are you with smartwatches? 1 2 3 4 5 6. Which is your dominant hand? Right Left Ambidextrous 	<p style="text-align: center;">Post-Study Questionnaire</p> <ol style="list-style-type: none"> 1. Did the smartwatch irritate you? Yes or No If yes, why? 2. On a scale of 1-5, how willing are you to perform choking first aid after watching the Red Cross Video Tutorial? 1 2 3 4 5 3. Did you feel that you performed choking first aid better after watching the Red Cross Tutorial Video? Yes or No why? 4. Did watching the Red Cross video tutorial reduce your fear of injuring the person you are performing choking first aid on? Yes or No why? 5. Any other comments? 	<p style="text-align: center;">Post-Study Questionnaire</p> <ol style="list-style-type: none"> 1. Did the smartwatch irritate you? Yes or No If yes, why? 2. On a scale of 1-5, how willing are you to perform choking first aid using a smartwatch with our app? 1 2 3 4 5 3. Did you feel that you performed choking first aid better with the smartwatch? Yes or No why? 4. Would using the smartwatch with our app reduce your fear of injuring the person you are performing choking first aid on? Yes or No why? 5. If you had a smartwatch, would you install our app? Yes or No why? 6. Any other comments?
(a) Pre-User Study	(b) Video Post-User Study	(c) BBAid Post-User Study

Figure 7.7: User Study Questionnaires

Parameters: We conducted our study in a lab setting. When our participants entered the lab, they were asked to fill out some demographical information and a Pre-Study Questionnaire. The questionnaire is shown in Figure 7.7a. With this questionnaire, we attempt to gauge each participant’s base knowledge of choking first aid and their willingness to perform it. Following this, we began the portion of the user study in which the participants performed choking first aid. Each participant was given two scenarios. In Scenario 1, we asked the participant to use any previous knowledge to perform choking first aid on the manikin. For Scenario 2, we randomly divided our participants into two groups. Group 1 served as our control group and was shown this training video [5] provided by the American Red Cross. Group 2 was instructed to open the BBAid application on the smartwatch and follow the instructions provided in the app. Finally, all participants were asked to fill out a Post-Study Questionnaire to gauge how their willingness to and fear

of performing choking first aid changed. Group 1 was asked to fill out the questionnaire shown in Figure [7.7b](#) and Group 2 was asked to fill out the questionnaire shown in Figure [7.7c](#).

Demographics: We recruited our study participants from the College of William and Mary and the surrounding areas. Our user study consisted of 16 participants: 12 male and 4 female. On average the participants were 28 years old with a standard deviation of 4.6 years. Overall our participants had an average BMI of 25.53 and a standard deviation of 4.5. All participants were right-handed. Prior to this study, only two participants had first aid training.

7.5.2 Study Results

7.5.2.1 Back Blow Classification

In this study, there were 80 possible real-time back blow classifications for BBAid to make. Of those 80 possible classifications, BBAid classified 75 in real-time achieving a classification accuracy of 93.75%. Of the five that were not correctly classified, three were recognized after a few seconds of lag time and two were not recognized. Post analysis of the two unclassified back blow events revealed that these back blows did not reach the maximum acceleration required by the application.

7.5.2.2 User Performance

We compared our two groups in terms of three metrics from the post-training scenario: simulating calling 9-1-1, manikin position, and max acceleration on their abdominal thrusts. We show the correct manikin position in Figure [7.8](#). For Group 1, we saw that two individuals simulated calling 9-1-1, six participants held the manikin horizontally, and only one made it to the recommended back blow acceleration. For Group 2, we saw that eight individuals simulated calling 9-1-1, eight participants held the manikin horizontally,

and only six made it to the recommended back blow acceleration. These results are shown in the Scenario 2 column of Table [7.2](#)

Group #	Scenario 1			Scenario 2		
	9-1-1	MP	Max Accel	9-1-1	MP	Max Accel
1	3	1	1	2	6	1
2	1	1	0	8	8	6

Table 7.2: Participant Performance



Figure 7.8: Correct Manikin Position

We also compared each group’s improvement between the first and second scenario. In Group 1, we saw that one less participant simulated calling 9-1-1, five additional participants positioned the manikin correctly and no additional participants were within the recommended maximum acceleration range after video training. In Group 2, we saw that seven additional participants simulated calling 9-1-1, seven additional participants positioned the manikin correctly and six additional participants were in the recommended maximum acceleration range when using BBAid. These results are shown in Table [7.2](#).

In our Post-Study Questionnaires, we asked each of our participants if they believed they had performed choking first aid better with either the tutorial video or BBAid and

why. This was asked in question three of both Post-Study Questionnaires shown in Figures [7.7b](#) and [7.7c](#). In Group 1, seven participants believed that they performed choking first aid better. In Group 2, all eight participants believed that they performed choking first aid better. We also opened up this question for a free response as to why they felt they had performed better or worse. Overall, Group 1's responses were centered around instructions and reminders of what they knew before. More specifically:

- “Because there were details I had forgotten from when I was trained.”
- “Clear and concise directions on what to do.”
- “I now know the correct way to perform the back blows and abdominal thrusts.”

In summary, Group 2's responses reflect the feedback they received for back blows. More specifically:

- “The feedback helped. I was able to adjust to it.”
- “The feedback helped me get to a green screen. I feel like I could save someone.”
- “Easy to follow instructions. Feedback is a great addition”

7.5.2.3 User Knowledge

In our study, two participants had prior first aid training. The first was trained and certified as a basic level emergency medical technician (EMT-B) from 2009 through 2012. The second was certified as a lifeguard in 2007 and in American Red Cross first aid in 2012. Both of these participants were randomly assigned to Group 1. The EMT-B trained participant was the only participant in Group 1 to make it to the recommended maximum acceleration. This participant correctly performed all of the metrics we measured except they did not position the manikin correctly in the first scenario. The American Red Cross first aid trained participant did simulate calling 9-1-1 pre and post-training but they did not reach the recommended max acceleration in either scenario and did not position

the dummy correctly in the first. From this, we see that previous training can improve performance in a choking first aid scenario but even those with training can use a reminder of the correct choking first aid procedure.

Of our sixteen participants, four did not attempt to perform first aid on the manikin in Scenario 1. These participants did not take the step to simulate calling 9-1-1 or even approach the manikin because they were not comfortable and lacked a basic knowledge of first aid. When randomly divided into groups, three of these were in Group 1 and one was in Group 2. Of those in Group 1, after the training video, none of the three simulated calling 9-1-1, two positioned the manikin correctly, and none got to the recommended acceleration. The participant in Group 2 simulated calling 9-1-1, positioned the manikin correctly, and made it to the recommended acceleration. This suggests that since BBAid provides instructions in real-time there is less chance for a step to be forgotten. Since BBAid provides feedback to the user as they perform back blows, our participants without any prior training were able to perform at the recommended maximum acceleration. This suggests that real-time feedback can help even those that have not been trained for an emergency situation.

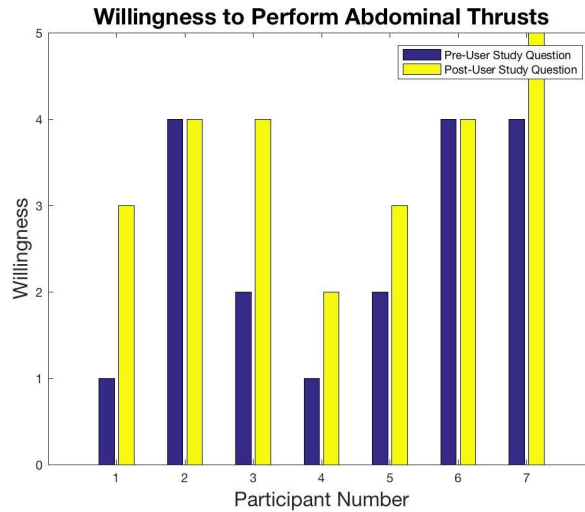


Figure 7.9: Choking First Aid Willingness

7.5.2.4 User Feedback

To combat the bystander effect in respect to choking first aid, we gauge how our users felt about performing back blows prior to and after training. We do this with questions numbers two and four in the Pre-Study Questionnaire [7.7a](#) and question numbers two and four in the Post-Study Questionnaires [7.7b](#) and [7.7c](#). First, we will address user willingness, followed by their comfort and fear level when performing choking first aid.

Comfort and Willingness: We asked our participants how willing they were to perform choking first aid before and after their training. We show the results per participant of these questions in Figure [7.9](#). From this figure, we see that regardless of their group, most individuals ranked highly on willingness and were more willing to perform choking first aid after being trained. Since both groups receive instructions on how to perform choking first aid, we conclude that information is the key to making our participants more willing to perform choking first aid.

We also asked how comfortable our participants were if they had to perform choking first aid prior to their training. Overall, our participants had an average comfort level of 2.2 out of 5. We had two participants with prior first aid training. Their comfort levels were a four and five out of five. The average comfort level for our untrained participants was 1.86 out of 5. Here we saw that our participants with training were much more comfortable with performing choking first aid than those who did not.

Fear: We survey our participants to see if they were fearful of injuring a choking victim after being trained by the video or the application. Of our sixteen participants, fourteen responded that they were not fearful. Their free response is as follows:

- “BBAid gave me more confidence in what I was doing because I know I am applying the right amount of force.”
- “I had no idea what I was doing but with your app I got to the point where I was doing it right .”

- “By watching the video I know the right way to perform the choking first aid. Thus, I am not afraid about it.”

The two participants that were fearful of injuring a choking victim had these responses to our free response question:

- “I had prior training and the video didn’t teach me anything I didn’t know.”
- “Isn’t it possible to break their ribs?”

7.6 Discussion and Future Work

7.6.1 Abdominal Thrusts

According to the American Red Cross recommended choking first aid procedure [3], there are two maneuvers to be performed on a choking victim: back blows and abdominal thrusts. Abdominal thrusts are described as: “Place a fist with the thumb side against the middle of the victim’s abdomen, just above the navel. Cover your fist with your other hand. Give five quick, upward abdominal thrusts” [3]. In this chapter, we only address back blows but to provide a complete choking first aid feedback application abdominal thrusts must also be addressed. Providing feedback on abdominal thrusts presents their own challenges as the force of impact, angle of thrust, and number of thrusts should be taken into account.

7.6.2 First Aid Training

Our application was mainly tested on individuals who had not had formal training in first aid. To see what effect BBAid would have on previously trained individuals it is necessary to complete a study where they are the targeted participants. During this study, it would be important to note if they were current on their certification, how long it had been since their training, and their current knowledge level. In our study, we saw that previously trained individuals did not perform every step recommended by the American

Red Cross, for example calling 9-1-1. Because of this, it is important to see how just those who train perform with the aid of the BBAid application.

7.7 Conclusion

In this chapter, we present BBAid: a novel Android smartwatch application for the improvement of choking first aid. Our application classifies and provides real-time feedback on the back blow portion of choking first aid using the data from a smartwatch accelerometer. Our application increases the user's performance of the back blows by providing instructions and feedback. BBAid combats the bystander effect by increasing user comfort and willingness to perform choking first aid. It also gives the user more confidence by decreasing their fear of injuring a choking victim. BBAid achieves a classification accuracy of 93.75% for back blows in real-time. Following the classification, BBAid analyzes the back blow and provides feedback on its quality. Because of this feedback, our participants are able to perform back blows within the recommended range 75% of the time.

Chapter 8

Conclusion and Future Work

This dissertation presented four projects contributing to the advancement of wearable technology research in healthcare and athletic performance.

First, we presented Magneto: a sensing system for joint motion analysis. Magneto uses the combination of an electromagnet and magnetometer to remove environmental interference from magnetic field readings in a dynamically changing environment. Given this purified reading, we localized the electromagnet with respect to the magnetic field reader which allowed us to apply Magneto in two pilot studies: elbow angle and shoulder position. We calculated elbow angles to the nearest 15° with 93.8% accuracy, calculated shoulder positions in two-degrees of freedom with 96.9% accuracy, and calculated shoulder positions in three-degrees of freedom with 75.8% accuracy.

Second, we presented TrackKnee a smart sensing knee sleeve that calculates knee angles via a conductive fabric sensor. This project demonstrated the ability for wearable technology to be soft and comfortable and functional. The sensor on the knee sleeve was created using conductive fabric and all wiring was done using conductive thread. We ran a user study using our knee sleeve in which we collected data on 240 knee angles from six individuals. We used this data to calculate knee angles using our models. Our results show that our model is 94.86% accurate to the nearest 15th degree angle and that our average error per angle is 3.69° .

Third, we evaluate a system named ServesUp that will improve the volleyball serve and present the future directions for the project. We designed a sensing shirt that is comfortable, unobtrusive, and washable. The sensors sewn into the shirt are made from fabric and instead of wires, we use conductive thread. This allows for the athlete to be able to perform as they would normally without being impeded by the sensors. This makes it ideal for athletes who want to improve their skills. With our sensing shirt, we collected data on 250 serves from a semi-professional volleyball player.

Finally, we presented two solutions for choking first aid: BreathEZ and BBAid. These solutions monitored abdominal thrusts and back blows via smartwatch applications and provided actionable insights to the user to increase their skill quality performance. Our findings show that our smartwatch applications combat the bystander effect by increasing user willingness and comfort when performing choking first aid skills. We also show that using our applications leads to enhanced performance of the choking first aid skill. With increased participation and enhanced performance, we believe that our applications can increase the chances of a favorable outcome in an emergency situation.

For future work, we are considering the following research directions:

- **Sports Performance**

A natural application for wearable technology is the field of sports performance. This field brings many challenges to the creation of wearable devices and their feedback systems. A device must be unobtrusive, impact-resistant, and comfortable to wear so that it does not impede an athlete's motion. Since many actions in sport are fast-paced, the device must provide high-quality data so that actions can be accurately sensed. Sports data provides unique opportunities for analysis as the data can be analyzed for the individual and the team as a whole. Actionable insights should be tailored to helping each player improve their game and to help the team win.

- **Wearable Sensors Upgrade**

As applications for wearable technology continue to evolve, the quality of the sensors should as well. Wearable sensors need to be soft, flexible and be able to stretch with body movement. They should not impede any movement made by the wearer or cause injury if the wearer were to land on the device. Advancements in Materials Science has brought us new conductive materials. These materials, such as graphene[145] and carbon nanotubes[62], should be considered when developing new wearable sensors. Fabric can be coated with these materials to make it conductive while still retaining the comfort of regular clothing.

- **Long-term Direction: Integration into Everyday Life**

Wearable technology, in the long term, should be integrated into the daily life of the wearer. Wearables should integrate seamlessly into the daily life of the wearer. When the wearer is getting ready for their day, they should be able to don their clothing as normal without thinking about the wearables integrated into them. The clothing with integrated sensors should not fit or feel different from their regular clothing. Data from these wearable devices will be recorded and sent to whatever parties that are approved for access. For example, biometric data can be sent to healthcare professionals for long term monitoring of health. Any anomalies in their data could be flagged or analyzed. This can lead to early diagnosis of health issues or even prevention of them entirely.

Bibliography

- [1] CHIWON AHN, JUNCHEOL LEE, JAEHOON OH, YEONGTAK SONG, YOUNGJOON CHEE, TAE HO LIM, HYUNGGOO KANG, AND HYUNGGOO SHIN. Effectiveness of feedback with a smartwatch for high-quality chest compressions during adult cardiac arrest: A randomized controlled simulation study. *PloS one*, 12(4):e0169046, 2017.
- [2] DEBORAH ALLEN. History and physical exam of the knee. <https://www.orthobullets.com/knee-and-sports/3003/history-and-physical-exam-of-the-knee> October 2016.
- [3] American Red Cross conscious choking. <http://www.redcross.org/flash/brr/English-html/conscious-choking.asp>.
- [4] American Red Cross pediatric first aid/cpr/aed. https://www.redcross.org/images/MEDIA_CustomProductCatalog/m4240175_Pediatric_ready_reference.pdf
- [5] American Red Cross: refresher- conscious choking- adult and child. <http://www.redcrossrefresher.com/media/videos/child-cc.html>
- [6] BOYD ANDERSON, MINGQIAN SHI, VINCENT YF TAN, AND YE WANG. Mobile gait analysis using foot-mounted uwb sensors. *Proceedings of the ACM on Interactive, Mobile, Wearable and Ubiquitous Technologies*, 3(3):73, 2019.

- [7] GREGORY S ANDERSON, MICHAEL GAETZ, AND JEFF MASSE. First aid skill retention of first responders within the workplace. *Scandinavian journal of trauma, resuscitation and emergency medicine*, 19(1):11, 2011.
- [8] MONIQUE L ANDERSON, MARGUERITTE COX, SANA M AL-KHATIB, GRAHAM NICHOL, KEVIN L THOMAS, PAUL S CHAN, PARAMITA SAHA-CHAUDHURI, EMIL L FOSBOL, BRIAN EIGEL, BILL CLENDENEN, ET AL. Rates of cardiopulmonary resuscitation training in the united states. *JAMA internal medicine*, 174(2):194–201, 2014.
- [9] Apple: iphone 6s. <https://www.apple.com/iphone-6s/specs/>.
- [10] Arduino. <https://www.arduino.cc>.
- [11] Arduino nano. <https://store.arduino.cc/usa/arduino-nano>.
- [12] M ASHIR AND K MARLOWE. Traffic lights: a practical clinical risk management system for community early intervention in psychosis teams po184. *Early Intervention in Psychiatry*, 2, 2008.
- [13] CMA ASHRUF. Thin flexible pressure sensors. *Sensor Review*, 2002.
- [14] Babylock verve. <https://babylock.com/machines/sewing/verve>.
- [15] MARC BÄCHLIN, MEIR PLOTNIK, DANIEL ROGGEN, INBAL MAIDAN, JEFFREY M HAUSDORFF, NIR GILADI, AND GERHARD TRÖSTER. Wearable assistant for parkinson’s disease patients with the freezing of gait symptom. *IEEE Trans. Information Technology in Biomedicine*, 14(2):436–446, 2010.
- [16] MARTIN A BAHR AND ROALD BAHR. Jump frequency may contribute to risk of jumper’s knee: a study of interindividual and sex differences in a total of 11 943 jumps video recorded during training and matches in young elite volleyball players. *Br J Sports Med*, 48(17):1322–1326, 2014.

- [17] SABA BAKHSHI AND MOHAMMAD H MAHOOR. Development of a wearable sensor system for measuring body joint flexion. In *2011 International Conference on Body Sensor Networks*, pages 35–40. IEEE, 2011.
- [18] LING BAO AND STEPHEN S. INTILLE. Activity Recognition from user -annotated acceleration data. In *PERVASIVE 2004*, 2004.
- [19] JEROEN HM BERGMANN, SALZITSA ANASTASOVA-IVANOVA, IRINA SPULBER, VIVEK GULATI, PANTELIS GEORGIU, AND ALISON MCGREGOR. An attachable clothing sensor system for measuring knee joint angles. *IEEE Sensors Journal*, 13(10):4090–4097, 2013.
- [20] MARILU BINTZ AND THOMAS H COGBILL. Gastric Rupture after the Heimlich Maneuver. *Journal of Trauma and Acute Care Surgery*, 40(1), 1996.
- [21] PETER BLANK, BENJAMIN H. GROH, AND BJOERN M. ESKOFIER. Ball speed and spin estimation in table tennis using a racket-mounted inertial sensor. *Proceedings of the 2017 ACM International Symposium on Wearable Computers - ISWC '17*, pages 2–9, 2017.
- [22] PETER BLANK, JULIAN HOSSBACH, DOMINIK SCHULDHAUS, AND BJOERN M. ESKOFIER. Sensor-based stroke detection and stroke type classification in table tennis. *Proceedings of the 2015 ACM International Symposium on Wearable Computers - ISWC '15*, pages 93–100, 2015.
- [23] DAVIDE BLONNA, PETER C. ZARKADAS, JAMES S. FITZSIMMONS, AND SHAWN W. O'DRISCOLL. Accuracy and inter-observer reliability of visual estimation compared to clinical goniometry of the elbow. *Knee Surgery, Sports Traumatology, Arthroscopy*, 20(7):1378–1385, Jul 2012.
- [24] Bluno beetle. <https://www.dfrobot.com/product-1259.html>

- [25] STEPHANE BONNET AND RODOLPHE HELIOT. A magnetometer-based approach for studying human movements. *IEEE Transactions on Biomedical Engineering*, 54(7):1353–1355, 2007.
- [26] VINCENT BONNET, CLAUDIA MAZZA, PHILIPPE FRAISSE, AND AURELIO CAPPOZZO. Real-time estimate of body kinematics during a planar squat task using a single inertial measurement unit. *IEEE Transactions on Biomedical Engineering*, 60(7):1920–1926, 2013.
- [27] THIAGO O BORGES, ALEXANDRE MOREIRA, RENATO BACCHI, RONALDO L FINOTTI, MAYARA RAMOS, CHARLES R LOPES, AND MARCELO S AOKI. Validation of the vert wearable jump monitor device in elite youth volleyball players. *Biology of sport*, 34(3):239, 2017.
- [28] RICHARD N BRADLEY, STAMATIOS LERAKIS, AND THE AMERICAN RED CROSS SCIENTIFIC ADVISORY COUNCIL. American red cross scientific review on obstructed airway-adults. 2015.
- [29] LEO BREIMAN. Random forests. *Machine learning*, 45(1):5–32, 2001.
- [30] LEO BREIMAN, JEROME FRIEDMAN, CHARLES J STONE, AND RICHARD A OLSEN. *Classification and regression trees*. CRC press, 1984.
- [31] BW BREWER, AE CORNELIUS, JL VAN RAALTE, JC BRICKNER, JH SKLAR, JR CORSETTI, MH POHLMAN, TD DITMAR, AND K EMERY. Rehabilitation adherence and anterior cruciate ligament reconstruction outcome. *Psychology, Health & Medicine*, 9(2):163–175, 2004.
- [32] OLIVIER BRUYÈRE. Rehabilitation in osteoarthritis. *Therapy*, 7(6):669–674, 2010.
- [33] ADRIAN BURNS, BARRY R GREENE, MICHAEL J MCGRATH, TERRANCE J O’SHEA, BENJAMIN KURIS, STEVEN M AYER, FLORIN STROIESCU, AND VICTOR

- CIONCA. Shimmer—a wireless sensor platform for noninvasive biomedical research. *IEEE Sensors Journal*, 10(9):1527–1534, 2010.
- [34] JOAO PAULO CARVALHO, NUNO HORTA, AND JOSE AB TOME. Fuzzy boolean nets based paediatrics first aid diagnosis. In *NAFIPS 2007-2007 Annual Meeting of the North American Fuzzy Information Processing Society*, pages 644–649. IEEE, 2007.
- [35] P.W.D. CHARLES. Bluno basic demo. <https://github.com/DFRobot/BlunoBasicDemo>
- [36] PAULA C. CHARLTON, CLAIRE KENNEALLY-DABROWSKI, JEREMY SHEPPARD, AND WAYNE SPRATFORD. A simple method for quantifying jump loads in volleyball athletes. *Journal of Science and Medicine in Sport*, 20(3):241–245, 2017.
- [37] HOWARD CHEN. The effects of movement speeds and magnetic disturbance on inertial measurement unit accuracy: the implications of sensor fusion algorithms in occupational ergonomics applications. 2017.
- [38] KE-YU CHEN, KENT LYONS, SEAN WHITE, AND SHWETAK PATEL. utrack: 3d input using two magnetic sensors. In *Proceedings of the 26th annual ACM symposium on User interface software and technology*, pages 237–244. ACM, 2013.
- [39] XI MEI CHEN, SHO VAN BARMA, SIO HANG PUN, MANG I VAI, AND PENG UN MAK. Direct measurement of elbow joint angle using galvanic couple system. *IEEE Transactions on Instrumentation and Measurement*, 66(4):757–766, 2017.
- [40] Cisco visual networking index: Global mobile data traffic forecast update, 2017–2022. <https://www.cisco.com/c/en/us/solutions/collateral/service-provider/visual-networking-index-vni/white-paper-c11-738429.pdf>
- [41] GLEN COOPER, IAN SHERET, LOUISE McMILLIAN, KONSTANTINOS SILVERDIS, NING SHA, DIANA HODGINS, LAURENCE KENNEY, AND DAVID HOWARD. Iner-

- tial sensor-based knee flexion/extension angle estimation. *Journal of biomechanics*, 42(16):2678–2685, 2009.
- [42] CORINNA CORTES AND VLADIMIR VAPNIK. Support-vector networks. *Machine learning*, 20(3):273–297, 1995.
- [43] NATIONAL SAFETY COUNCIL, NATIONAL SAFETY COUNCIL. RESEARCH, AND STATISTICS DEPT. *Injury facts*. The Council, 2017.
- [44] NATIONAL SAFETY COUNCIL, NATIONAL SAFETY COUNCIL. RESEARCH, AND STATISTICS DEPT. *Injury facts*. The Council, 2015.
- [45] T. COVER AND P. HART. Nearest neighbor pattern classification. *IEEE Transactions on Information Theory*, 13(1):21–27, 1967.
- [46] Crucial compression premium knee brace compression sleeve. <https://crucialcompression.com/products/knee-brace-compression-sleeve>.
- [47] A. CRUZ AND J. P. LOUSADO. A survey on wearable health monitoring systems. In *2018 13th Iberian Conference on Information Systems and Technologies (CISTI)*, pages 1–6, June 2018.
- [48] L PONCE CUSPINERA, SAKURA UETSUJI, FJ ORDONEZ MORALES, AND DANIEL ROGGEN. Beach volleyball serve type recognition. In *Proceedings of the 2016 ACM International Symposium on Wearable Computers*, pages 44–45, 2016.
- [49] J.J. D. *Classical Electrodynamics*. John Wiley, 1975.
- [50] JOHN M DARLEY AND BIBB LATANE. Bystander intervention in emergencies: diffusion of responsibility. *Journal of personality and social psychology*, 8(4p1):377, 1968.
- [51] ZELAI SÁENZ DE URTURI, AMAIA MÉNDEZ ZORRILLA, AND BEGOÑA GARCÍA ZAPIRAIN. Serious game based on first aid education for individuals with autism

- spectrum disorder (asd) using android mobile devices. In *2011 16th International Conference on Computer Games (CGAMES)*, pages 223–227. IEEE, 2011.
- [52] Dechoker breathing is mandatory. <https://www.dechoker.com/collections/anti-choking-devices/products/dechoker-for-adults>.
- [53] Dechoker clinical evaluation. https://cdn.shopify.com/s/files/1/0852/1468/files/Clinical_47817b71-d0b2-4916-8446-a549ae2c5c50.pdf?15898932315925775175.
- [54] LUCA DELLA TOFFOLA, SHYAMAL PATEL, MUZAFFER Y OZSECEN, RAVI RAMACHANDRAN, AND PAOLO BONATO. A wearable system for long-term monitoring of knee kinematics. In *Proceedings of 2012 IEEE-EMBS International Conference on Biomedical and Health Informatics*, pages 188–191. IEEE, 2012.
- [55] BHUSHAN R DESHPANDE, JEFFREY N KATZ, DANIEL H SOLOMON, EDWARD H YELIN, DAVID J HUNTER, STEPHEN P MESSIER, LISA G SUTER, AND ELENA LOSINA. Number of persons with symptomatic knee osteoarthritis in the us: impact of race and ethnicity, age, sex, and obesity. *Arthritis care & research*, 68(12):1743–1750, 2016.
- [56] LAURA DOLKAS, CHRISTINA STANLEY, ALAN M SMITH, AND GARY M VILKE. Deaths associated with choking in san diego county. *Journal of forensic sciences*, 52(1):176–179, 2007.
- [57] Dritz quilting adhesive spray. <https://www.joann.com/dritz-quilting-adhesive-spray-5.62-oz/7139991.html#q=adhesive&start=1>.
- [58] LUCY E. DUNNE, SARAH BRADY, RICHARD TYNAN, KIM LAU, BARRY SMYTH, DERMOT DIAMOND, AND G. M.P. O’HARE. Garment-based body sensing using foam sensors. *Conferences in Research and Practice in Information Technology Series*, 50:155–161, 2006.

- [59] LUCY E DUNNE, RICHARD TYNAN, GREGORY MP O’HARE, BARRY SMYTH, SARAH BRADY, AND DERMOT DIAMOND. Coarse sensing of upper arm position using body-garment interactions. In *Proc. 2nd Int. Forum Appl. Wearable Comput*, pages 138–141, 2005.
- [60] PHILIP EISENBURGER AND PETER SAFAR. Life supporting first aid training of the public—review and recommendations. *Resuscitation*, 41(1):3–18, 1999.
- [61] MAHMOUD EL-GOHARY AND JAMES MCNAMES. Shoulder and elbow joint angle tracking with inertial sensors. *IEEE Transactions on Biomedical Engineering*, 59(9):2635–2641, 2012.
- [62] MORINOBU ENDO, SUMIO IJIMA, AND MILDRED S DRESSELHAUS. *Carbon nanotubes*. Elsevier, 2013.
- [63] Eeontex conductive stretchable fabric. <https://www.sparkfun.com/products/retired/14112>
- [64] LORENZ ERTL AND FRANK CHRIST. Significant improvement of the quality of bystander first aid using an expert system with a mobile multimedia device. *Resuscitation*, 74(2):286–295, 2007.
- [65] DARIO FARINA, THOMAS LORRAIN, FRANCESCO NEGRO, AND NING JIANG. High-density EMG E-textile systems for the control of active prostheses. In *2010 Annual International Conference of the IEEE Engineering in Medicine and Biology Society, EMBC’10*, 2010.
- [66] JULIEN FAVRE, BM JOLLES, RACHID AISSAOUI, AND K AMINIAN. Ambulatory measurement of 3d knee joint angle. *Journal of biomechanics*, 41(5):1029–1035, 2008.

- [67] NICOLE M FEARING AND PAUL B HARRISON. Complications of the heimlich maneuver: case report and literature review. *Journal of Trauma and Acute Care Surgery*, 53(5):978–979, 2002.
- [68] A FERRETTI, P PAPANDREA, AND F CONTEDEUCA. Knee injuries in volleyball. *Sports Medicine*, 10(2):132–138, 1990.
- [69] GIANCARLO FORTINO AND RAFFAELE GRAVINA. A cloud-assisted wearable system for physical rehabilitation. In *ICTs for Improving Patients Rehabilitation Research Techniques*, pages 168–182. Springer, 2014.
- [70] BRETT E GAGE, NATALIE M MCILVAIN, CHRISTY L COLLINS, SARAH K FIELDS, AND R DAWN COMSTOCK. Epidemiology of 6.6 million knee injuries presenting to united states emergency departments from 1999 through 2008. *Academic emergency medicine*, 19(4):378–385, 2012.
- [71] FRANCISCO GARCÍA-MURO, ÁNGEL L RODRÍGUEZ-FERNÁNDEZ, AND ANGEL HERRERO-DE LUCAS. Treatment of myofascial pain in the shoulder with kinesio taping. a case report. *Manual therapy*, 15(3):292–295, 2010.
- [72] M. GHOLAMI, A. EJUPI, A. REZAEI, A. FERRONE, AND C. MENON. Estimation of knee joint angle using a fabric-based strain sensor and machine learning: A preliminary investigation. In *2018 7th IEEE International Conference on Biomedical Robotics and Biomechatronics (Biorob)*, pages 589–594, Aug 2018.
- [73] GUIDO GIOBERTO. Garment-integrated wearable sensing for knee joint monitoring. In *Proceedings of the 2014 ACM International Symposium on Wearable Computers: Adjunct Program*, pages 113–118. ACM, 2014.
- [74] GUIDO GIOBERTO AND LUCY DUNNE. Garment-Integrated Bend Sensor. *Electronics*, 3(4):564–581, 2014.

- [75] GUIDO GIOBERTO AND LUCY E DUNNE. Overlock-Stitched Stretch Sensors: Characterization and Effect of Fabric Property. *Journal of textile and Apparel, Technology and Management*, 2013.
- [76] GUIDO GIOBERTO, CHEOL-HONG MIN, CRYSTAL COMPTON, AND LUCY E. DUNNE. Lower-Limb Goniometry using Stitched Sensors : Effects of Manufacturing and Wear Variables. In *Proceedings of the 2014 ACM International Symposium on Wearable Computers (ISWC '14)*, 2014.
- [77] GABRIEL GOMEZ, PATRICIA HERRERA LÓPEZ, DANIEL LINK, AND BJOERN ESKOFIER. Tracking of Ball and players in beach volleyball videos. *PLoS ONE*, 9(11), 2014.
- [78] Google pixel - smartphone. https://store.google.com/us/product/pixel_phone?hl=en-US.
- [79] Google pixel 2. https://store.google.com/us/product/pixel_2?hl=en-US.
- [80] MAHANTH GOWDA, ASHUTOSH DHEKNE, SHENG SHEN, ROMIT ROY CHOUDHURY, LEI YANG, SURESH GOLWALKAR, AND ALEXANDER ESSANIAN. Bringing IoT to Sports Analytics. *14th {USENIX} Symposium on Networked Systems Design and Implementation, {NSDI} 2017, Boston, MA, USA, March 27-29, 2017*, pages 499–513, 2017.
- [81] BENJAMIN H GROH, MARTIN FLECKENSTEIN, AND BJOERN M ESKOFIER. Wearable trick classification in freestyle snowboarding. In *2016 IEEE 13th International Conference on Wearable and Implantable Body Sensor Networks (BSN)*, pages 89–93. IEEE, 2016.
- [82] BENJAMIN H. GROH, MARTIN FLECKENSTEIN, THOMAS KAUTZ, AND BJOERN M. ESKOFIER. Classification and visualization of skateboard tricks using wearable sensors. *Pervasive and Mobile Computing*, 40:42–55, 2017.

- [83] BENJAMIN H GROH, THOMAS KAUTZ, DOMINIK SCHULDHAUS, AND BJOERN M ESKOFIER. Imu-based trick classification in skateboarding. In *KDD Workshop on Large-Scale Sports Analytics*, volume 17, 2015.
- [84] BENJAMIN H. GROH, FRANK WARSCHUN, MARTIN DEININGER, THOMAS KAUTZ, CHRISTINE MARTINDALE, AND BJOERN M. ESKOFIER. Automated Ski Velocity and Jump Length Determination in Ski Jumping Based on Unobtrusive and Wearable Sensors. *Proceedings of the ACM on Interactive, Mobile, Wearable and Ubiquitous Technologies*, 1(3):1–17, 2017.
- [85] AGNES GRUENERBL, GERALD PIRKL, ELOISE MONGER, MARY GOBBI, AND PAUL LUKOWICZ. Smart-watch life saver: Smart-watch interactive-feedback system for improving bystander cpr. In *Proceedings of the 2015 ACM International Symposium on Wearable Computers*, pages 19–26. ACM, 2015.
- [86] AGNES GRUENERBL, GERALD PIRKL, ELOISE MONGER, MARY GOBBI, AND PAUL LUKOWICZ. Smart-watch life saver: smart-watch interactive-feedback system for improving bystander cpr. In *Proceedings of the 2015 ACM International Symposium on Wearable Computers*, pages 19–26, 2015.
- [87] CHARLES WAYNE GUILDNER, DOUG WILLIAMS, AND TOM SUBITCH. Airway obstructed by foreign material: the heimlich maneuver. *Journal of the American College of Emergency Physicians*, 5(9):675–677, 1976.
- [88] HAODONG GUO, LING CHEN, GENCAI CHEN, AND MINGQI LV. Smartphone-based activity recognition independent of device orientation and placement. *International Journal of Communication Systems*, 2016.
- [89] PIYUSH GUPTA AND TIM DALLAS. Feature selection and activity recognition system using a single triaxial accelerometer. *IEEE Transactions on Biomedical Engineering*, 2014.

- [90] KRISTIE HADDEN. The stoplight method: a qualitative approach for health literacy research. *HLRP: Health Literacy Research and Practice*, 1(2):e18–e22, 2017.
- [91] MARK HALL, EIBE FRANK, GEOFFREY HOLMES, BERNHARD PFAHRINGER, PETER REUTEMANN, AND IAN H. WITTEN. The WEKA data mining software: an update. *SIGKDD Explorations*, 11(1):10–18, 2009.
- [92] ANTHONY J HANDLEY. Basic life support. *British journal of anaesthesia*, 79(2):151–158, 1997.
- [93] H. J. HEIMLICH, M. H. UHLEY, AND F. H. NETTER. The heimlich maneuver. *Clinical symposia (Summit, N.J. : 1957)*, 31(3):1–32, 1979.
- [94] RICHARD HELMER, IAN BLANCHONETTE, DAMIAN FARROW, JOHN BAKER, AND ELISSA PHILLIPS. Interactive biomechanics and electronic textiles. In *ISBS-Conference Proceedings Archive*, 2012.
- [95] KUMAR HEMANT, ERWAN THÉBAULT, MIOARA MANDEA, DHANANJAY RAVAT, AND STEFAN MAUS. Magnetic anomaly map of the world: merging satellite, airborne, marine and ground-based magnetic data sets. *Earth and Planetary Science Letters*, 260(1-2):56–71, 2007.
- [96] TIMOTHY E HEWETT, GREGORY D MYER, KEVIN R FORD, ROBERT S HEIDT JR, ANGELO J COLOSIMO, SCOTT G MCLEAN, ANTONIE J VAN DEN BOGERT, MARK V PATERNO, AND PAUL SUCCOP. Biomechanical measures of neuromuscular control and valgus loading of the knee predict anterior cruciate ligament injury risk in female athletes: a prospective study. *The American journal of sports medicine*, 33(4):492–501, 2005.
- [97] THOMAS HOLLECZEK, JONA SCHOCH, BERT ARNRICH, AND GERHARD TR??STER. Recognizing turns and other snowboarding activities with a gyroscope. *Proceedings - International Symposium on Wearable Computers, ISWC*, 2010.

- [98] CHING TANG HUANG, CHIEN LUNG SHEN, CHIEN FA TANG, AND SHUO HUNG CHANG. A wearable yarn-based piezo-resistive sensor. *Sensors and Actuators, A: Physical*, 2008.
- [99] TODD J HULLFISH, FEINI QU, BRENDAN D STOECKL, PETER M GEBHARD, ROBERT L MAUCK, AND JOSH R BAXTER. Measuring clinically relevant knee motion with a self-calibrated wearable sensor. *Journal of biomechanics*, 89:105–109, 2019.
- [100] FELIX H. SAVOIE III. Elbow anatomy & biomechanics. <https://www.orthobullets.com/shoulder-and-elbow/3078/elbow-anatomy-and-biomechanics>.
- [101] MARC JAEGER, MARCO MUELLER, DANIEL WETTACH, TIMUR OEZKAN, JOHANN MOTSCH, THOMAS SCHAUER, ROBERT JAEGER, AND ARMIN BOLZ. First-aid sensor system: New methods for single-point detection and analysis of vital parameters such as pulse and respiration. In *2007 29th Annual International Conference of the IEEE Engineering in Medicine and Biology Society*, pages 2928–2931. IEEE, 2007.
- [102] CAROLIN JAKOB, PATRICK KUGLER, FELIX HEBENSTREIT, SAMUEL J REINFELDER, ULF JENSEN, DOMINIK SCHULDHAUS, MATTHIAS LOCHMANN, AND BJØERN ESKOFIER. Estimation of the knee flexion-extension angle during dynamic sport motions using body-worn inertial sensors. In *BodyNets*, pages 289–295. Citeseer, 2013.
- [103] JON M JARNING, KAM-MING MOK, BJØRGE H HANSEN, AND ROALD BAHR. Application of a tri-axial accelerometer to estimate jump frequency in volleyball. *Sports biomechanics*, 14(1):95–105, 2015.
- [104] STEPHAN JONAS, ANDREAS HANNIG, CORD SPRECKELSEN, AND THOMAS M DESERNO. Wearable technology as a booster of clinical care. In *Medical Imaging 2014:*

PACS and Imaging Informatics: Next Generation and Innovations, volume 9039, page 90390F. International Society for Optics and Photonics, 2014.

- [105] THOMAS KAUTZ, BENJAMIN H GROH, AND BJOERN M ESKOFIER. Sensor fusion for multi-player activity recognition in game sports. In *Workshop on Large-Scale Sports Analytics, 21st ACM SIGKDD Conference on Knowledge Discovery and Data Mining*, 2015.
- [106] THOMAS KAUTZ, BENJAMIN H GROH, JULIUS HANNINK, ULF JENSEN, HOLGER STRUBBERG, AND BJOERN M ESKOFIER. Activity recognition in beach volleyball using a deep convolutional neural network. *Data Mining and Knowledge Discovery*, 31(6):1678–1705, 2017.
- [107] THOMAS KAUTZ, BENJAMIN H GROH, JULIUS HANNINK, ULF JENSEN, HOLGER STRUBBERG, AND BJOERN M ESKOFIER. Activity recognition in beach volleyball using a deep convolutional neural network. *Data Mining and Knowledge Discovery*, 31(6):1678–1705, 2017.
- [108] VASSILIS KILINTZIS, CHRISTOS MARAMIS, AND NICOS MAGLAVERAS. Wrist sensors—an application to acquire sensory data from android wear® smartwatches for connected health. In *2017 IEEE EMBS International Conference on Biomedical & Health Informatics (BHI)*, pages 125–128. IEEE, 2017.
- [109] JI-SUN KIM, A-HEE KIM, HAN-BYEOL OH, JUN-SIK KIM, BONG-JUN GOH, EUN-SUK LEE, JU-HYEON CHOI, JIN-YOUNG BAEK, AND JAE-HOON JUN. Study of an optical goniometer using a multi-photodiode sensor. *Journal of the Optical Society of Korea*, 20(1):22–28, 2016.
- [110] K&j magnetics - neodymium magnet information. <https://www.kjmagnetics.com/neomaginfo.asp>

- [111] JOERG KOENIGSTORFER, ANDREA GROEPPPEL-KLEIN, AND FRIEDERIKE KAMM. Healthful food decision making in response to traffic light color-coded nutrition labeling. *Journal of Public Policy & Marketing*, 33(1):65–77, 2014.
- [112] N C KRISHNAN, D COLBRY, AND C JUILLARD. Real time human activity recognition using tri-axial accelerometers. *Sensors*, 2008.
- [113] LIU KUN, YOSHIO INOUE, KYOKO SHIBATA, AND CAO ENGUO. Ambulatory estimation of knee-joint kinematics in anatomical coordinate system using accelerometers and magnetometers. *IEEE Transactions on Biomedical Engineering*, 58(2):435–442, 2011.
- [114] JENNIFER R. KWAPISZ, GARY M. WEISS, AND SAMUEL A. MOORE. Activity recognition using cell phone accelerometers. *ACM SIGKDD Explorations Newsletter*, 2011.
- [115] Laerdal little annie cpr training manikin. <http://www.laerdal.com/us/doc/60/Little-Anne-CPR-Training-Manikin>
- [116] OSCAR D LARA, ALFREDO J PÉREZ, MIGUEL A LABRADOR, AND JOSÉ D POSADA. Centinela: A human activity recognition system based on acceleration and vital sign data. *Pervasive and mobile computing*, 8(5):717–729, 2012.
- [117] GUO XIONG LEE AND KAY-SOON LOW. A factorized quaternion approach to determine the arm motions using triaxial accelerometers with anatomical and sensor constraints. *IEEE Transactions on Instrumentation and Measurement*, 61(6):1793–1802, 2012.
- [118] GUO XIONG LEE, KAY SOON LOW, AND TAWFIQ TAHER. Unrestrained measurement of arm motion based on a wearable wireless sensor network. *IEEE transactions on instrumentation and measurement*, 59(5):1309–1317, 2010.

- [119] S. I. LEE, J. DANEALU, L. WEYDERT, AND P. BONATO. A novel flexible wearable sensor for estimating joint-angles. In *2016 IEEE 13th International Conference on Wearable and Implantable Body Sensor Networks (BSN)*, pages 377–382, June 2016.
- [120] JAMES LENZ AND S EDELSTEIN. Magnetic sensors and their applications. *IEEE Sensors journal*, 6(3):631–649, 2006.
- [121] LG lg urbane - smartwatch. <http://www.lg.com/us/smart-watches/lg-W150-lg-watch-urbane>
- [122] HONGQIANG LI, HAIJING YANG, ENBANG LI, ZHIHUI LIU, AND KEJIA WEI. Wearable sensors in intelligent clothing for measuring human body temperature based on optical fiber Bragg grating. *Optics Express*, 2012.
- [123] JULIANA LOCKMAN, ROBERT S FISHER, AND DONALD M OLSON. Detection of seizure-like movements using a wrist accelerometer. *Epilepsy & Behavior*, 20(4):638–641, 2011.
- [124] ELENA LOSINA, A DAVID PALTIEL, ALEXANDER M WEINSTEIN, EDWARD YELIN, DAVID J HUNTER, STEPHANIE P CHEN, KRISTINA KLARA, LISA G SUTER, DANIEL H SOLOMON, SARA A BURBINE, ET AL. Lifetime medical costs of knee osteoarthritis management in the united states: impact of extending indications for total knee arthroplasty. *Arthritis care & research*, 67(2):203–215, 2015.
- [125] Y MA, W JIA, C LI, J YANG, Z-H MAO, AND M SUN. Magnetic hand motion tracking system for human–machine interaction. *Electronics letters*, 46(9):621–623, 2010.
- [126] YINGHONG MA, ZHI-HONG MAO, WENYAN JIA, CHENGLIU LI, JIAWEI YANG, AND MINGUI SUN. Magnetic hand tracking for human-computer interface. *IEEE Transactions on Magnetics*, 47(5):970–973, 2011.

- [127] YINGHONG MA, ZHI-HONG MAO, WENYAN JIA, CHENGLIU LI, JIAWEI YANG, AND MINGUI SUN. Magnetic hand tracking for human-computer interface. *IEEE Transactions on Magnetics*, 47(5):970–973, 2011.
- [128] KERRY MACDONALD, ROALD BAHR, JENNIFER BALTICH, JACKIE L WHITTAKER, AND WILLEM H MEEUWISSE. Validation of an inertial measurement unit for the measurement of jump count and height. *Physical Therapy in Sport*, 25:15–19, 2017.
- [129] PAUL H MAHONY, ROBIN F GRIFFITHS, PETER LARSEN, AND DAVID POWELL. Retention of knowledge and skills in first aid and resuscitation by airline cabin crew. *Resuscitation*, 76(3):413–418, 2008.
- [130] E MCFEE, Y DAS, AND RO ELLINGSON. Locating and identifying compact ferrous objects. *IEEE Transactions on Geoscience and Remote Sensing*, 28(2):182–193, 1990.
- [131] JOHN E MCFEE, ROBERT O ELLINGSON, AND YOGADHISH DAS. A total-field magnetometer system for location and identification of compact ferrous objects. *IEEE transactions on instrumentation and measurement*, 43(4):613–619, 1994.
- [132] JOHAN ERNEST MEBIUS. Derivation of the euler-rodriques formula for three-dimensional rotations from the general formula for four-dimensional rotations. *arXiv preprint math/0701759*, 2007.
- [133] Medigauge digital protractor goniometer for medical applications. <http://www.medigauge.com/digital-protractor-goniometer-for-medical-applications/>
- [134] MICHAŁ MEINA, KRZYSZTOF RYKACZEWSKI, AND ANDRZEJ RUTKOWSKI. Position tracking using inertial and magnetic sensing aided by permanent magnet. In *2016 Federated Conference on Computer Science and Information Systems (FedCSIS)*, pages 105–111. IEEE, 2016.

- [135] YIĞIT MENGÜÇ, YONG-LAE PARK, HAO PEI, DANIEL VOGT, PATRICK M AUBIN, ETHAN WINCHELL, LOWELL FLUKE, LEIA STIRLING, ROBERT J WOOD, AND CONOR J WALSH. Wearable soft sensing suit for human gait measurement. *The International Journal of Robotics Research*, 33(14):1748–1764, 2014.
- [136] HADRIEN O MICHAUD, JOAN TEIXIDOR, AND STÉPHANIE P LACOUR. Soft flexion sensors integrating stretchable metal conductors on a silicone substrate for smart glove applications. In *2015 28th IEEE International Conference on Micro Electro Mechanical Systems (MEMS)*, pages 760–763. IEEE, 2015.
- [137] EMILIANO MILUZZO, NICHOLAS D. LANE, KRISTÓF FODOR, RONALD PETERSON, HONG LU, MIRCO MUSOLESI, SHANE B. EISENMAN, XIAO ZHENG, AND ANDREW T. CAMPBELL. Sensing meets mobile social networks. In *Proceedings of the 6th ACM conference on Embedded network sensor systems - SenSys '08*, 2008.
- [138] CHEOL-HONG MIN, CRYSTAL COMPTON, AND LUCY E DUNNE. Sensing lower body lifting posture through disposable sensing coveralls. *International Textile and Apparel Association (ITAA) Annual Conference Proceedings*, 2015.
- [139] EDMOND MITCHELL, DAVID MONAGHAN, AND NOEL E. O’CONNOR. Classification of sporting activities using smartphone accelerometers. *Sensors (Switzerland)*, 13(4):5317–5337, 2013.
- [140] Motorola moto 360 - smartwatch. <https://www.motorola.com/us/products/moto-360>
- [141] SUBHAS CHANDRA MUKHOPADHYAY. Wearable sensors for human activity monitoring: A review. *IEEE sensors journal*, 15(3):1321–1330, 2015.
- [142] National Institute of Neurological Disorders and Stroke: cerebral hypoxia. <https://espanol.ninds.nih.gov/trastornos/anoxia.htm?css=print>, Dec 2016.

- [143] LE NGUYEN NGU NGUYEN, DANIEL RODRÍGUEZ-MARTÍN, ANDREU CATALÀ, CARLOS PÉREZ-LÓPEZ, ALBERT SAMÀ, AND ANDREA CAVALLARO. Basketball Activity Recognition using Wearable Inertial Measurement Units. *Proceedings of the XVI International Conference on Human Computer Interaction - Interacción '15*, pages 1–6, 2015.
- [144] DOMEN NOVAK AND ROBERT RIENER. A survey of sensor fusion methods in wearable robotics. In *Robotics and Autonomous Systems*, 2015.
- [145] KOSTYA S NOVOSELOV, ANDRE K GEIM, SERGEI V MOROZOV, D JIANG, Y. ZHANG, SERGEY V DUBONOS, IRINA V GRIGORIEVA, AND ALEXANDR A FIRSOV. Electric field effect in atomically thin carbon films. *science*, 306(5696):666–669, 2004.
- [146] KAROL J O'DONOVAN, ROMAN KAMNIK, DEREK T O'KEEFFE, AND GERARD M LYONS. An inertial and magnetic sensor based technique for joint angle measurement. *Journal of biomechanics*, 40(12):2604–2611, 2007.
- [147] NINJA P. OESS, JOHANN WANER, AND ARMIN CURT. Design and evaluation of a low-cost instrumented glove for hand function assessment. *Journal of NeuroEngineering and Rehabilitation*, 2012.
- [148] STEVEN OSMAN. Magnetic tracking of glove fingertips with peripheral devices, May 30 2017. US Patent 9,665,174.
- [149] VAIBHAV PANDE, SYED MOHD ALI, SUBODH KUMAR, AND PUNEET GOYAL. Automated first aid and medication system for burn victims. In *2014 IEEE International Advance Computing Conference (IACC)*, pages 623–627. IEEE, 2014.
- [150] E. PAPI, I. SPULBER, M. KOTTI, P. GEORGIU, AND A. H. MCGREGOR. Smart sensing system for combined activity classification and estimation of knee range of motion. *IEEE Sensors Journal*, 15(10):5535–5544, Oct 2015.

- [151] ENRICA PAPI, GED M MURTAGH, AND ALISON H MCGREGOR. Wearable technologies in osteoarthritis: a qualitative study of clinicians' preferences. *BMJ open*, 6(1):e009544, 2016.
- [152] YONG LAE PARK, BOR RONG CHEN, DIANA YOUNG, LEIA STIRLING, ROBERT J. WOOD, EUGENE GOLDFIELD, AND RADHIKA NAGPAL. Bio-inspired active soft orthotic device for ankle foot pathologies. In *IEEE International Conference on Intelligent Robots and Systems*, 2011.
- [153] JUHA PARKKA, MIIKKA ERMES, PANU KORPIPAA, JANI MANTYJARVI, JOHANNES PELTOLA, AND ILKKA KORHONEN. Activity classification using realistic data from wearable sensors. *IEEE Transactions on information technology in biomedicine*, 10(1):119–128, 2006.
- [154] Pasport goniometer sensor. <https://www.pasco.com/prodCompare/goniometer-sensor/index.cfm>
- [155] SHYAMAL PATEL, HYUNG PARK, PAOLO BONATO, LEIGHTON CHAN, AND MARY RODGERS. A review of wearable sensors and systems with application in rehabilitation. *Journal of neuroengineering and rehabilitation*, 9(1):21, 2012.
- [156] TANMAY PAWAR, SUBHASIS CHAUDHURI, AND SIDDHARTHA P DUTTAGUPTA. Body movement activity recognition for ambulatory cardiac monitoring. *IEEE transactions on biomedical engineering*, 54(5):874–882, 2007.
- [157] F. PEDREGOSA, G. VAROQUAUX, A. GRAMFORT, V. MICHEL, B. THIRION, O. GRISEL, M. BLONDEL, P. PRETTENHOFER, R. WEISS, V. DUBOURG, J. VANDERPLAS, A. PASSOS, D. COURNAPEAU, M. BRUCHER, M. PERROT, AND E. DUCHESNAY. Scikit-learn: Machine Learning in Python . *Journal of Machine Learning Research*, 12:2825–2830, 2011.

- [158] IVAN POUPYREV, NAN-WEI GONG, SHIHO FUKUHARA, MUSTAFA EMRE KARAGÖZLER, CARSTEN SCHWESIG, AND KAREN E. ROBINSON. Project Jacquard: Interactive Digital Textiles at Scale. In *Proceedings of the 2016 CHI Conference on Human Factors in Computing Systems*, 2016.
- [159] YONGBIN QI, CHEONG SOH, ERRY GUNAWAN, KAY-SOON LOW, AND RIJIL THOMAS. Lower extremity joint angle tracking with wireless ultrasonic sensors during a squat exercise. *Sensors*, 15(5):9610–9627, 2015.
- [160] YONGBIN QI, CHEONG BOON SOH, ERRY GUNAWAN, AND KAY-SOON LOW. A wearable wireless ultrasonic sensor network for human arm motion tracking. In *2014 36th Annual International Conference of the IEEE Engineering in Medicine and Biology Society*, pages 5960–5963. IEEE, 2014.
- [161] YONGBIN QI, CHEONG BOON SOH, ERRY GUNAWAN, KAY-SOON LOW, AND ARASH MASKOOKI. A novel approach to joint flexion/extension angles measurement based on wearable uwb radios. *IEEE journal of biomedical and health informatics*, 18(1):300–308, 2014.
- [162] FEINI QU, BRENDAN D STOECKL, PETER M GEBHARD, TODD J HULLFISH, JOSH R BAXTER, AND ROBERT L MAUCK. A wearable magnet-based system to assess activity and joint flexion in humans and large animals. *Annals of biomedical engineering*, 46(12):2069–2078, 2018.
- [163] 100 μ h rf choke: Radioshack. <https://www.radioshack.com/products/radioshack-100-h-rf-choke> [Online; accessed 10-October-2019].
- [164] NISHKAM RAVI, NIKHIL DANDEKAR, PREETHAM MYSORE, AND MICHAEL L LITTMAN. Activity recognition from accelerometer data. In *Aaai*, volume 5, pages 1541–1546, 2005.

- [165] MIKE RAYNER, PETER SCARBOROUGH, ANNA BOXER, AND LYNN STOCKLEY. Nutrient profiles: development of final model. *London: Food Standards Agency*, 2005.
- [166] Remington industries 28 gauge awg magnet wire, enameled copper wire, 4 oz, 0.0135" diameter, 507' length, red. https://www.amazon.com/Remington-Industries-28SNSP-25-Enameled-Diameter/dp/B00I53B2TC/ref=sr_1_3?keywords=magnet+wire&qid=1563292790&s=gateway&sr=8-3 [Online; accessed 10-October-2019].
- [167] MARKUS ROTHMAIER, MINH PHI LUONG, AND FRANK CLEMENS. Textile pressure sensor made of flexible plastic optical fibers. *Sensors*, 2008.
- [168] Schmetz metallic needles. <https://www.schmetzneedles.com/schmetz-metallic-needles/>.
- [169] DOMINIK SCHULDHAUS, CONSTANTIN ZWICK, HARALD KÖRGER, EVA DORSCHKY, ROBERT KIRK, AND BJOERN M. ESKOFIER. Inertial Sensor-Based Approach for Shot / Pass Classification During a Soccer Match. *Proc. 21st ACM KDD Workshop on Large-Scale Sports Analytics*, 27:1–4, 2015.
- [170] SKIPPER SEABOLD AND JOSEF PERKTOLD. Statsmodels: Econometric and statistical modeling with python. In *Proceedings of the 9th Python in Science Conference*, volume 57, page 61. Scipy, 2010.
- [171] SYED ZAFAR ALI SHAH, IFTIKHAR AHMED KHAN, IMRAN MAQSOOD, TAIMOOR ALI KHAN, AND YASIR KHAN. First-aid application for illiterates and its usability evaluation. In *2015 13th International conference on frontiers of information technology (FIT)*, pages 125–131. IEEE, 2015.
- [172] JEROLD S SHINBANE AND LESLIE A SAXON. Digital monitoring and care: virtual medicine. *Trends in cardiovascular medicine*, 26(8):722–730, 2016.

- [173] K. ALEX SHORTER, GZA F. KOGLER, ERIC LOTH, WILLIAM K. DURFEE, AND ELIZABETH T. HSIAO-WECKSLER. A portable powered ankle-foot orthosis for rehabilitation. *The Journal of Rehabilitation Research and Development*, 2011.
- [174] PETE B. SHULL, WISIT JIRATTIGALACHOTE, MICHAEL A. HUNT, MARK R. CUTKOSKY, AND SCOTT L. DELP. Quantified self and human movement: A review on the clinical impact of wearable sensing and feedback for gait analysis and intervention, 2014.
- [175] TIEN-WEI SHYR, JING-WEN SHIE, CHANG-HAN JIANG, AND JUNG-JEN LI. A textile-based wearable sensing device designed for monitoring the flexion angle of elbow and knee movements. *Sensors*, 14(3):4050–4059, 2014.
- [176] ANA S SILVA, ANDRÉ CATARINO, MIGUEL V CORREIA, AND ORLANDO FRAZÃO. Design and characterization of a wearable macrobending fiber optic sensor for human joint angle determination. *Optical Engineering*, 52(12):126106, 2013.
- [177] RAMANDEEP SINGH, HAVNEET SINGH, AND ANOOP KANT GODIYAL. Wearable knee joint angle measurement system based on force sensitive resistors. In *2018 IEEE Long Island Systems, Applications and Technology Conference (LISAT)*, pages 1–3. IEEE, 2018.
- [178] CHRISTOPHER SKAZALSKI, ROD WHITELEY, CLINT HANSEN, AND ROALD BAHR. A valid and reliable method to measure jump-specific training and competition load in elite volleyball players. *Scandinavian journal of medicine & science in sports*, 28(5):1578–1585, 2018.
- [179] Sparkfun bluetooth modem - bluesmirf silver. <https://www.sparkfun.com/products/12577>
- [180] Sparkfun: conductive thread bobbin - 12m (smooth, stainless steel). <https://www.sparkfun.com/products/13814>

- [181] Sparkfun: lipower - boost converter. <https://www.sparkfun.com/products/10255>.
- [182] DANA ELLIOT SRITHER AND FATIMAH LATEEF. A novel cpr training method using a smartphone app. *Journal of Acute Disease*, 5(6):517–520, 2016.
- [183] DRAGAN Z STUPAR, JOVAN S BAJIC, LAZO M MANOJLOVIC, MILOŠ P SLANKAMENAC, ANA V JOZA, AND MILOŠ B ZIVANOV. Wearable low-cost system for human joint movements monitoring based on fiber-optic curvature sensor. *IEEE Sensors Journal*, 12(12):3424–3431, 2012.
- [184] AMARNAG SUBRAMANYA, ALVIN RAJ, JEFF A BILMES, AND DIETER FOX. Recognizing activities and spatial context using wearable sensors. *arXiv preprint arXiv:1206.6869*, 2012.
- [185] Syscom advanced materials amberstrand fiber. <http://www.metalcladfibers.com/amberstrand/>.
- [186] SHIGERU TADANO, RYO TAKEDA, AND HIROAKI MIYAGAWA. Three dimensional gait analysis using wearable acceleration and gyro sensors based on quaternion calculations. *Sensors (Switzerland)*, 2013.
- [187] EMMANUEL MUNGUIA TAPIA, STEPHEN S INTILLE, WILLIAM HASKELL, KENT LARSON, JULIE WRIGHT, ABBY KING, AND ROBERT FRIEDMAN. Real-time recognition of physical activities and their intensities using wireless accelerometers and a heart rate monitor. In *Wearable Computers, 2007 11th IEEE International Symposium on*, pages 37–40. IEEE, 2007.
- [188] CAITLIN N TEAGUE, SINAN HERSEK, HAKAN TÖREYİN, MINDY L MILLARD-STAFFORD, MICHAEL L JONES, GÉZA F KOGLER, MICHAEL N SAWKA, AND OMER T INAN. Novel methods for sensing acoustical emissions from the knee for

- wearable joint health assessment. *IEEE Transactions on Biomedical Engineering*, 63(8):1581–1590, 2016.
- [189] ALESSANDRO TOGNETTI, FEDERICO LORUSSI, GABRIELE DALLE MURA, NICOLA CARBONARO, MARIA PACELLI, RITA PARADISO, AND DANILO DE ROSSI. New generation of wearable goniometers for motion capture systems. *Journal of Neuro-Engineering and Rehabilitation*, 2014.
- [190] MARK H TOTMAN. Method of measuring abdominal thrusts for clinical use and training, September 9 2014. US Patent 8,827,721.
- [191] Toyobo pbo fiber: Zylon. <http://www.toyobo-global.com/seihin/kc/pbo/>.
- [192] Underarmour coldgear authentic mock. <https://www.underarmour.com/en-us/womens-coldgear-fitted-mock/pid1215968-001>.
- [193] ANTONIE J. VAN DEN BOGERT, THOMAS GEIJTENBEEK, OSHRI EVEN-ZOHAR, FRANS STEENBRINK, AND ELIZABETH C. HARDIN. A real-time system for biomechanical analysis of human movement and muscle function. *Medical and Biological Engineering and Computing*, 2013.
- [194] PETER H. VELTINK AND DANILO DE ROSSI. Wearable technology for biomechanics: E-textile or micromechanical sensors?, 2010.
- [195] VERT wearable for athletes. <https://www.myvert.com>. Accessed: 2018-03-37.
- [196] ROBERT E VISINTINE AND CHOONG H BAICK. Ruptured stomach after heimlich maneuver. *Jama*, 234(4):415–415, 1975.
- [197] PO T WANG, CHRISTINE E KING, AN H DO, AND ZORAN NENADIC. A durable, low-cost electrogoniometer for dynamic measurement of joint trajectories. *Medical engineering & physics*, 33(5):546–552, 2011.

- [198] AMANDA WATSON, MINGLONG SUN, SAMHITA PENDYAL, AND GANG ZHOU. Tracknee: Knee angle measurement using stretchable conductive fabric sensors. *Smart Health*, 15:100092, 2020.
- [199] AMANDA WATSON AND GANG ZHOU. Breathez: Using smartwatches to improve choking first aid. *Smart Health*, 13:100058, 2019.
- [200] TIM V WRIGLEY. Motion sensors in osteoarthritis: Prospects and issues. *Healthcare Sensor Networks: Challenges Toward Practical Implementation*, page 183, 2011.
- [201] YANXIN ZHANG, DAVID G LLOYD, AMITY C CAMPBELL, AND JACQUELINE A ALDERSON. Can the effect of soft tissue artifact be eliminated in upper-arm internal-external rotation? *Journal of applied biomechanics*, 27(3):258–265, 2011.
- [202] CHUN ZHU AND WEIHUA SHENG. Realtime recognition of complex human daily activities using human motion and location data. *IEEE Transactions on Biomedical Engineering*, 59(9):2422, 2012.